

**DEFINING THE STRATIGRAPHIC AND PALEOENVIRONMENTAL RECORD
OF RAPID SEA-LEVEL RISE DURING THE LATE PLEISTOCENE TO HOLOCENE
IN THE ALBEMARLE SOUND REGION OF NORTH CAROLINA**

By

Erik Kenneth Gudmunson

July, 2022

Directors of Thesis: Dr. D.J. Mallinson and Dr. S.J. Culver

Department: Geological Sciences

Abstract

Sea-level fluctuations throughout the late Quaternary Period are recorded in the shallow stratigraphy and modern geomorphology of coastal North Carolina. In the Albemarle Sound region, four distinct Pleistocene sea-level highstand units occur between the late Pleistocene shoreline, marked by the Suffolk Scarp, and the modern ocean shoreline (a distance up to 120 km). Lithofacies and geophysical (ground penetrating radar and CHIRP seismic) data reveal the presence of multiple paleoenvironments during these highstand periods. These deposits are chronostratigraphically and lithostratigraphically categorized into depositional sequences (DS1-4), each separated by a subaerial unconformity or transgressive ravinement surface. DS1 and DS2 contain marine facies (shoreline, shallow shelf, and shoal) with DS1 representing marine deposition during either MIS5e or MIS5c and DS2 representing MIS5a transgressive deposits based on OSL age estimates (91.8 ± 6.3 ka and 93.4 ± 6.3). Overlying DS2, DS3 is dominated by marginal marine and fluvial facies interpreted to include estuarine, tidal flat, and braidplain paleoenvironments. Radiocarbon and OSL age data from this sequence suggest deposition

occurred during MIS3. The uppermost sequence DS4, consists of Holocene valley-fill primarily within the Albemarle Sound, and marsh and swamp forest peat.

Correlations of facies throughout the Albemarle Sound, paired with those interpreted in comparable studies in the region reveal how coastal North Carolina's geomorphology responded to relative sea-level changes during the late Pleistocene. The geologic characteristics of these depositional sequences and their corresponding depositional environments provide an analog for future conditions. The results of this study indicate that with current rates of regional sea-level rise (3.4 mm/yr) the wave dominated estuarine system of the present Albemarle Sound region will likely transition to an extensive tidal flat system comparable to the interpreted MIS3 paleoenvironment.

DEFINING THE STRATIGRAPHIC AND PALEOENVIRONMENTAL RECORD OF
RAPID SEA-LEVEL RISE DURING THE LATE PLEISTOCENE TO HOLOCENE IN THE
ALBEMARLE SOUND REGION OF NORTH CAROLINA

A Thesis

Presented to

The Faculty of the Department of Geological Sciences

East Carolina University

In Partial Fulfillment

of the Requirements for the Degree

Masters of Science in Geology

by

Erik K. Gudmunson

July, 2022

© Erik K. Gudmunson, 2022

DEFINING THE STRATIGRAPHIC AND PALEOENVIRONMENTAL RECORD OF
RAPID SEA-LEVEL RISE DURING THE LATE PLEISTOCENE TO HOLOCENE IN THE
ALBEMARLE SOUND REGION OF NORTH CAROLINA

By

Erik K. Gudmunson

Approved by:

Co-Director of Thesis

Dr. David J. Mallinson

Co-Director of Thesis

Dr. Stephen J. Culver

Committee Member

Dr. Eduardo Leorri

External Committee Member

Dr. Regina DeWitt

Chair of the Department of
Geological Sciences

Dr. Eric Horsman

Interim Dean of the Graduate School

Kathleen T Cox, PhD

DEDICATION

To my parents, Garry and Allison Gudmunson.

ACKNOWLEDGEMENTS

First, I would like to thank my family for their endless support and motivation throughout this whole process, especially my grandparents who at times seemed to be as interested in my research as myself. I would like to thank Drs. Mallinson and Culver for the numerous edits provided for me over the past year. A special thanks to Dr. Mallinson whose patience and guidance aided significantly in my completion of this research. Thank you, Dr. DeWitt, for taking the time to help me prepare and analyze my OSL samples at ECU. Another special thank you to Marah Dahn and Scott Rose for assisting me with field work operations including land and marine coring, as well as CHIRP seismic surveying. I would again like to thank all of my committee members, Drs. Mallinson, Culver, DeWitt, and Leorri for their guidance. Finally, I would like to thank the NSF grant (06040000 OCE) and the Department of Geological Sciences at ECU for funding this research.

Table of Contents

LIST OF TABLES.....	ix
LIST OF FIGURES.....	x
1.0 Introduction.....	1
<i>1.1 Objectives</i>	2
<i>1.2 Study Area</i>	3
<i>1.2.1 Geologic Setting</i>	3
<i>1.2.2 Stratigraphic Framework</i>	6
2.0 Methods.....	7
<i>2.1 Geophysical Analysis</i>	7
<i>2.2 Core Collection and Analysis</i>	8
<i>2.3 Optically Stimulated Luminescence Dating</i>	8
<i>2.4 Radiocarbon Dating</i>	9
<i>2.5 Foraminiferal Analysis</i>	10
3.0 Results.....	11
<i>3.1 Geophysical Data</i>	11
<i>3.1.1 Ground Penetrating Radar</i>	11
<i>3.1.1.1 Radar facies 1 (RF1)</i>	11
<i>3.1.1.2 Radar surface 1 (RS1)</i>	11
<i>3.1.1.3 Radar facies 2 (RF2)</i>	12
<i>3.1.1.4 Radar surface 2 (RS2)</i>	13
<i>3.1.1.5 Radar facies 3 (RF3)</i>	13

3.1.1.6 Radar Surface 3 (RS3)	18
3.1.2 CHIRP Seismic.....	18
3.1.2.1 Seismic stratigraphic unit 0 (SSU0)	18
3.1.2.2 Seismic horizon 1 (SH1)	18
3.1.2.3 Seismic stratigraphic unit 1 (SSU1)	18
3.1.2.4 Seismic horizon 2 (SH2)	19
3.1.2.5 Seismic stratigraphic unit 2 (SSU2)	19
3.1.2.6 Seismic horizon 3 (SH3)	19
3.1.2.7 Seismic stratigraphic unit 3 (SSU3)	20
3.1.2.8 Seismic horizon 4 (SH4)	20
3.1.2.9 Seismic stratigraphic unit 4 (SSU4)	20
3.2 Lithofacies.....	26
3.3 Age Analysis.....	31
3.3.1 Optically Stimulated Luminescence Analysis.....	31
3.3.2 Radiocarbon Analysis.....	32
3.4 Sedimentology Data.....	33
3.5 Foraminiferal Data.....	33
4.0 Discussion.....	34
4.1 Defining the Lithostratigraphy and Chronostratigraphy.....	34
4.1.1 Depositional Sequence 1 (DS-1)	34
4.1.2 Depositional Sequence 2 (DS-2)	38
4.1.3 Depositional Sequence 3 (DS-3)	41

4.1.4	<i>Depositional Sequence 4 (DS-4)</i>	48
4.2	<i>Evolution of the System and Implications for Sea Level Changes and Isostatic Adjustment</i>	55
4.2.1	<i>Marine Isotope Stage 5</i>	56
4.2.2	<i>Marine Isotope Stage 3</i>	60
4.3	<i>Expectations for the Future</i>	68
5.0	Conclusion.....	72
	References	73
	Appendix A: Geoprobe and Vibracore Locations.....	78
	Appendix B: Grain Size Analysis Data.....	79
	Appendix C: Radiocarbon Data.....	81
	Appendix D: Optically Stimulated Luminescence Data.....	82
	Appendix E: Core Logs.....	83

List of Tables

Table 1. Distinct radar facies observed in GPR data. Each facies define the characteristics of a Radar facies defined in this paper. Black scale bars are included for each radar facies example (vertical scale = 1 m and horizontal scale = 5 m).

Table 2. List of lithofacies and their characteristics.

Table 3. Marine isotope stages displayed with their corresponding Geophysical facies (radar and seismic) and denoted depositional sequences associated with this study.

Table 4. Sea level rise estimates (meters) along the Atlantic coast of the United States. These data were collected from the IPCC A6 climate report (IPCC, 2021).

List of Figures

- Figure 1.** Maps defining the study area location. A) Regional map of eastern North Carolina, defining major water bodies and structural features discussed in the study. The figure includes an inset map of the southeastern United States with the regional map outlined in black. B) LiDAR map of study area including core locations and geophysical survey lines.
- Figure 2.** Ground penetrating radar profile along the northern shoreline of the Albemarle Sound, east of Edenton, NC. A) Processed GPR profile, displaying signal attenuation towards the right side of the profile. B) Defined radar facies and horizons are outlined in black.
- Figure 3.** Ground penetrating radar profile collected along the southern coast of the Albemarle Sound, southeast of the mouth of the Roanoke River. A) Processed GPR profile. B) Defined GPR facies and horizons. C) These profiles were collected along Mackey's Rd. 1 GPR transect defined in this inset map.
- Figure 4.** Ground penetrating radar profile collected along the southern coast of the Albemarle Sound, southeast of the mouth of the Roanoke River. A) Processed GPR profile. B) Defined GPR facies and horizons. C) These profiles were collected along the *Mackey's rd.* 1 GPR transect defined in this inset map.
- Figure 5.** Seismic profile along the north shore of the Albemarle sound west of the Yeopim River. Major seismic horizons including SSU1, SSU2, and SSU4. Dipping clinoforms also outlined within SSU2. C) Location of the seismic profile outlined in red.
- Figure 6.** CHIRP seismic crossing line, extending north to south towards the center of the sound. Defined in the inset map, this profile is the eastern most crossing line.
- Figure 7.** CHIRP seismic profile along the southern coast of the Albemarle sound, outlined in the inset map. Processed seismic profile with water column removed and core SAS20-VC1 marked. Seismic horizons defined as SH.
- Figure 8.** CHIRP seismic crossing line, extending north to south towards the center of the sound. Signal attenuation present beneath the outlined paleochannel.
- Figure 9.** CHIRP seismic N-S profile collected within the Albemarle sound, ~5 km north of Bull Bay.
- Figure 10.** Dose rate plot depicting contrasting dose component ranges. Lower dose range was utilized for the calculation of the OSL 5 age.
- Figure 11.** Cross section across the northern shoreline of the Albemarle Sound, between the Chowan river and Edenton Bay. Dashed lines define the boundaries between depositional sequences. Each paleoenvironment and their associated Depositional Sequence are defined in

the cross section with a letter (corresponding to their paleoenvironment defined in the legend) followed by a number representing the Depositional Sequence.

Figure 12. Interpreted cross section adapted from Parham et al. (2013), 10 km north of the Albemarle Sound. Interpretations displayed here are based on extrapolated lithofacies of sediment cores GH 19-21 collected by Parham et al. (2013). Lithofacies are grouped into distinct depositional sequences, correlative to those discussed in this study.

Figure 13. CHIRP seismic W-E profile. Depositional sequences are interpreted from seismic units defined previously in Table 3. Much of the data in this profile is attenuated from gas release in the subsurface.

Figure 14. Cross section of the three interfluves on the northern shoreline of the Albemarle Sound, between the Yeopim and Pasquotank rivers. Dashed lines define the boundaries between depositional sequences. Each paleoenvironment and their associated Depositional Sequence are defined in the cross section with a letter (corresponding to their paleoenvironment defined in the legend) followed by a number representing the Depositional Sequence. Red lines within cores mark OSL dated samples.

Figure 15. Cross section across the northern shoreline of the Albemarle Sound, west of the Yeopim River. Dashed lines define the boundaries between depositional sequences. Each paleoenvironment and their associated Depositional Sequence are defined in the cross section with a letter (corresponding to their paleoenvironment defined in the legend) followed by a number representing the Depositional Sequence.

Figure 16. Images of shell material recovered from core NAS20-GP12 compared with documented shell samples from Porter and Houser (2010). **A.** Sample of *Anadara floridana* from this study area. **B.** *Anadara floridana* identified by Porter and Houser, 2010. **C.** Sample of *Spisula solidissima raveneli* from the study area. **D.** *Spisula solidissima raveneli* identified by Porter and Houser, 2010.

Figure 17. Cross section across the southern shoreline of the Albemarle Sound, West of the Roanoke river. Dashed lines define the boundaries between depositional sequences. Each paleoenvironment and their associated Depositional Sequence are defined in the cross section with a letter (corresponding to their paleoenvironment defined in the legend) followed by a number representing the Depositional Sequence.

Figure 18. Cross section adapted from Parham et al. (2013). Interpretations presented in this cross section based on 11 sediment cores taken south of the Albemarle Sound between the Suffolk Scarp Lake Mattamuskeet. Here Parham et al. (2013) has defined four late Pleistocene depositional sequences correlative to those in this study.

Figure 19. CHIRP seismic N-S crossing line with interpreted depositional sequences based on seismic units defined previously in Table 3. Paleochannel here emitting gas attenuate the seismic data in two locations along this profile. This distinguishable data here is mostly Holocene channel fill (DS-4).

Figure 20. GPR profile collected along the southern shoreline of the Albemarle Sound. Here the depositional sequences (DS) are interpreted from their associated radar facies. DS are bound by subaerial unconformities.

Figure 21. CHIRP seismic W-E profile. Here the depositional sequences (DS) are interpreted from their seismic units. DS are bound by subaerial unconformities including transgressive ravinement surfaces. Vibracore SAS20-VC1 location superimposed on the profile.

Figure 22. CHIRP seismic N-S crossing line. Here the depositional sequences (DS) are interpreted from their seismic units. DS are bound by subaerial unconformities including transgressive ravinement surfaces.

Figure 23. CHIRP seismic N-S crossing line, east of the Yeopim river. Here the depositional sequences (DS) are interpreted from their seismic units. DS are bound by subaerial unconformities including transgressive ravinement surfaces.

Figure 24. Marine benthic foraminiferal $\delta^{18}\text{O}$ data adapted from Railsback (2015), including marine isotope stages, from 140kya to the present. **a.** Extended $\delta^{18}\text{O}$ data showing marine isotope stages 1-9 (From termination IV). **b.** Enhanced view of figure 16a focusing on the marine isotope stages relevant to this study (MIS 1-5). **c.** North Atlantic marine record (MIS 1-5).

Figure 25. Sea-level curve (solid black line) and glacioisostasy curve (dashed black line) compared with $\delta^{18}\text{O}$ data for the last glacial/interglacial cycle (MIS 5-2). Colored polygons point out periods within MIS5 (blue/purple) and MIS3 (green) where relative sea level extended above the Virginia coastal plain (adapted from Scott et al., 2010).

Figure 26. Map showing interpreted extent of paleoenvironments throughout the study area during MIS 5c and 5a.

Figure 27. Modified figure from Pico et al. (2017) depicting a compilation of sea-level indicators from various studies done in North Carolina and Virginia. Upward pointing triangles represent lower bounding marine markers and downward pointing triangles signify upperbounding terrestrial markers. Open triangles represent data from this study. The upper bound marker represents the interpreted upper limit of MIS3 age deposits.

Figure 28. Map showing interpreted extent of paleoenvironments throughout the study area during early MIS 3.

Figure 29. GPR profile along the southern shoreline of the Albemarle Sound, south of the Roanoke River mouth. Geoprobe core SAS20-GP3 is superimposed on this profile where it was collected. GP3 recovers a fining upward sequence representing a succession of paleoenvironments during MIS 3 (Deposited as DS-3).

Figure 30. Map showing interpreted extent of paleoenvironments throughout the study area during middle MIS 3.

Figure 31. Seismic profile along the northern shore of the Albemarle Sound west of the Yeopim River. Vibracore NAS20-VC3 is superimposed on this profile where it was collected. VC3 shows a coarsening upward lithology.

Figure 32. Seismic profile along the southern shore of the Albemarle Sound. Geoprobe SAS20-VC1 is superimposed on this profile where it was collected. GP1 penetrates RS1, the subaerial unconformity forming the boundary between MIS 5a (DS-2) and MIS 3 (DS-3).

Figure 33. Map showing interpreted extent of paleoenvironments throughout the study area during late MIS 3.

Figure 34. Bathymetry map (m) of the Wadden Sea along the northern shoreline of the Netherlands. Map is adapted from Scheel (2012)

DEFINING THE STRATIGRAPHIC AND PALEOENVIRONMENTAL RECORD OF RAPID SEA-LEVEL RISE DURING THE LATE PLEISTOCENE TO HOLOCENE IN THE ALBEMARLE SOUND REGION OF NORTH CAROLINA

1. Introduction

The relationship between oceanic and geologic processes in coastal environments is dynamic and complex. As a result, the geomorphology associated with coastal regions is also susceptible to a great deal of change over time. The fluctuating levels of accommodation space associated with sea-level rise and fall produce a geologic record cataloging the dynamic interactions between coastal processes and adjacent mainland areas (Miall et al., 1995; Catuneanu, 2006). Such a record is preserved within the stratigraphy of North Carolina's coastal system. The Quaternary geologic record, specifically, has been studied here by numerous researchers (e.g., Riggs et al., 1996; Mallinson et al., 2005, 2008, 2010, 2018; Corbett et al., 2007; Parham et al., 2007; Culver et al., 2007, 2011, 2016; Parham et al., 2013; Kopp et al., 2015; Zaremba et al., 2016). However, there remain numerous gaps in the understanding of morphodynamic and paleoenvironmental response to Quaternary sea-level changes.

The Albemarle-Pamlico estuaries of North Carolina are one of many estuarine systems dominating the present Atlantic coastal plain of North America (Dame et al., 2000; Corbett et al., 2007). A barrier island system, the North Carolina Outer Banks, constrains the eastern margin of these estuaries and acts as a buffer from oceanic processes, controlling the hydraulic connectivity between these environments and dampening the effect of tides. Thus, North Carolina's estuaries are predominantly micro-tidal and wave dominated (Mallinson et al., 2008, 2018). However, relative sea level (RSL) on the coast is forecast to increase over one meter during the next century in response to increases in global sea level related to ice sheet melting and thermal expansion of seawater (Kopp et al., 2015; IPCC, 2021). In combination with glacio-isostatic

adjustment, storm activity, and antecedent topography, North Carolina's coastal system is extremely susceptible to inundation (Riggs et al. 1996; Zaremba et al., 2016). Sea-level rise has proven to increase erosion of coastal geomorphology, specifically that of barrier islands, affecting the hydrologic characteristics (salinity distribution and hydrologic stratification) within adjacent estuarine systems (Scavia et al., 2002; Chua and Xu, 2014; Mulligan et al., 2019). The inevitability of regional sea-level rise along coastal North Carolina, accelerating from a global average rate of 1.7 mm/yr during the twentieth century to 3.4 mm/y currently (Kemp et al., 2009; IPCC 2021), makes it vitally important to understand the morphodynamic responses of this area to regional transgression.

The last interglacial (the Eemian) and subsequent interstadial events during the late Pleistocene are represented stratigraphically and temporally in eastern North Carolina by Marine Isotope Stage (MIS) 5 (~130–80 ka) and MIS 3; ~57–29 ka) (Shackleton and Turner 1967; Volker et al., 2002; Shackleton et al. 2003; Siddall et al., 2008; Parham, 2009). These events produced episodes of RSL (relative sea level) rise possibly analogous with projected sea-level rise over the next century (Mallinson et al., 2008; Scott et al., 2010). Several studies have defined portions of the late Pleistocene stratigraphy in parts of North Carolina's coastal system (Mallinson et al., 2008, 2010; Culver et al. 2011, 2016; Parham et al., 2007, 2013; Lazar et al., 2016). However, a complete geologic framework is required if accurate predictions are to be made regarding the response of this low gradient coastal system to sea-level rise.

1.1 Objectives

The fundamental goal of this project is to identify deposits associated with MIS 5 and 3 in the shallow stratigraphy of the Albemarle Sound region and understand the changes of

depositional environments associated with the highstand conditions. This will be achieved by addressing the following objectives.

1. Define the stratigraphic surfaces of MIS3 and MIS5 deposits in the Albemarle region using geophysical methods, including ground penetrating radar and high-resolution chirp seismic surveys.
2. Collect cores at locations along surveyed geophysical transects and define lithofacies and biofacies where possible.
3. Use optically stimulated luminescence (OSL) dating techniques on cored siliciclastic sediments, combined with geophysical data to develop a chronostratigraphic framework for the Quaternary units observed in the study area, and determine regional facies correlations and changes within chronostratigraphic units.
4. Interpret paleoenvironments based on microfossil and lithofacies analysis.
5. Synthesize data to develop a geomorphic model that incorporates facies, stratigraphic surfaces and depositional environment relationships.

1.2 Study Area

The study area for this project, the Albemarle Sound trunk estuary, is a microtidal, wave energy dominated, drowned river valley estuary in northeastern North Carolina (Riggs et al., 1992; Riggs et al., 1996; Mallinson et al., 2005). Today, seven major tributaries including the Chowan and Roanoke rivers (Figure 1) discharge water containing sediment composed of sand, and organic rich muds, into the 7,540 km² Albemarle basin, of which the Roanoke River constitutes ~55% of the Albemarle freshwater influx (Moody et al., 1986; Riggs et al., 1996).

1.2.1 Geologic Setting

The Albemarle Embayment, a structural low occupied by the Albemarle Sound (Figure 1), contains a ~90 m thick sedimentary wedge representing deposition and erosion associated

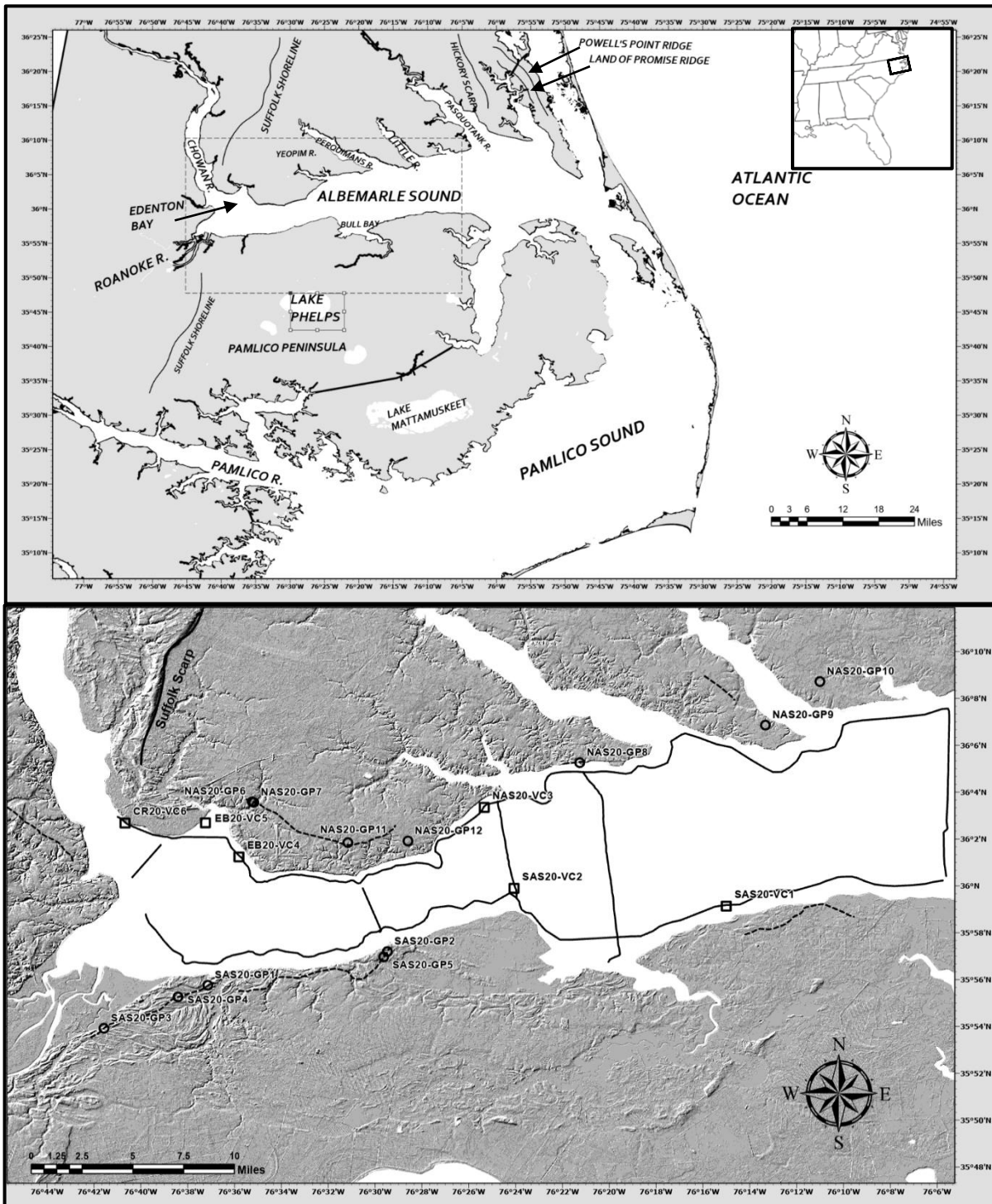


Figure 1. Maps defining the study area location. **A.** Regional map of eastern North Carolina, defining major water bodies and structural features discussed in the study. The figure includes an inset map of the southeastern United States with the regional map outlined in black. **B.** LiDAR map of study area including core locations and geophysical survey lines.

with ~15 regional cycles of Quaternary sea-level fluctuations (Riggs et al. 1996; Mallinson et al., 2005; 2010; Wehmiller et al., 2010; Parham et al., 2013; Culver et al., 2016). Late Pleistocene and Holocene units were deposited in the paleo-Roanoke River valley (PRVC), a paleo-valley, incised into early Pleistocene strata establishing a subaerial unconformity during lowstand conditions of the Last Glacial Maximum (LGM) (Riggs et al., 1996; Boss et al., 2002; Mallinson et al., 2005). Since the late Pleistocene, the geomorphologic and geologic characteristics of the Albemarle Sound have evolved substantially. Following the MIS 6-5 deglaciation of Termination II, ~130 ka (Lisiecki and Raymo, 2005) and simultaneous retreat of the Laurentide Ice Sheet, subsequent subsidence of the peripheral forebulge produced a relative sea-level rise along portions of the U.S. east coast (Artyushkov, 1967; Milne and Mitrovica 1996; Peltier, 1996; Potter and Lambeck, 2003; Mallinson et al. 2008; Scott et al., 2009). Based on conclusions drawn from Scott et al. (2009) regarding isostatic adjustment in Virginia's coastal plain, forebulge subsidence continued through MIS 5 and MIS 4 (~130 ka – 52 ka) allowing for relative sea-level rise and the deposition of highstand deposits of MIS 5 (~130 ka – 70 ka) and MIS 3 (60 ka – 40 ka) age. Mallinson et al. (2008) identified several paleoshorelines in the geomorphology of coastal North Carolina associated with these sea-level highstands, deposited and preserved as a result of the region's "relaxed isostatic position". This includes the Suffolk shoreline (a.k.a. Suffolk Scarp; Figure 1), a product of Pleistocene transgression during MIS 5, associated with the Sedgefield Member of the Tabb Formation (Peebles, 1984; Mallinson et al., 2008; Parham, 2009). East of the Suffolk Scarp (~45 km), the Hickory Shoreline Scarp and Land of Promise Ridge are interpreted by Mallinson et al. (2008) to represent peak sea-level highstand conditions corresponding with MIS 3 ages (52 ka – 45 ka) and comprise the Poquoson Member of the Tabb Formation.

1.2.2 Stratigraphic Framework

Several seismic reflections identified from seismic surveys in the Albemarle Embayment (Mallinson et al., 2005, 2010; Culver et al., 2008) define Pleistocene stratal boundaries; reflections most relevant to this study including Q50 and Q99. These reflections include the transgressive ravinement surface formed during Termination II (Q50), and the LGM subaerial unconformity approximating the Pleistocene/Holocene boundary (Q99). Late Pleistocene units of this section thin westward and are limited by the Suffolk Scarp (Mallinson et al., 2008; Parham, 2009). Incision as a result of the MIS 2 lowstand, hinders the ability to easily determine the continuity of these units from the Albemarle Embayment, west the Albemarle trunk estuary. However, based on facies models presented by Peebles et al. (1984), Parham et al. (2013) demonstrated that the lithofacies of incised paleo-valleys can be observed along modern estuarine shorelines, where a majority of the sediment core samples and geophysical surveys have been collected for this study.

2. Methods

2.1 Geophysical Analysis

In the spring and summer of 2020, subsurface geophysics data were acquired within the Albemarle Sound and on adjacent mainland areas (Figure 1). Land-based data were acquired using a GSSI SIR-3000 ground-penetrating radar (GPR) unit (Geophysical Survey System Inc.) with a 200 MHz antenna and a sampling interval of 1024 samples/scan. The antenna was towed at 3–5 mph along 13, 5– 6 mile long transects. Waypoints were recorded using a WAAS-enabled Garmin GPS unit during the survey to aid in locating core sites. GPR data collected from these transects were filtered, stacked, and gain-enhanced using Radan v.7 software and digitized with Canvas X software. Determination of vertical scales and velocities for GPR profiles were done through the Radan 7 software using Kirchoff Migration.

Imaging within the Albemarle Sound required the use of a sub-bottom profiling system for high-resolution CHIRP seismic data collection (Figure 1). These CHIRP data were collected using the RV Tomcat with survey lines running parallel to the Albemarle Sound shoreline (approximately E-W) and additional N-S transects to create a coarse grid. The acoustic data were processed and digitized using SonarWiz v.7 (Chesapeake Technology, Inc.) seismic interpretation software. Unit boundaries and geometries were interpreted and digitized for both geophysical data sets using Canvas X graphics software.

2.2 Core Collection/Analysis

Core locations (Appendix A; Figure 1) were determined based on the facies and stratigraphic surfaces interpreted from the digitized geophysical images. Collection of on-land cores, from the GPR-located sites, was done with a truck-mounted Geoprobe. In Albemarle Sound, a vibracorer was used with a 10m-long coring tube. The target depths for each core

varied based on the boundary geometry of interest, identified during the geophysical analysis, and the physical limitations of the equipment in use. Penetration of the vibracores within the Albemarle Sound was limited to a maximum depth of 3.2 m below the sediment-water interface.

A total of 16 cores were collected throughout the study area, including ten land Geoprobe cores and six vibracores collected within the sound (Table 1). All cores, except those collected for OSL dating, were split, photographed, and logged using techniques outlined in Farrell et al. (2013). Once all the cores were logged they were sampled for grain size analysis, OSL dating, and microfossil analysis.

Twenty-five sediment samples, 4 cm long segments in Geoprobe cores and 2 cm segments from vibracores, were collected. The outer ca. 1 mm of sediment in core in contact with the core liner was not used to avoid contamination related to sediment smearing. Samples were dried, weighed, disaggregated and wet-sieved over a 63 μ mesh screen to determine the sand/mud ratio. Disaggregation, required the dried samples to be placed into a 300 ml beaker, covered with DI water, and stirred with 1/8 teaspoon of sodium hexametaphosphate. Further grain-size analysis used nested sieves of 0.5 ϕ intervals (from -2 ϕ to 4 ϕ) placed in a ROTAP shaker for 15 minutes. Subsequent statistical analysis was performed using the GRADISTAT Excel worksheet program developed by Blott and Pye (2001).

2.3 OSL Dating

Quartz grains extracted from cores have been analyzed using the OSL single-aliquot regenerative-dose protocol (Murray and Wintle, 2000). OSL dating of five samples took place in the ECU Physics Department's OSL laboratory. Results from this analysis have been used to delineate Holocene and late Pleistocene strata and more specifically, outline a chronostratigraphic framework of MIS 3 and MIS 5 deposits in the Albemarle sound region.

To acquire accurate age results the samples chosen for OSL analysis were collected using opaque Geoprobe cores and cut in the OSL dark room laboratory, to protect samples from unwanted light exposure prior to testing. Samples were removed from the cores in 10 cm sections, avoiding sediment in contact with the core wall, as these grains may have been displaced during the coring process. Laboratory procedures were carried out under red light conditions, beginning with the wet sieving of all five samples to isolate the >125 microns fraction used for processing. To remove unwanted carbonates and organic material each sample is treated with 10% HCL and 29% H₂O₂ and subsequently etched for 40 mins with 48% HF to remove the quartz rind, removing portions of the quartz grain damaged by alpha radiation. Following the completion of chemical treatment, density separation is carried out using lithium polytungstate (2.75 g/cm³) separating quartz grains from heavy minerals and feldspars in each sample. Measurements for determining D_e were conducted using a Risø TL/OSL-DA-20 reader using the single regenerative dose protocol on at least 32 aliquot per sample.

Following the calculation of the D_e, uranium, ²³²Th and potassium within excess material from each sample is collected for high resolution gamma spectrometry to calculate the radiation dose rate.

2.4 Radiocarbon Analysis

In this study, radiocarbon dating is used to date organic material based on the decay of ¹⁴C in the organic matter being tested. Following the death of an organism, ¹⁴C is converted via β decay, to ¹⁴N with a half-life of 5730 years. According to Bradley (1999) through the method of radiocarbon dating, organic material can be dated to ~40 kya B.P.

Two samples were taken from separate vibracores (SAS20-VC1 and NAS-VC3) and radiocarbon dated at the National Ocean Sciences Accelerator Mass Spectrometry Facility. These

samples consist of organic plant debris from VC3 taken -4.33 meters relative to sea level (mrs) and woody material from VC1 -4.4 mrs. In the context of this study radiocarbon analyses are utilized to constrain ages corresponding to MIS 3 and earlier (< ~57 ka).

2.5 Foraminiferal Analysis

Samples for foraminiferal analyses were collected in 4 cm long segments from Geoprobe cores and 2 cm segments from vibracores. Once removed, samples were dried overnight at 50° C and subsequently weighed. To disaggregate organic material binding to the sediment, the sample was placed into a 300 ml beaker filled with ~150 ml of deionized water and 1/8 teaspoon of sodium hexametaphosphate. After the solution had sat for at least 24 hours, the sample was washed over a sieve-stack composed of 710 μ and 63 μ sieves. Prior to sieving both sieves were sprayed with methylene blue to stain any leftover sediment that may have been stuck in the mesh from prior use, so they could be distinguished. Once sieved, each sample fraction (63–710 μ and >710 μ) was placed into individual weigh boats, subsequently dried overnight, and weighed to determine the mud fraction. >710 μ fractions were placed in a capped vial and stored. Density separation following the Sodium polytungstate floating method (Munsterman and Kerstholt, 1996) was used on the 63–710 μ fraction to separate foraminifera from quartz grains..

3. Results

3.1 Geophysical Data

The two forms of geophysical data utilized in this study provide the context for the regional stratigraphy. GPR provided ~60 km of land-based data with maximum penetration depth of ~6 m. The stratigraphy interpreted from the GPR profiles collected consist of radar facies (RF) bound above and below by radar surfaces (RS). Each radar facies display distinct geophysical characteristics which are catalogued in Table 1 below. These survey lines were not continuous around the study area (Figure 1) due to time constraints. ~140 km of CHIRP data collected within the Albemarle sound provide data to ~22 m below sea level. Interpreted geophysical units and facies from these data are described below.

3.1.1 GPR

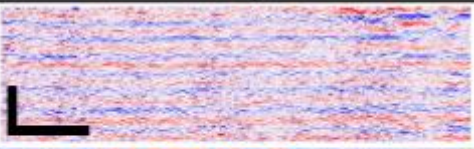
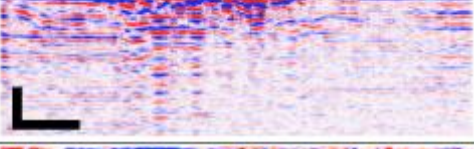
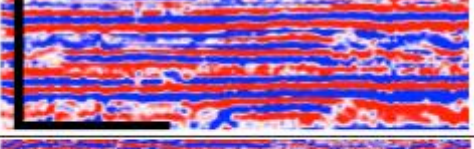
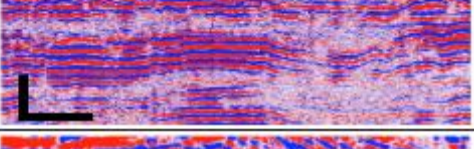
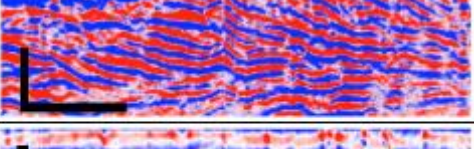
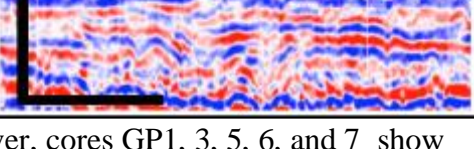
Radar Facies 1 (RF₁)

RF₁ is observed as the stratigraphically deepest unit present in the GPR data, bounded at the top by RS₁. GPR >4 m below the ground surface (mbgs) become heavily attenuated, thus making it difficult to identify a bounding bottom surface for this unit. While the GPR reflections beneath RS₁ are mostly indistinguishable in the study area, data along the northern shoreline of the sound (Figure 2) provide insight for the geophysical characteristics of this unit. Here, RF₁ consists of subhorizontal, medium amplitude reflections at 4–6 mbgs (radar facies A, Table 1).

Radar Surface 1 (RS₁)

This semicontinuous, medium to high reflection is the deepest horizon observed in the GPR data of this study. RS₁ is present along the northern and southern shores of the Albemarle Sound (Figs. 2–3). The most horizontally continuous observation of this boundary extends for ~450 m along the southern shore (Figure 3). Depths of this reflection range from 3–5.5 mbgs but, GPR

Table 1. Distinct radar facies observed in GPR data. Each facies define the characteristics of a Radar facies defined in this paper. Black scale bars are included for each radar facies example (vertical scale = 1 m and horizontal scale = 5 m).

Radar Facies	Amplitude	Radar Unit	Continuity	Geometry	Example
A	Medium	1	Semi-continuous	Sub-horizontal	
B	Low-Medium	2a	Semi-continuous	Horizontal	
C	High	3b	Continuous	Horizontal	
D	High	2a	Semi-continuous	Sub-Horizontal	
E	High	2c	Discontinuous	East-dipping	
F	Low-medium	3a	Discontinuous	Wavy	

data become heavily attenuated below ~4 m depth. However, cores GP1, 3, 5, 6, and 7 show evidence of a distinct lithologic transition from sand above (RF_1) to gravelly sand below between 3–4 mbgs.

Radar Facies 2 (RF_2)

This unit is present intermittently throughout the study area (Figs. 3–4) beneath RS_2 . RF_2 ranges in thickness from 1–3 m and is composed of three major radar facies (2a and 2c shown in Table. 1)

Radar facies 2a is the deepest facies observed in the RF₂, bounded by RS₁ at its base. This facies is continuous, high amplitude and consists of wavy to subhorizontal reflectors (radar facies D, Table 1).

Facies 2b, the upper most facies of RF₂, consists of low amplitude, horizontal reflectors and is 0–1.5 m thick (see radar facies B in Table 1). The inconsistent thickness of this facies is due to the undulating nature of RS₂ which forms the bounding surface above.

The third facies of RF₂, 2c, is a discontinuous facies, only observed in GPR data along the southern coast of the Albemarle Sound (Figure 3-4). This facies consists of high amplitude dipping clinoform reflectors (radar facies E, Table 1), with a maximum thickness of 1 m. Facies 2c is bounded on the bottom by facies 2a and above by RS₂.

Radar Surface 2 (RS₂)

RS₂ is a continuous, medium to high amplitude reflection observed in the GPR data north and south of Albemarle Sound. The depth of this horizon varies between 0–2.5 mbgs. This horizon undulates throughout the study area, incising RF₂ (Figs. 2- 4).

Radar Facies 3 (RF₃)

RF₃ is the uppermost unit observed in the GPR data. Bounded above by RS₃ and beneath by RS₂, this unit includes two distinct radar facies, 3a and 3b, shown in Table 1 (facies C and F). Facies 3a is medium to high amplitude, continuous, and displays horizontal geometry. Below C, radar facies F is low to medium amplitude, semicontinuous, subhorizontal consisting of wavy reflectors (Table 1) with a thickness of (0–0.8 m). Based on evidence in SAS20-GP1, SAS20-GP4, SAS20-GP5, NAS20-GP6, the lithologic composition of facies 3a is interpreted as mud/sandy peat. This facies fills the undulating paleochannels defined by GPR reflection, RS₂ (Figure 3). The reflection separating these two facies is discontinuous and medium amplitude,

occurring at a relatively consistent depth of 0–2.5 mbgs. This reflection is present along the southern and northern shores of Albemarle Sound (Figs. 2–4). Cores SAS20-GP1, SAS20-GP4, and SAS20-GP5 penetrate this reflection along the southern shoreline GPR line (Figs. 2–4).

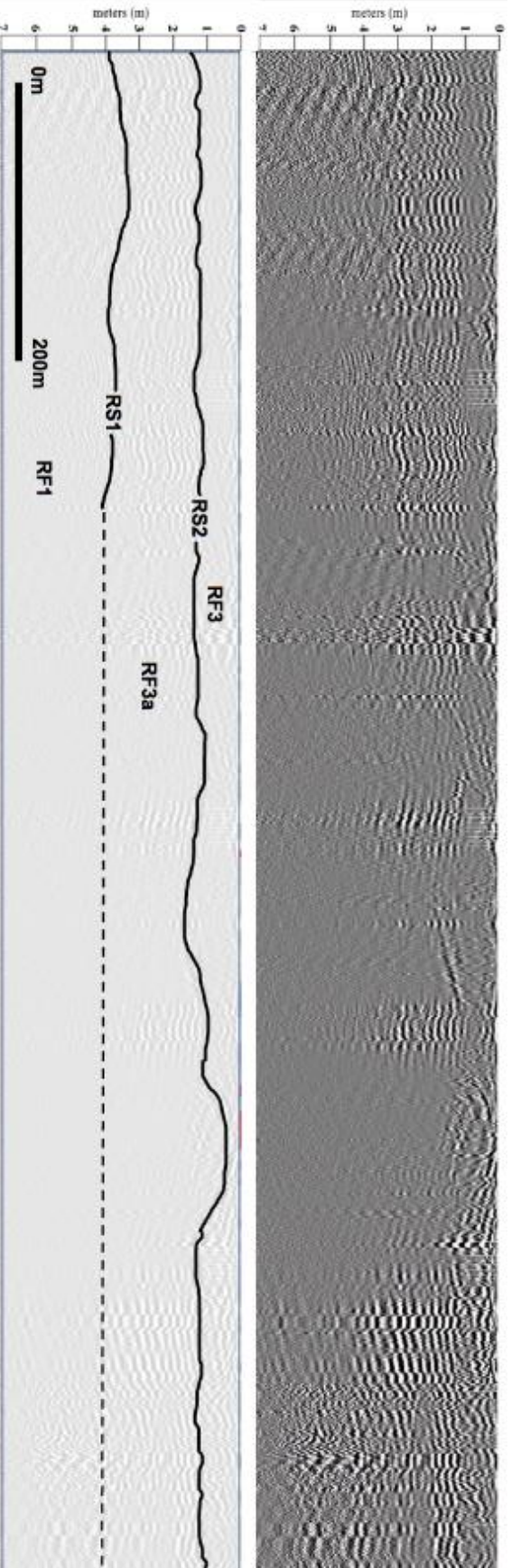
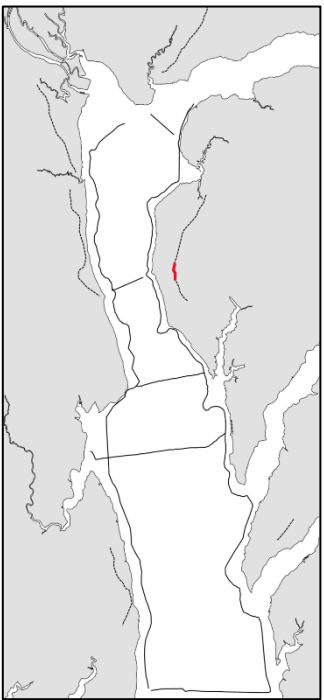


Figure 2. Ground penetrating radar profile along the northern shoreline of the Albemarle Sound, east of Edenton, NC. **A)** Processed GPR profile, displaying signal attenuation towards the right side of the profile. **B)** Radar facies defined and horizons are outlined in black.



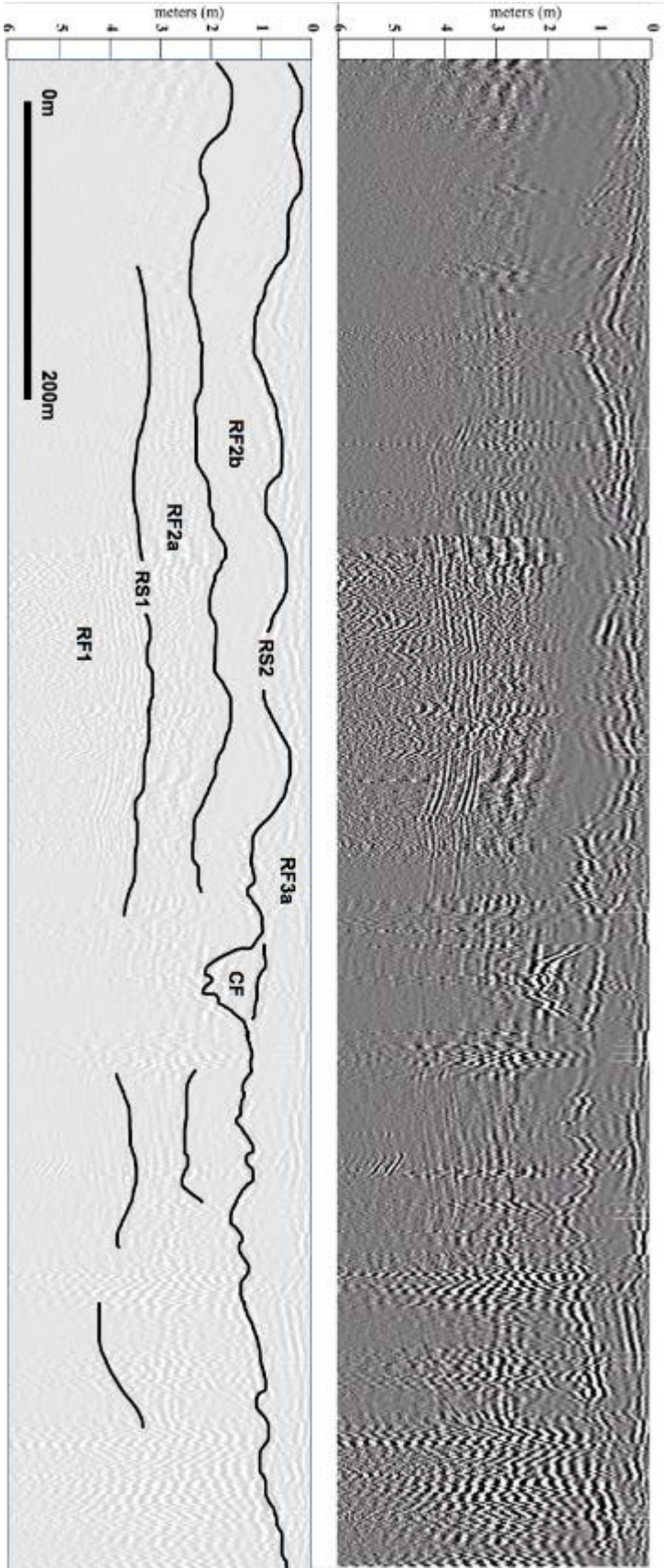
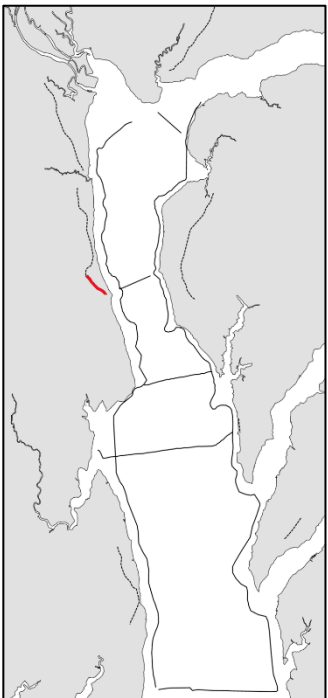


Figure 3. Ground penetrating radar profile collected along the southern coast of the Albemarle Sound, southeast of the mouth of the Roanoke River. A) Processed GPR profile. B) Defined GPR facies and horizons. C) These profiles were collected along the *Mackey's rd.* 1 GPR transect defined in this inset map.



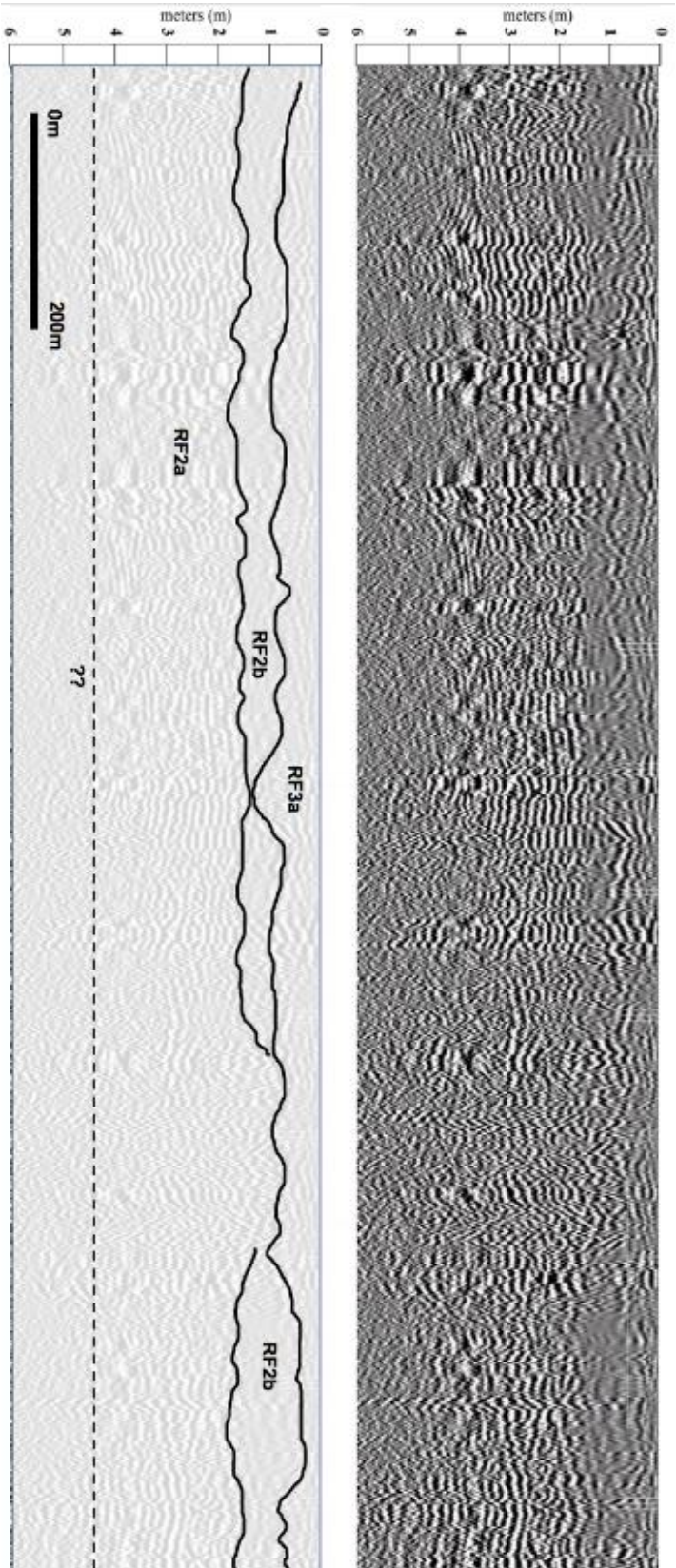
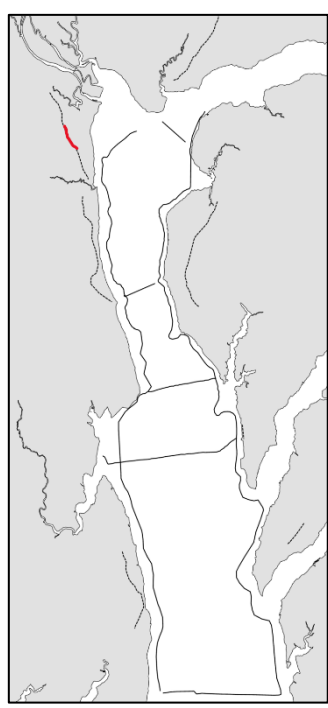


Figure 4. Ground penetrating radar profile collected along the southern coast of the Albemarle Sound, southeast of the mouth of the Roanoke River. A) Processed GPR profile. B) Defined GPR facies and horizons. C) These profiles were collected along the *Mackey's rd.* 1 GPR transect defined in this inset map.



An abrupt transition is observed in these cores from mud (GP1 and GP4) or peat (GP5 and GP6) lithofacies (facies 3a) below to medium to fine sand above (facies 3b). This boundary marks the upper limit to multiple paleochannel fills (Figure 3).

Radar Surface 3 (RS₃)

The ground surface in all GPR profiles is defined by a high amplitude, horizontal, and continuous reflection, RS₃.

3.1.2 CHIRP

Seismic Stratigraphic Unit 0 (SSU0)

SSU0 is the basal unit observed in the seismic data. The unit is bounded on top by SH₁, however the unit itself does not display any distinct reflections. With no distinguishable bottom bounding horizon, an estimated thickness for SSU0 is unattainable based on the seismic data.

Seismic Horizon 1 (SH₁)

SH₁ is a discontinuous, medium to high amplitude reflection observed west of the Yeopim River (Figure 5) and along the crossing line in Figure 6 at depths of -8 – -12 mrsImrsl. SH₁ is attenuated by gas crossing the mouth of the Yeopim River. Along the southern shoreline of the sound, east of Bull Bay, (Figure 7) SH₁ is observed at -6 mrsImrsl. The reflection is discontinuous in this region and thus is difficult to distinguish anywhere else in the CHIRP data. However, lithologic evidence from SAS20-VC1 present a transition at ~-6 mrsImrsl (Appendix D) from mud facies below to muddy sand above. This is interpreted as the transition from SSU1 up core to SSU2.

Seismic stratigraphic unit 1 (SSU1)

Seismic stratigraphic unit 1 consists of medium to high amplitude, discontinuous, subhorizontal reflections, incised heavily by SH₂ throughout the study area (Figure 5–9). SSU1

is bounded above by SH₂ only along the northern shore west of the Yeopim River, where SSU2 is observed above (Figure 5). Here, SSU1 is present with a maximum thickness of ~7 m, thinning eastward until the mouth of the Yeopim River and south towards the center of the Albemarle Sound (Figure 6) where in both instances it pinches out.

Seismic Horizon 2 (SH₂)

SH₂ is characterized by low to medium amplitude and discontinuous reflections and occurs -3 – -8 mrs/mrsl (Figure 5–6 and 8). Along the northern shoreline of the sound, west of the mouth of the Yeopim River, underlies a unit of highly reflective clinoforms (SSU2) (Figure 5). Moving east SH₂ fluctuates in depth between 1.5 – 10 mbsf until the signal becomes indistinguishable at the mouth of the Yeopim River.

Seismic stratigraphic Unit 2 (SSU2)

Seismic stratigraphic unit 2 is a medium to high amplitude, discontinuous unit composed of gently to steeply dipping (10–20°) clinoforms. SSU2 is only observed along the northern shoreline of Albemarle Sound, west of Yeopim River (Figure 6). Here, SSU2 is partially incised by SH₄ and bounded by SH₂ at the base. Thickness along this transect varies from 1–10 m. This unit terminates against SH₄ west of the crossing line displayed figure 7.

Seismic Horizon 3 (SH₃)

SH₃ is a semicontinuous medium to high amplitude reflection present throughout the study area. This reflection defines the upper boundary of paleochannel fills observed intermittently along the northern and southern coasts of the Sound, with a depth range fairly consistent at <1– 3 mbsf. Based on evidence from cores SAS-VC1 and SAS20-VC2, SH₃ marks a lithologic transition from sand above, to mud below, interpreted to represent the transition from SSU2 to SSU3.

Seismic Stratigraphic Unit 3 (SSU3)

Seismic stratigraphic unit 3 is composed of low amplitude, discontinuous, subhorizontal reflections and underlies SSU4, separated by SH₄ above (Figure 8). SSU3 is composed of fine mud based on lithofacies observed in SAS20-VC1 and SAS20VC2. Thickness of this unit varies drastically between 3 m, in the center of the Sound, and 0 m as it frequently terminated by the overlying seismic unit.

Seismic Horizon 4 (SH₄)

SH₄ is a subaerial unconformity (SU), characterized as a continuous reflection defining paleovalleys and paleochannels within Albemarle Sound. Depth of the SH₃ reflection varies significantly due to its undulating nature. When observed in E-W survey transects along the northern and southern shoreline SH₃ occurs 0.5 – 3 mbsf (Figure 6 and 9). Approaching the center of the Sound the reflection deepens (5 – 6 mbsf) and becomes slightly segmented due to attenuation from gas pockets in incised valleys (Figure 9). This reflection often amalgamates with SH₃ along E-W transects, at which point SH₄ is observed to come within 1 m of the sediment/water interface (Figure 7). Based on lithologic evidence from vibracore SAS20-VC1, this boundary represents an abrupt transition from coarse sand below to mud with a clayey texture above; a similar transition to those observed in land cores GP1 and 3-8.

Seismic Stratigraphic unit 4 (SSU4)

Seismic stratigraphic unit 4 is the uppermost unit observed in the seismic data, bounded by the sediment water interface above and SH₄ below. This unit consists of medium – high amplitude and horizontal reflections. Lithologic evidence from vibracores SAS20- VC1, SAS20-VC2, EB20-VC4, and NAS20-VC3 suggests this unit is composed of sand with modern bivalve shell fragments present in SAS20-VC2.

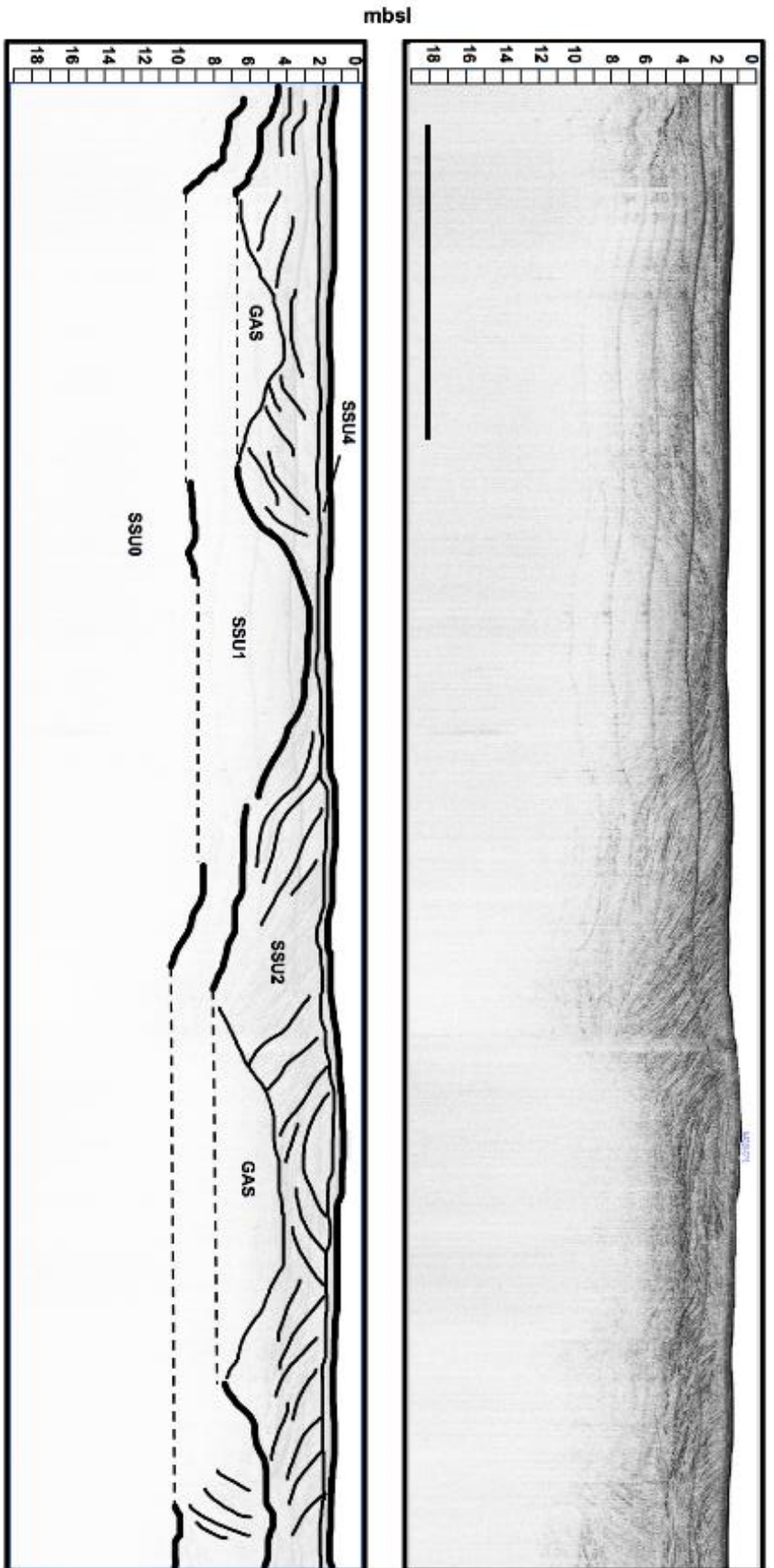


Figure 5. Seismic profile along the north shore of the Albemarle sound west of the Yeopim River. Major seismic horizons including SSU1, SSU2, and SSU4. Dipping cliniforms also outlined within SSU2. C) Location of the seismic profile outlined in red.

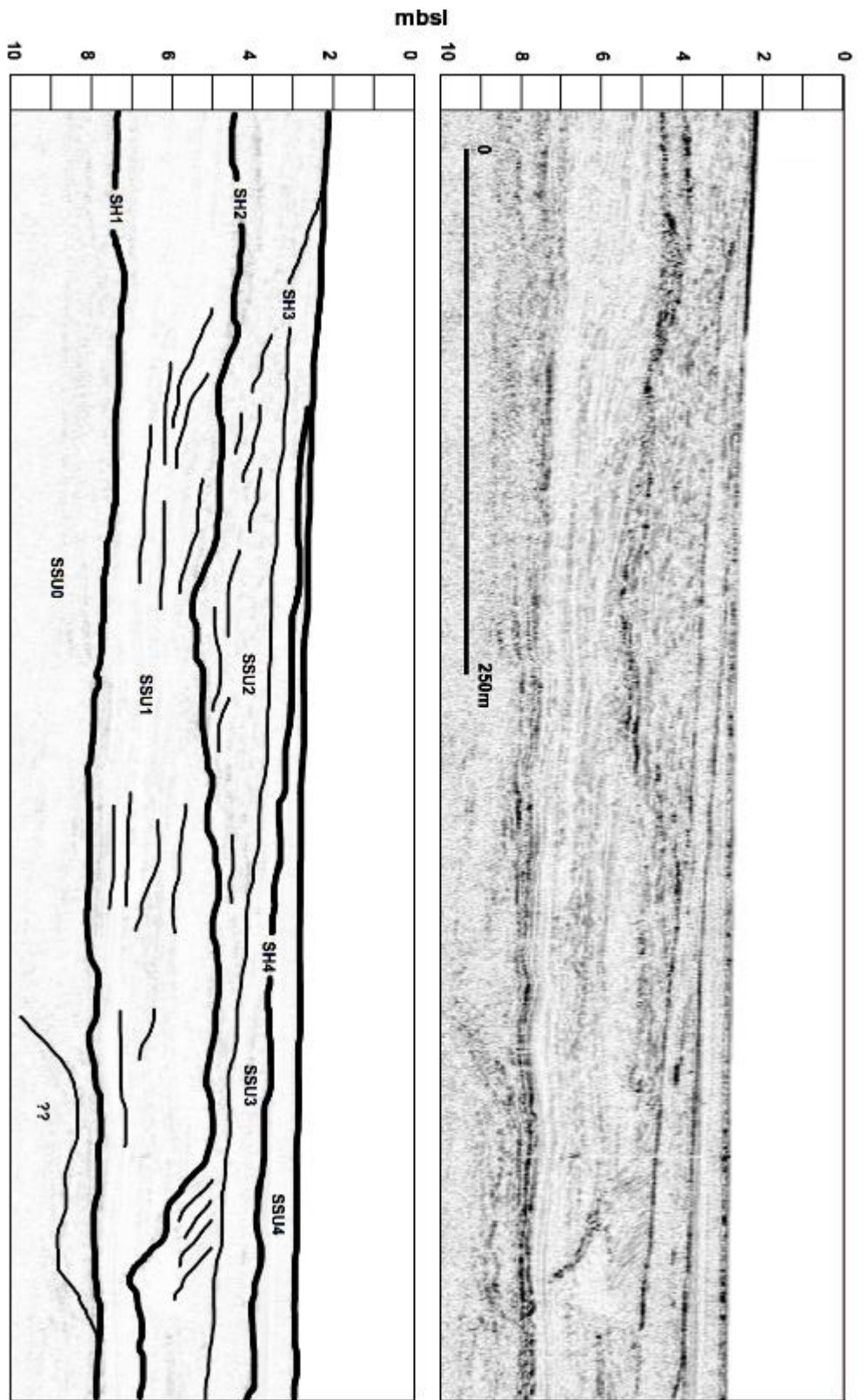
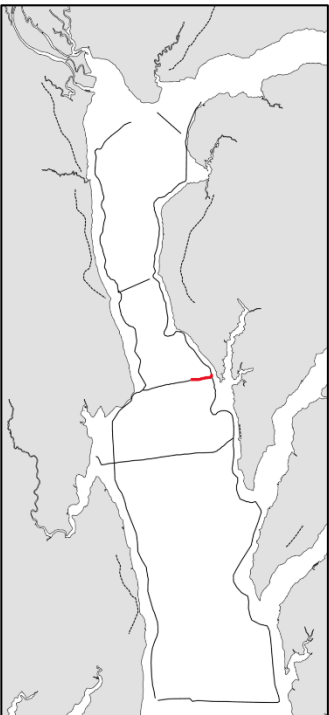


Figure 6. CHIRP seismic crossing line, extending north to south towards the center of the sound. Defined in the inset map, this profile is the eastern most crossing line.



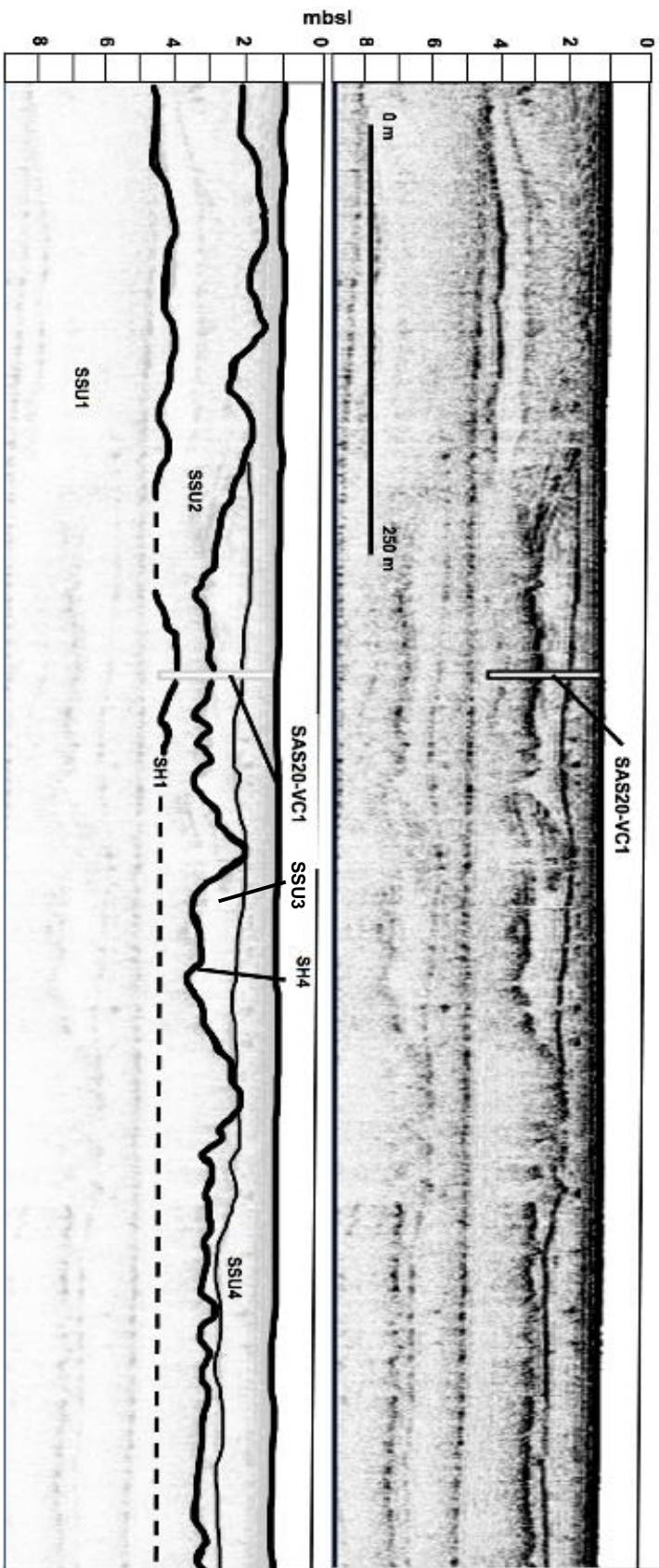
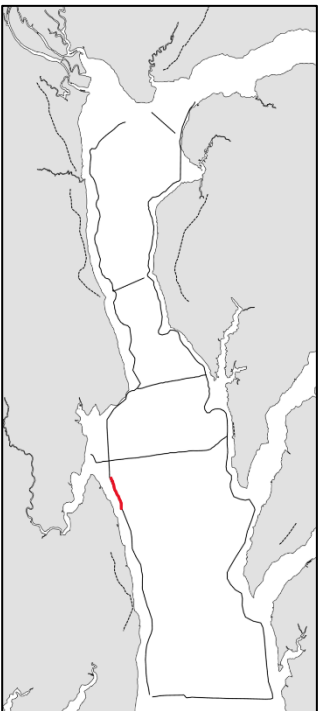


Figure 7. CHIRP seismic profile along the southern coast of the Albatrarre sound, outlined in the inset map. Processed seismic profile with water column removed and core SAS20-VC1 marked. Seismic horizons defined as SH.



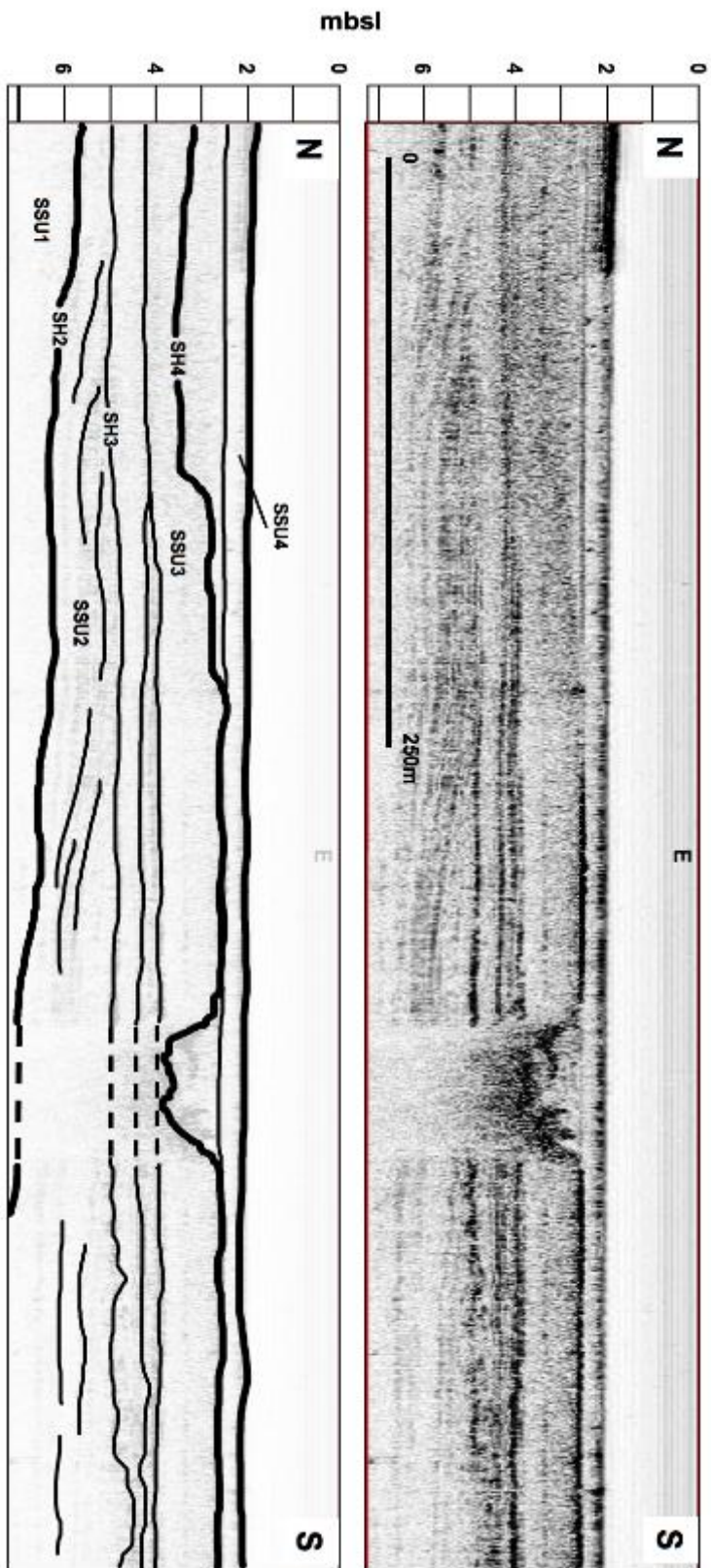
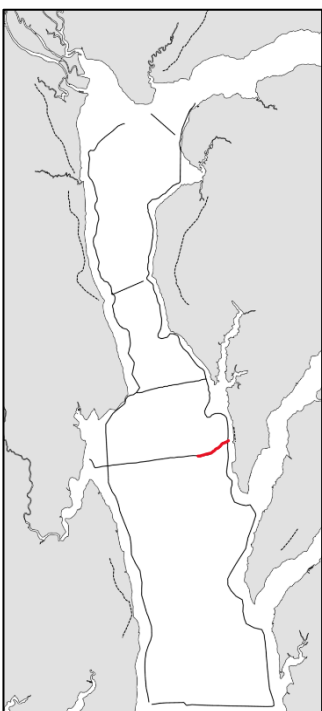


Figure 8. CHIRP seismic crossing line, extending north to south towards the center of the sound. Signal attenuation present beneath the outlined paleochannel.



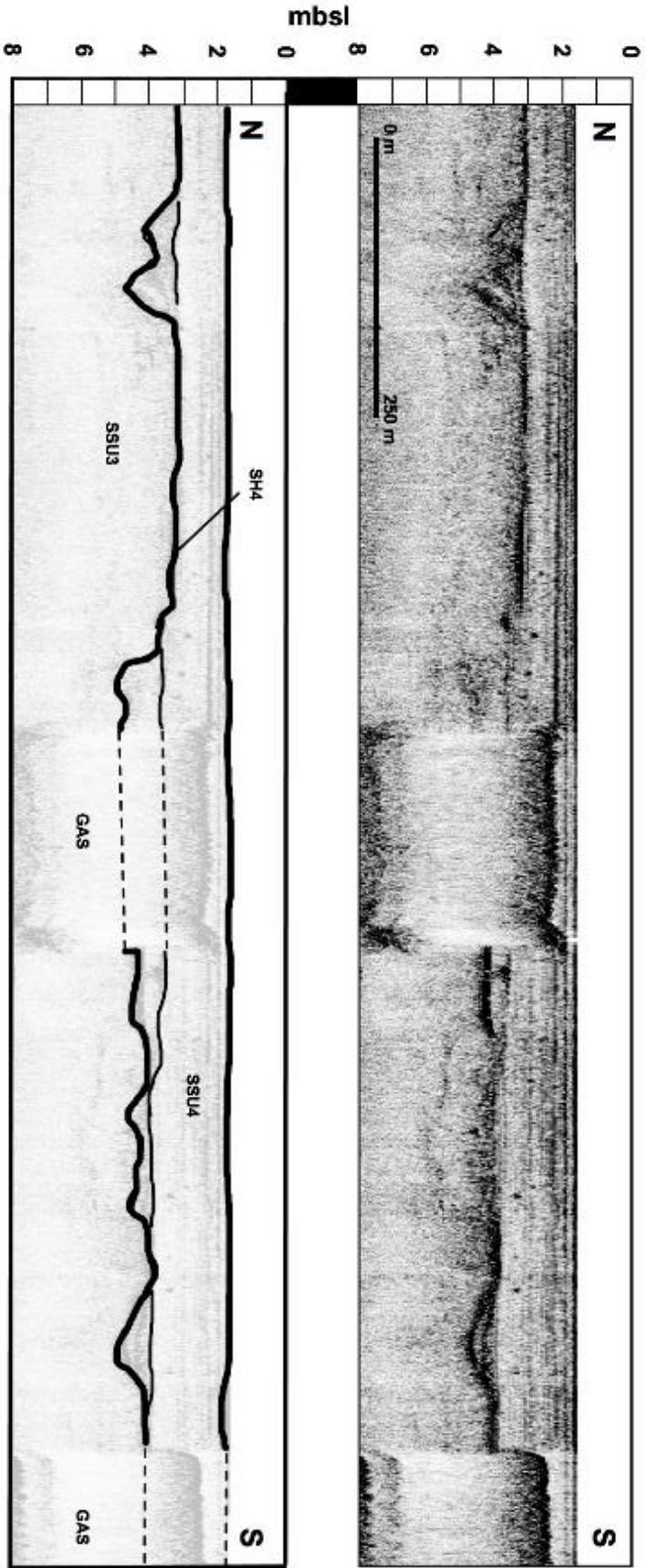
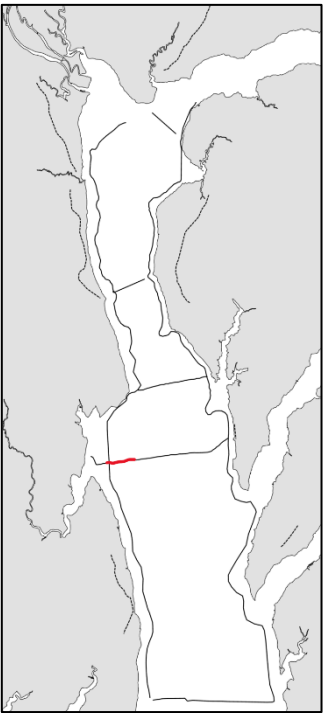


Figure 9. CHIRP seismic N-S profile collected within the Albemarle sound, ~5 km north of Bull Bay.



3.2 Lithofacies

Distinction of lithofacies are based on the visual descriptions from cores (Geoprobe and vibracores) and grain size analysis of 24 sediment samples (Appendix B). Lithofacies are categorized based on lithofacies codes described by Farrell et al. (2013). The characteristics of lithofacies described in this study are summarized in Table 2. The sand component in all lithofacies is dominated by quartz grains. Feldspar grains were not recognized in these lithofacies, however contamination of OSL sample 5 suggests the presence of feldspars in the sand lithofacies of core NAS20-GP10. Heavy minerals (magnetite) are present intermittently in all lithofacies (0-20%) with the exception of the mud lithofacies.

Sand - (S)

The sand facies is light brown/tan to gray present in all cores except NAS20-GP6. Features include occasional flaser bedding and lenses of plant debris. Normal graded bedding of sand is present in SSU3 of Geoprobe cores NAS20- GP10, NAS20-GP11, NAS20-GP12, SAS20-GP4, and SAS20-GP5. This facies exhibits reverse grading in SSU3 of SAS20-GP2 and massive bedding in SSU1 from SAS20-VC2 and SSU4 from EB20-VC4. The composition is entirely sand except where flaser bedding or burrowing are present. The minerology of this lithofacies dominated by quartz grains with 10 – 20 % heavy minerals. Burrows and flaser bedding in sand lithofacies contain silt while those observed in vibracores (SAS20-VC2 and SAS20-VC1) are mostly sand filled. Organics include plant fragments and roots (roots are only found in Geoprobe cores). Roots are modern and are not found deeper than 6 cm bs (below surface) in any core.

Slightly gravelly sand - (g)S

Table 2. List of lithofacies and their characteristics

Lithofacies	Sedimentary Description	Sedimentary Features	Organic material (%)	Bioturbation (%)
Sand (S)	Reddish brown; brown; tan; gray	Massive;	Geoprobe <40%	<5%
	Moderately - well sorted	Organic lens Plant debris and burrowing Flaser bedding	Vibracore <20%	
Muddy Sand (mS)	Reddish brown; dark brown	Sand filled burrows common	<20%	30-40%
	Moderately - well sorted	Occasional sand filled burrowing Flaser bedding common Frequently oxidized		
Slightly Gravelly Sand (g)S	Light brown; gray	Occasional plant debris	<20%	None
	Moderately sorted			
Slightly Muddy Sand (m)S	Orange; reddish brown	Flaser bedding	Geoprobe <30%	40-50%
	Dark-light brown (vibracore)	Mud filled burrowing Sand filled burrows (vibracore)	Vibracore <5%	
Laminated Sand Slam	Light brown; tan; gray	Laminations of heavy minerals	<5%	Geoprobe <5%
	Well sorted	Laminations occasionally discontinuous Occasionally bioturbated		Vibracore None
Gravelly Sand gS	Dark gray; tan	Gravel commonly pebble size	Geoprobe 10%	<5%
	Poorly sorted	Occasional plant debris Large Scale shell fragments 2-3 cm (vibracore)	Vibracore None	
Mud (M)	Brown; light-dark gray	Bioturbation common	<10%	Geoprobe <5%
	Well sorted	Plant debris common Occasional lamination		Vibracore None
Sandy Mud sM	Light-dark gray; brown	Occasionally bioturbated	<20%	40%
	Moderately - poorly sorted	Convolute oxidized laminations common (Geoprobe) Flaser bedding		
Slightly Sandy Mud (s)M	Dark gray; brown	Commonly bioturbated	<10%	50%
	Moderately sorted			
Laminated Mud Mlam	Light brown; gray	Laminations oxidized and frequently subhorizontal	None	<5%
	Well sorted			
Sandy Peat sP	Dark brown	Frequently contain large (2 cm) roots	60-90%	90%
	Moderately - poorly sorted	Undifferentiated burrows Sand filled burrows		
Slightly gravelly Muddy Sand	Dark gray	Gravel mostly 1 cm diameter	None	None
	Moderately - poorly sorted			
Peat (P)	Black; dark brown	Commonly contains coarse plant debris	95%	100%
	Poorly sorted	Abundant large scale roots (3 cm) Structureless		

The slightly gravelly sand lithofacies is light brown to dark gray and occasionally contains plant debris (< %15). Slightly gravelly sand is present only in SSU2 from cores NAS20-GP6 and SAS20-GP2. In SAS20-GP2 the slightly gravelly sand lithofacies exists as part of the modern soil profile, whereas in NAS20-GP6 it marks a gradational transition from muddy sand below to gravelly sand above.

Gravelly sand - gS

The gravelly sand facies is dark gray to tan and poorly sorted. Gravel makes up 10-50% of the facies with gravel grains of pebble size (2-20 mm). These facies are observed in SSU2 from Geoprobe cores SAS20-GP1, SAS20-GP3–5, and NAS20-GP6. Lenses of detrital plant debris are present in SAS20-GP3. Gravel in SAS20-VC1 and SAS20-VC2 consists of mollusc shell fragments (2-3 cm).

Slightly gravelly muddy sand – (g)mS

Observed only in SSU1 from EB20-VC5, the slightly gravelly muddy sand lithofacies is dark gray and poorly sorted. The lithofacies is composed of <5% gravel, 10-20% mud where gravel grains are ~1 cm in diameter.

Muddy sand (Geoprobe) - mS

The muddy sand lithofacies is reddish to dark brown and is heavily oxidized in terrestrial cores and brown to dark yellow in marine cores. Bioturbation is common including sand-filled burrows, burrow laminations, and undifferentiated burrows. The muddy sand lithofacies is present in SSU1-4 from cores NAS20-VC5–6, SAS20-GP1–5, NAS20-GP6–7, and NAS20-GP9–10. Organic material includes detrital plant debris and small isolated plant fragments. Of the marine cores, organic material, composed of decomposed plant debris, is only present in EB20-VC5 (1.1–1.4 mbsf).

Slightly muddy sand – (m)S

The slightly muddy sand lithofacies is orange to reddish brown and moderately sorted. The percentage of bioturbation is fairly high (40-50%). Features include flaser bedding and organic material. Organics include modern roots (< 1.5 mbsf) in Geoprobe cores and plant fragments (1–2 cm) in vibrocores. Slightly muddy sand is recognized in SSU3 from Geoprobe cores

SAS20-GP1, SAS20-GP2, SAS20-GP5, NAS20-GP6, NAS20-GP11, and one vibracore (SAS20-VC1). The lithofacies in SAS20-VC1 is partially bioturbated (40%) by undifferentiated burrowing.

Laminated Sand – S_{lam}

The laminated sand lithofacies is light brown/tan to gray and well sorted. These lithofacies are present in SSU1, SSU3, and SSU4. Laminated sand are recovered in Geoprobe cores SAS20-GP2, SAS20-GP3, SAS20-GP5, NAS20-GP7–10, NAS20-GP12, and vibracores EB20-VC4–5 and CR20-VC6. Laminations are composed of heavy minerals and are occasionally discontinuous (SAS20-GP5 at 4.9 and 5.6 mbsf). It is common for these laminations to display a concave-down geometry in Geoprobe cores as the result of deformation from the coring process. Laminations in vibracores include wavy, inclined (10°-20°), and concave-down. Organic material is rare (<5%) and bioturbation is not observed in laminated sand lithofacies from vibracores.

Mud – M

The mud lithofacies appear brown to dark gray and well sorted. Bioturbation is common (50%) in Geoprobe cores (extensive undifferentiated burrowing) but absent in vibracores. Mud is a distinct lithofacies and can be correlated between SAS20-GP4, SAS20-GP1, and SAS20-GP5 along the southern shore of the Albemarle Sound. Similarly, mud is correlative north of the sound between NAS20-GP7-9. SAS20-VC1 and NAS20-VC3 contain the only observed mud lithofacies within the sound.

Laminated mud - M_{lam}

The laminated mud lithofacies is light brown to gray and well sorted. Laminations are composed of oxidized mud. Laminated mud is considered a subfacies of the Mud lithofacies as it is present in Geoprobe core NAS20-GP8 from SSU3.

Sandy mud – sM

The sandy mud lithofacies is gray to brown and moderately to poorly sorted, with undifferentiated burrowing common (40%). This lithofacies is present in SSU3–4 from NAS20-GP9-10, NAS20-VC3, and CR20-VC6. Sandy mud lithofacies root traces in CR20-VC6 related to heavily rooted sandy peat lithofacies above. The thickest sandy mud lithofacies is observed in vibracore, NAS20-VC3, between 0.85-1.10 mbsf and is heavily bioturbated by undifferentiated burrowing.

Slightly sandy mud – (s)M

The sandy mud lithofacies is dark gray to brown, moderately sorted, and only observed in Geoprobe cores. This lithofacies is found in SSU3 from Geoprobe cores NAS20-GP11–12. Bioturbation is common (50%) including horizontal sand-filled burrows and undifferentiated burrows. Laminations within the slightly sandy mud lithofacies are present in NAS20-GP8 between 1.22-2.06 mbsf. Geometries of these laminations include subhorizontal, concave-down (product of coring deformation), wavy, and convoluted.

Sandy peat – sP

The sandy peat lithofacies is dark brown and poorly sorted. Bioturbation, including undifferentiated burrows and tube-shaped sand filled structures, along with organic material are frequently present (90%) with 2 cm long roots, common in Geoprobe cores. Sandy peat is observed in SAS20-GP5 (1.82-2.18 mbsf), SAS20-VC1 (2.60-2.94 mbsf), and EB20-VC5 within SSU4 only. All sandy peat lithofacies are bounded by sand and muddy sand facies.

Peat - P

The peat lithofacies is black to dark brown, poorly sorted and observed only in SSU4 from EB20-VC5 (-2.5 – -3.5 mrsf). This lithofacies represents an accumulation of modern plant debris from a swamp forest near Edenton Bay. Composed entirely of coarse plant fragments including large roots (3 cm), and other woody debris. The peat is heavily bioturbated and structureless.

Slightly sandy peat – (s)P

The slightly sandy peat lithofacies is dark gray to brown, poorly sorted and only observed in SSU4 from CR20-VC6 (0.26-0.40 mbsf). This lithofacies is structureless and composed of <10% and 90% plant debris including roots and other woody debris.

3.3 Age Analysis

3.3.1 OSL Analysis

OSL ages were attained from five medium- to fine-grained sand samples collected from Geoprobe cores (Appendix E). OSL determines the length of time transpired since a mineral's last exposure to sunlight (Murray and Wintle 2000; Rhodes, 2011). Two components are required for this dating method; equivalent dose (D_e) and the dose rate which are then substituted into the following formula to attain an estimated age (ka).

$$age(ka) = \frac{D_e}{dose\ rate}$$

OSL proved accurate for constraining MIS5 and MIS3 ages in similar coastal environments in North Carolina (Mallinson, 2008; Parham et al., 2013; Lazar et al., 2016). All five samples produced Pleistocene luminescence ages ($61.6 \pm 3.8 - 93.4 \pm 5.3$ ka). Several outliers with high doses were identified when processing samples 3 and 5. Large aliquot fractions from sample 3 were produced by possible feldspar contamination, indicated by a high (<0.9) **IR** depletion (Figure 10). Two distinct dose component ranges were observed for sample 5 aliquots when

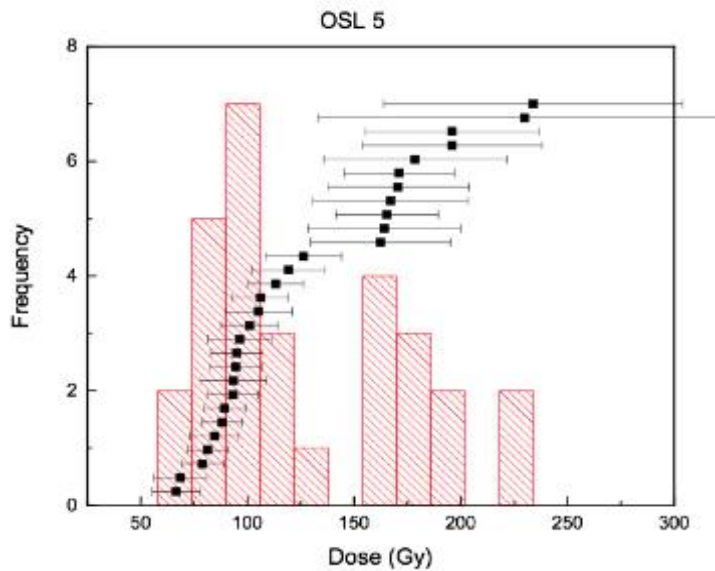


Figure 10. Dose rate plot depicting contrasting dose component ranges. Lower dose range was utilized for the calculation of the OSL 5 age.

plotting the dose rate, however the upper range doses were not included in the dose calculation. OSL ages collected from cores NAS20-GP9 and NAS20-GP10, the easternmost Geoprobe cores (Figure 1) on the northern coast of the Albemarle Sound produced MIS5a ages. However, 10 km west of NAS20-GP9, OSL 3 collected from NAS20-GP8 produced an age of 68.8 ± 5.4 ka (MIS 3 age), suggesting a major chronostratigraphic transition near the Perquimans River (Figure 1). MIS 3 ages are also observed in cores SAS20-GP1 and SAS20-GP5 collected along the southern shoreline, ~20-25 km southwest of NAS20-GP8 (Figure1).

3.3.2 Radiocarbon Analyses

Radiocarbon analysis of two samples produced ages correlative with MIS 3 and MIS 1 deposition (Appendix D). Detrital plant debris collected from NAS20-VC3 at ~ -4.33 msl provided an age of $35,600 \pm 1,300$ yr B.P. suggesting deposition during late MIS3. Woody debris sampled from SAS20-VC1 -4.4 msl produced a Holocene age of $3,830 \pm 20$ yrs B.P.

3.4 Sedimentology Data

Sedimentological analysis of 24 samples present varied results for grain size patterns throughout the cores (Table 3). For samples containing between 1-5% $<63\mu$, the mud fraction was ignored in the grain-size analysis and only sand to gravel sediment fractions were recorded (Blott and Pye, 2001). Sediments are mostly fine to very fine sand, and moderately to well sorted. Data acquired from core NAS20-GP7 sampled at 5.39-5.43 mbsf are outliers with sediment defined here as medium sand and poorly sorted. Results for skewness vary the most with results between coarse and fine skewed.

Relationships between statistical analysis and lithofacies are presented in Appendix B. Due to the exclusion of mud fractions from the grain size analysis, statistics calculated for the mud-dominated lithofacies represent the sand fraction only.

Sand-dominated lithofacies (sand, muddy sand, and slightly muddy sand) range from very well to moderately sorted with sorting (ϕ) values of 0.295-0.386 (Appendix B). These are slightly better sorted than sand in the mud-dominated lithofacies (mud, sandy mud, and slightly sandy mud) which produced sorting (ϕ) values of 0.605-0.702. Sand-dominated lithofacies (excluding slightly muddy sand due to low sample size) on average produced grain size results more coarsely skewed (0.157 ϕ) than those calculated for mud dominated lithofacies (1.07 ϕ).

3.5 Foraminifera Data

Samples collected for microfossil analysis were barren of foraminifera.

4. Discussion

4.1 Defining the Lithostratigraphy and Chronostratigraphy

The extent of observed depositional sequences (DS) is described based on correlations made between geophysical facies and their corresponding lithologies (Figure 17-22). Lateral correlations of DS are depicted in four cross sections (Figure 11-14). Each DS consists of a vertical lithostratigraphic succession, representing a sequence of paleoenvironments, which change in response to sea-level fluctuations during MIS 5 to MIS 1. Unconformities or correlative conformities form the upper and lower boundaries of each DS (Catuneanu, 2006), marking transitions into bounding depositional sequences. OSL and radiocarbon ages define the chronostratigraphic framework and provide additional evidence for lateral facies correlations. One Holocene and three Pleistocene chronostratigraphic units were interpreted from the data mentioned above, each corresponding to marine isotope stages discussed herein (Appendix B).

4.1.1 Depositional Sequence 1 (DS-1)

Age constraints for DS-1 are based on OSL samples and lithological correlations with Parham et al. (2013). DS-1 is interpreted to represent MIS 5c (~110 ka) strata, and is observed in the seismic data as SSU0 (Table 3). With no distinguishable bottom boundary present in the geophysical data for SSU0, determining the lateral extent of this seismic unit is dependent on the

Table 3. Marine isotope stages displayed with their corresponding Geophysical facies (radar and seismic) and denoted depositional sequences associated with this study.

MIS and Geophysical Facies Relationships			
Depositional Sequence/Erosional surface	Radar facies	Seismic Facies	Marine Isotope Stage
DS-4	N/A	SSU4	MIS 1
Erosional Surface	N/A	SH3+SH4	MIS 2
DS-3	RU2-4	SSU3 + SSU2	MIS 3
Erosional Surface	RH1	SH2	MIS 4
DS-2	RU1	SSU1	MIS 5a
Erosional Surface	N/A	SH1	MIS 5b
DS-1	N/A	SSU0	MIS 5c

presence of SH1 (Table 3), the upper bounding unconformity, possibly formed during MIS 5b lowstand conditions.

At the mouth of the Chowan River, ~1 km west of the Suffolk shoreline (Figure 1), core CR20-VC6 penetrated SH1 erosional surface (Figure 11) and recovered coarse sands of DS-2 at -5.7 mrs. Seismic data at this location are heavily attenuated, thus no seismic boundary is distinguishable beneath SSU0 (Figure 13). Parham et al. (2013) defines a possible MIS 5c or 5c age sequence ~10 km north of CR20-VC6, interpreted from three cores along a W-E transect (Figure 12). Along this cross section, ~0.75 km west of the Suffolk shoreline, east-dipping sand clinofolds are depicted within the MIS 5c sequence from -3 to +6 meters relative to sea level and interpreted by Parham et al. (2013) to represent seaward progradation of shoreface sands associated with the Chowan Spit complex (CSC). Eastward along this cross section, the dip of these clinofolds decreases and they are overlain by gently dipping lithofacies of muddy sand and flaser bedded sand described by Parham et al. (2013) as shallow shelf deposits. This lithologic succession is correlative to DS-1 recovered by CR20-VC6, -3 – -6 mrs (Figure 11).

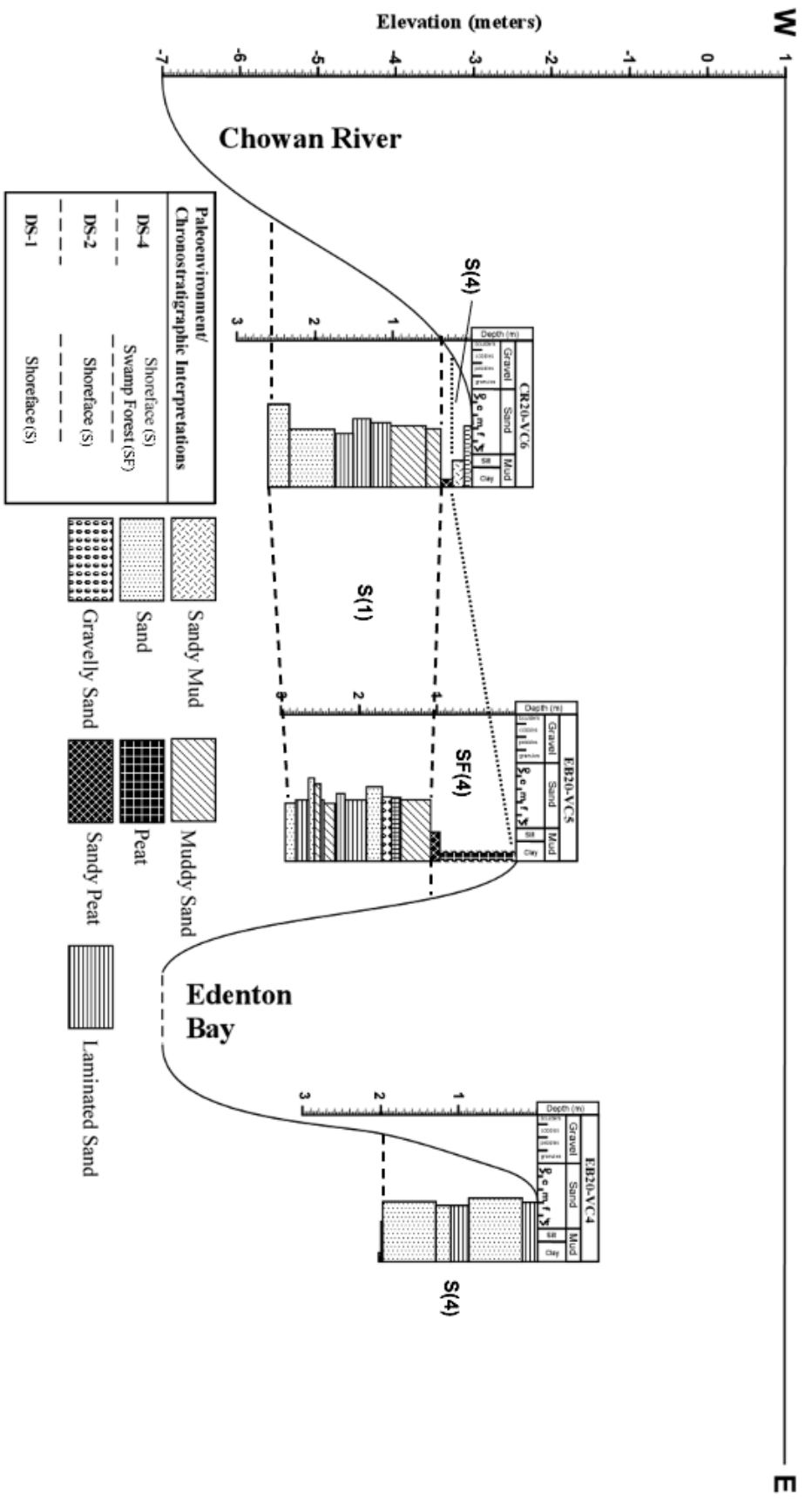


Figure 11. Cross section across the northern shoreline of the Albemarle Sound, between the Chowan river and Edenton Bay. Dashed lines define the boundaries between depositional sequences. Each paleoenvironment and their associated Depositional Sequence are defined in the cross section with a letter (corresponding to their paleoenvironment defined in the legend) followed by a number representing the Depositional Sequence. See figure 1 for core locations.

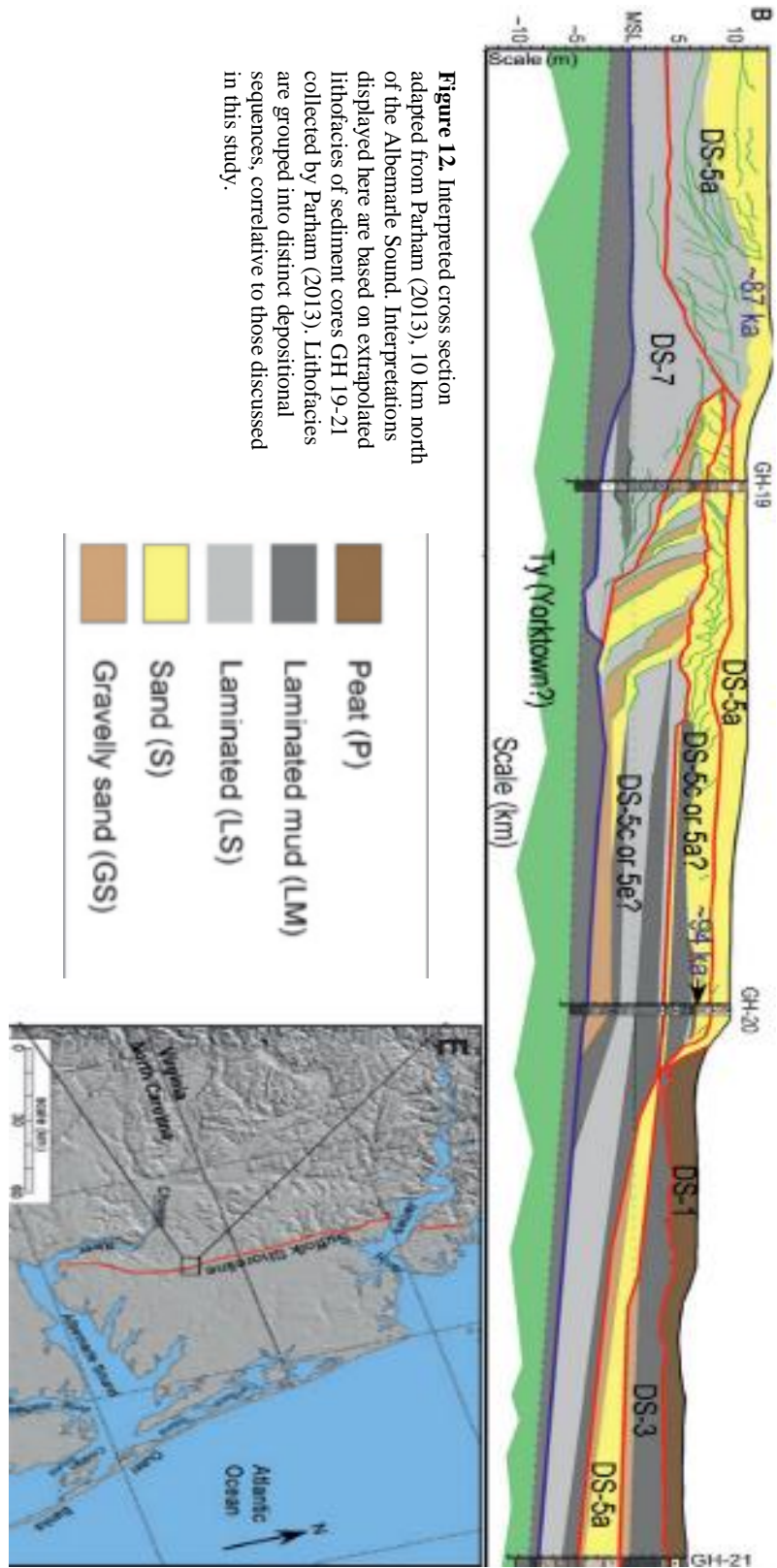
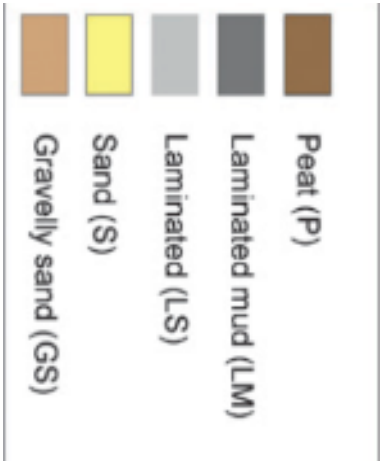


Figure 12. Interpreted cross section adapted from Parham (2013), 10 km north of the Albemarle Sound. Interpretations displayed here are based on extrapolated lithofacies of sediment cores GH 19-21 collected by Parham (2013). Lithofacies are grouped into distinct depositional sequences, correlative to those discussed in this study.



Moving east of CR20-VC6, the SH1 boundary is visible in the seismic data (Figure 13) 4 km west of the mouth of the Yeopim River, at ~ -8 mrsL. Here, SH1 incises to -13 mrsL into DS-1 (SSU0) during MIS 5d. Considering the extent of erosion here during a substage of MIS 5 it is inferred that the present Yeopim River was heavily incised during the MIS 4 glacial period (60-75 ka) (Scott et al., 2010), producing a river channel extending ≥ 4 km west of the present channel bank. Thus, subsequent depositional sequences, first being DS-3 and DS-4, fill in this extended channel of the Yeopim river (Figure 13).

Cores NAS20-GP9-10, collected on modern interfluves east of Perquimans River, penetrate burrowed sandy shoal deposits -2 to -5 mrsL with OSL samples from these deposits producing MIS 5c ages, 93.4 ± 5.3 ka and 91.8 ± 6.3 ka (Figure 14).

4.1.2 Depositional Sequence 2 (DS-2)

Above DS-1, DS-2 defines the MIS 5a age sequence present in the study area (Table 3), represented in the geophysical data as SSU1 and RF1 (Table 3). This interpretation is consistent with those made by Parham et al. (2013) north of the study area (Figure 15). East of Edenton Bay (Figure 11), medium sands found in cores VC6 with mean and mode grain sizes of 2.01 phi and 1.75 phi (Appendix B) and are correlative to shoreface deposits defined by Parham et al. (2013) along the Suffolk shoreline north of the study area (Figure 12).

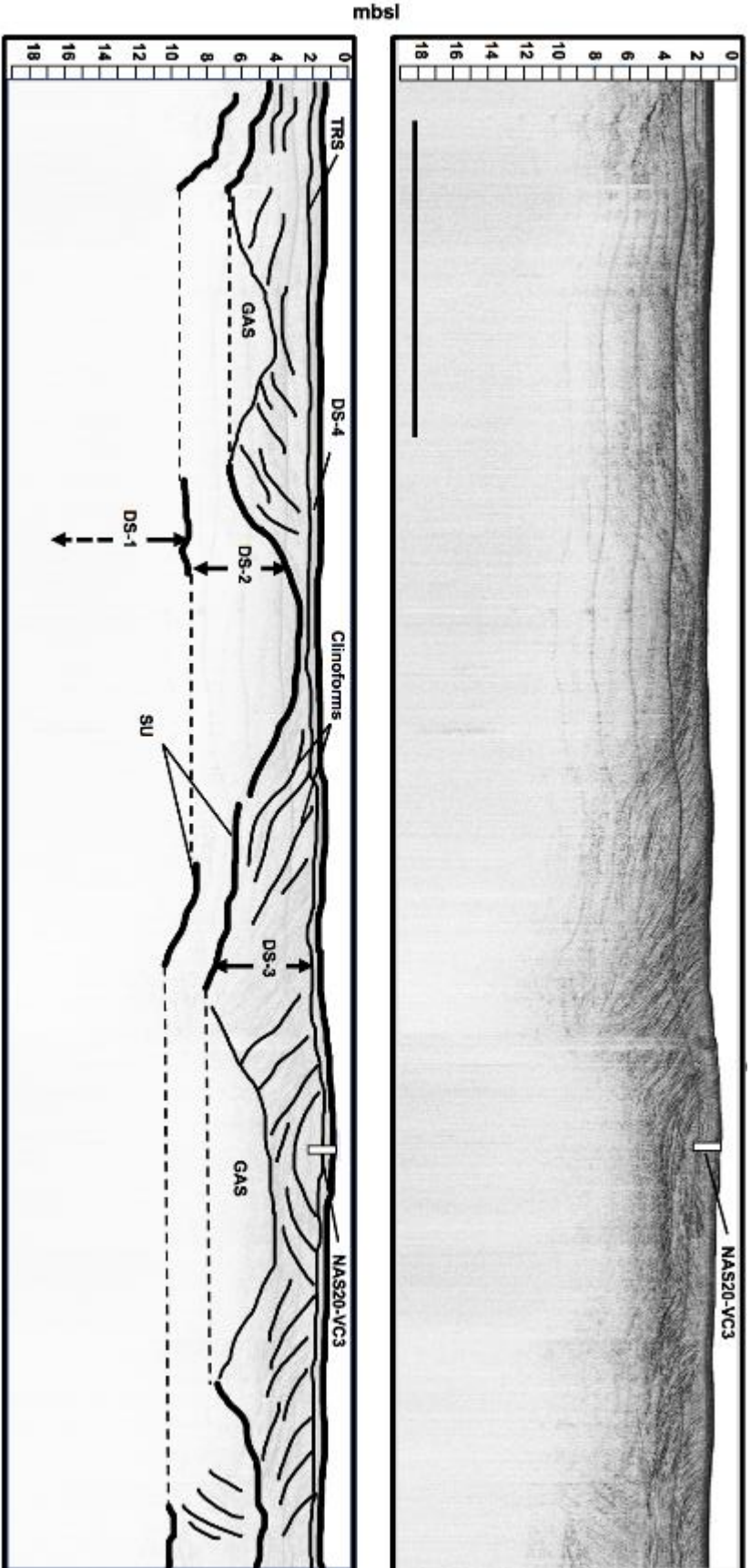
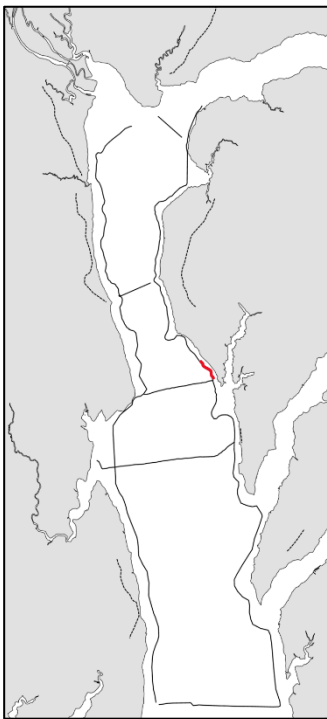


Figure 13. CHIRP seismic W-E profile. Depositional sequences are interpreted from seismic units defined previously in Figure x. Much of the data in this profile is attenuated from gas release in the subsurface.



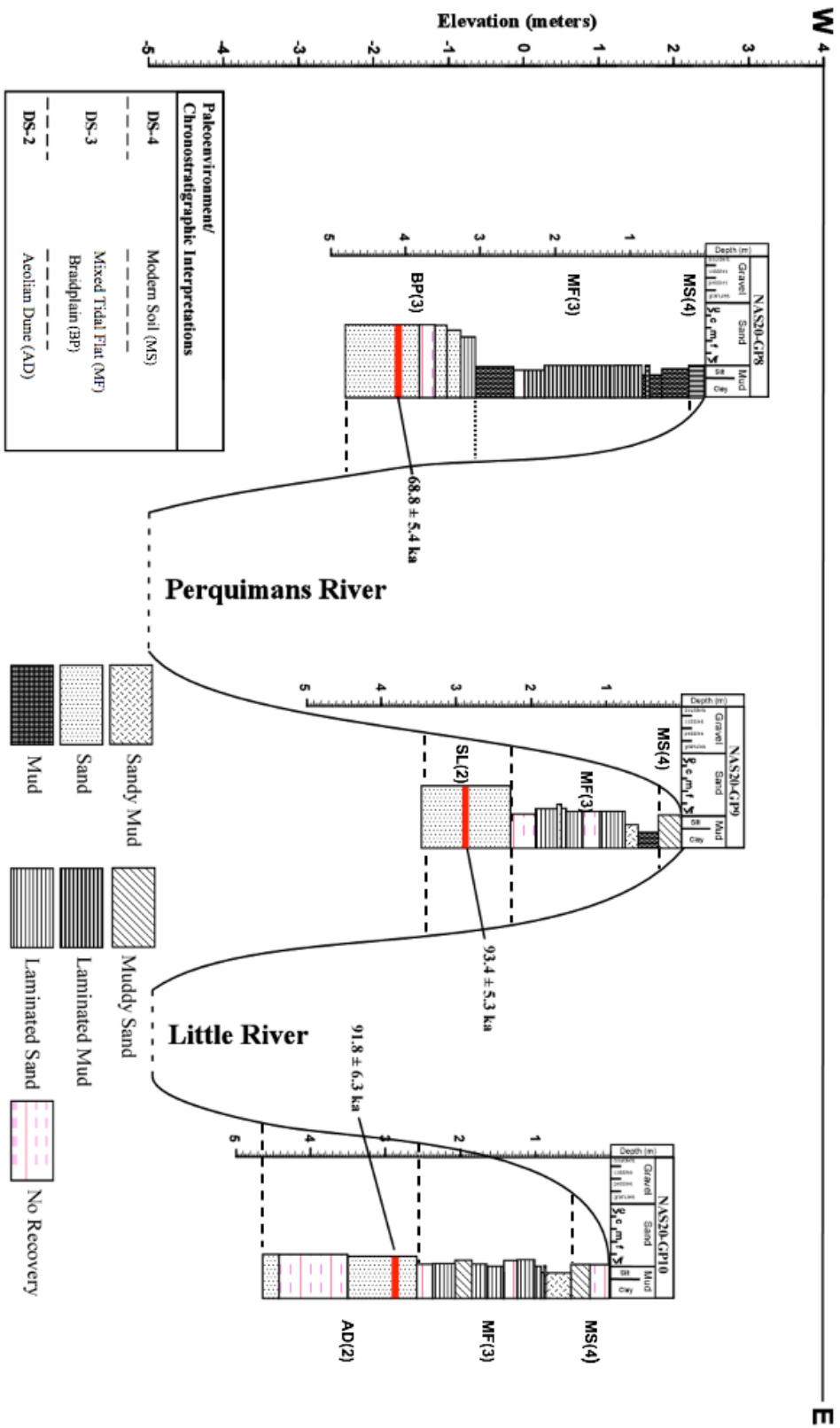


Figure 14. Cross section of the three interfluvies on the northern shoreline of the Albemarle Sound, between the Yeopim and Pasquotank rivers. Dashed lines define the boundaries between depositional sequences. Each paleoenvironment and their associated Depositional Sequence are defined in the cross section with a letter (corresponding to their paleoenvironment defined in the legend) followed by a number representing the Depositional Sequence. Red lines within cores mark OSL dated samples. See figure 1 for core locations.

Here, DS-2 is 2–2.5 m thick and incised by SH4 at -3.5 mrs. Incision of DS-2 occurs from -1 to -3.5 mrs. DS-2 is observed in the sound -3 to -5 mrs and is ~8 m thick (Figure 13). Eastward within DS-2, there is a lateral lithofacies change from heavy mineral laminated, shallow shoreface coarse sands to shelly muddy sand shallow shelf deposits < -1.5 mrs (Figure 15). The thin shelled bivalve samples observed here are identified as *Spisula solidissima raveneli* (Figure 16). Juvenile and adult *Spisula solidissima raveneli* live on the shallow Atlantic shelf at depths 8–66m below sea level (Cargnelli, 1999). This suggests deposition in a shallow shelf environment. Parham et al. (2013) defines an MIS 5c or 5a aged sequence of shelly muddy sand ~10 km north of the study area, containing *Spisula* as well and interpreted as a shallow shelf paleoenvironment. Calcareous shell material does not occur in cores NAS20-GP11 and GP6 (Figure 15), however the lithologic composition (muddy sand) remains the same as that observed in NAS20-GP12.

DS-2 thickens towards the present day Yeopim River where incision of a paleo-river (Figure 13) channel created 13 m of accommodation space during MIS 4. Filling this valley are laterally accreting tidal deposits represented by dipping clinofolds in the seismic data, which are overlain by tidal flat mud deposits shown as high amplitude wavy reflections (Figure 13

4.1.3 Depositional Sequence 3 (DS-3)

DS-3 is interpreted to represent deposits of MIS3 age, bounded below by the SH3 unconformity (Table 3). Above, DS-3 is bounded by the Holocene bay ravinement surface in the sound and by the modern land surface on the uplands, where soil processes modify the

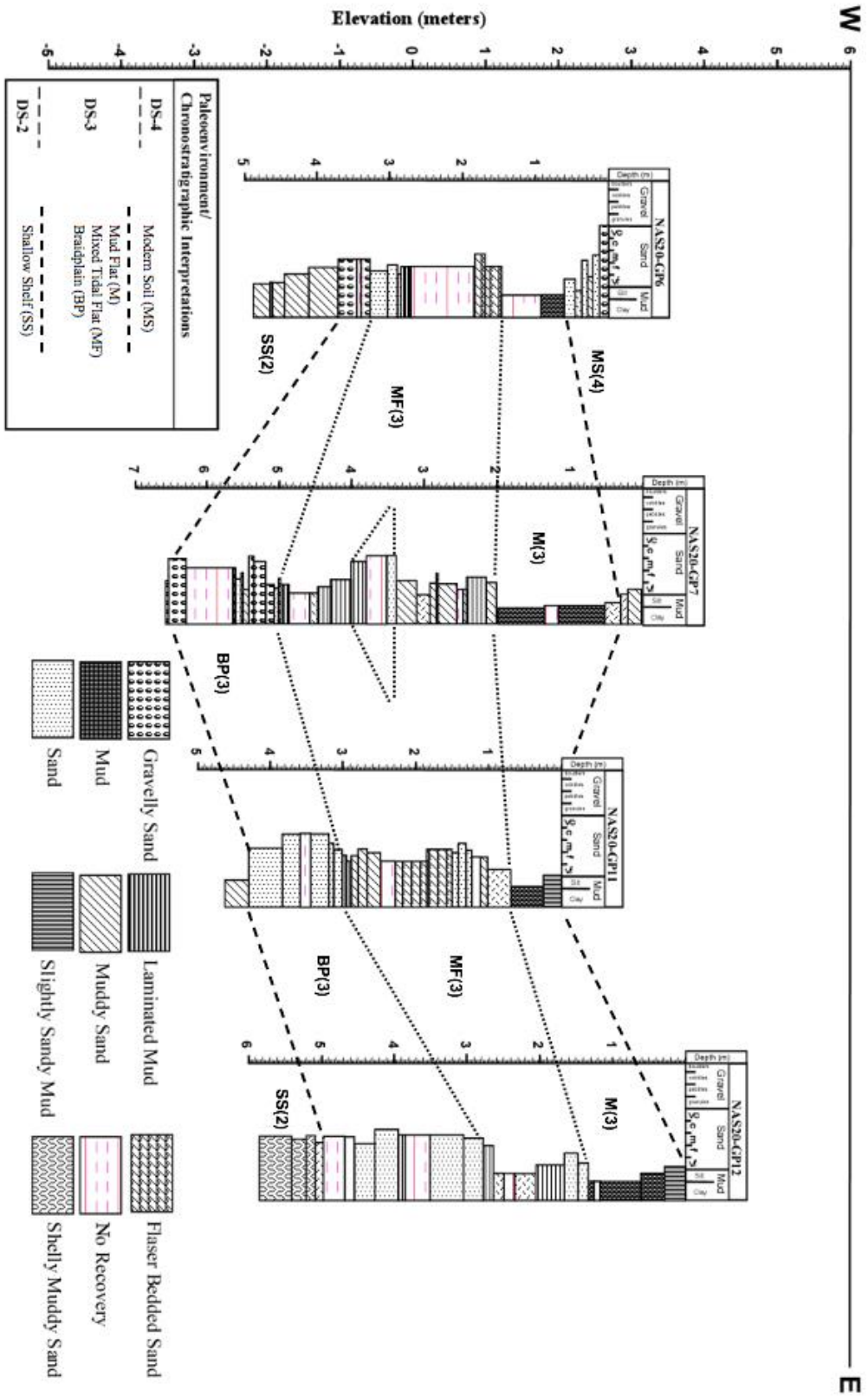


Figure 15. Cross section across the northern shoreline of the Albemarle Sound, west of the Yeopim River. Dashed lines define the boundaries between depositional sequences. Each paleoenvironment and their associated Depositional Sequence are defined in the cross section with a letter (corresponding to their paleoenvironment defined in the legend) followed by a number representing the Depositional Sequence. See figure 1 for core locations.

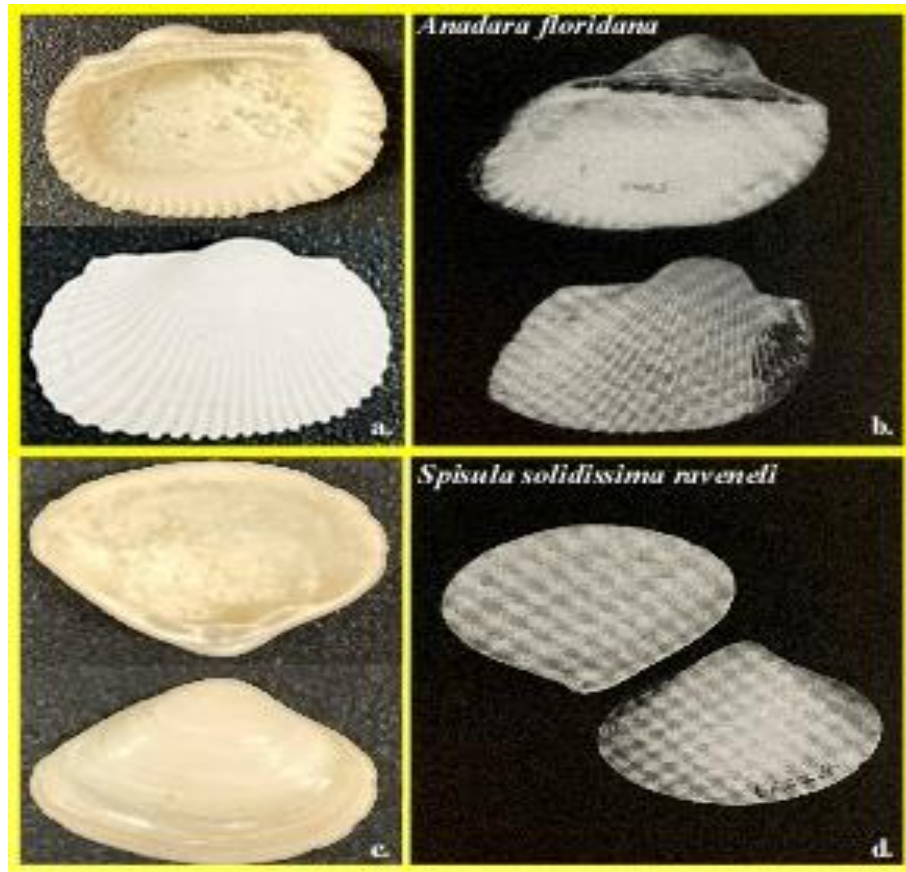


Figure 16. Images of shell material recovered from core NAS20-GP12 compared with documented shell samples from Porter and Houser, 2010. **A.** Sample of *Anadara floridana* from this study area. **B.** *Anadara floridana* identified by Porter and Houser, 2010. **C.** Sample of *Spisula solidissima raveneli* from the study area. **D.** *Spisula solidissima raveneli* identified by Porter and Houser, 2010.

sediments. This unit is best preserved in Geoprobe land cores along the southern and northern shorelines of the Albemarle Sound, where three OSL ages constrain the chronostratigraphy. Along the southeastern flank of the Roanoke River and the Albemarle Sound (Figure 17), gravelly sand deposits of a braidplain paleoenvironment, aged 61.6 ± 3.8 ka and 54.5 ± 3.1 ka are observed at the base of DS-3, ~ -2 mrsf in Geoprobe cores SAS20-GP1, SAS20-GP3, and SAS20GP-5. Lidar data support the interpretation of a braidplain environment at this location during MIS 3 (Figure 1). As seen in figure 1, the LiDAR data reveal remnants of

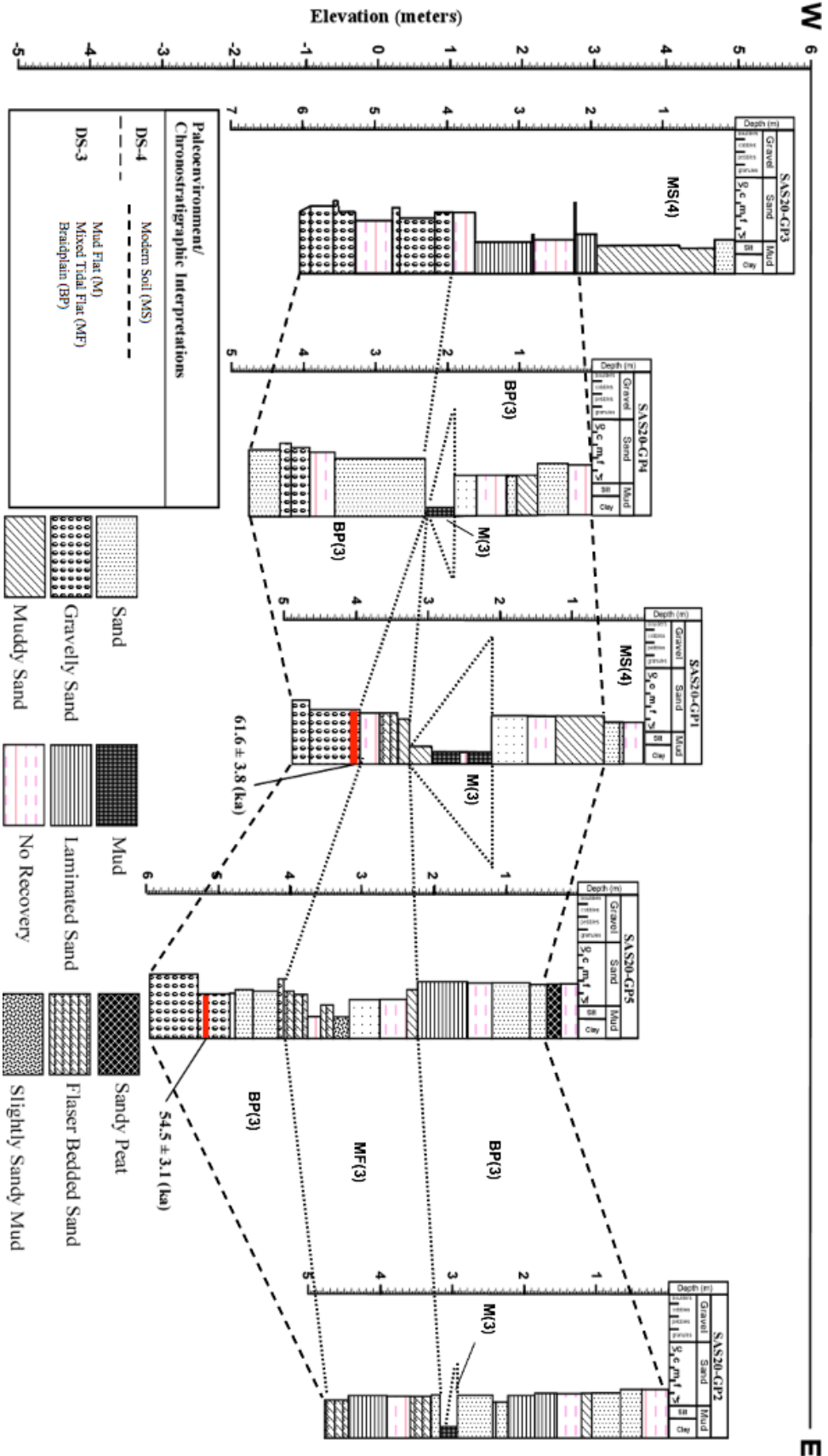


Figure 17. Cross section across the southern shoreline of the Albemarle Sound, West of the Roanoke river. Dashed lines define the boundaries between depositional sequences. Each paleoenvironment and their associated Depositional Sequence are defined in the cross section with a letter (corresponding to their paleoenvironment defined in the legend) followed by a number representing the Depositional Sequence. See figure 1 for core locations

braid bars and channels south of the present-day mouth of the Roanoke River. The braidplain lithofacies consists of gravelly sand containing ~20% mica flakes. Sedimentologic data collected from these braidplain facies in SAS20-GP5 produced a negative skewness of -0.07 and a 2.22 phi mean grain size (Appendix B). Similar gravelly sand lithofacies at -2 mrs1 containing ~15% mica flakes are found in NAS20-GP7 near present day Edenton Bay along the northern shoreline (Figure 15). Sedimentologic data collected from NAS20-GP7 are consistent with those observed in SAS20-GP5, yielding a negative skewness of -0.163 phi (Appendix B), providing evidence for a braidplain paleoenvironment along the northern and southern shore of the modern Albemarle Sound. Moving east at the same elevation there is a lateral transition in lithology to fine sand in NAS20-GP11 and NAS20-GP12 along the northern shoreline and fine flaser bedded sands along the southern shoreline in SAS20-GP2, marking a paleoenvironment transition from braidplain to sand and mixed tidal flat eastward (Figure 15 and 17). Due to the lack of sedimentological data in SAS20-GP2, paleoenvironment interpretations were made based on correlations with the W-E cross section south of the study area by Parham et al. (2013) (Figure 18).

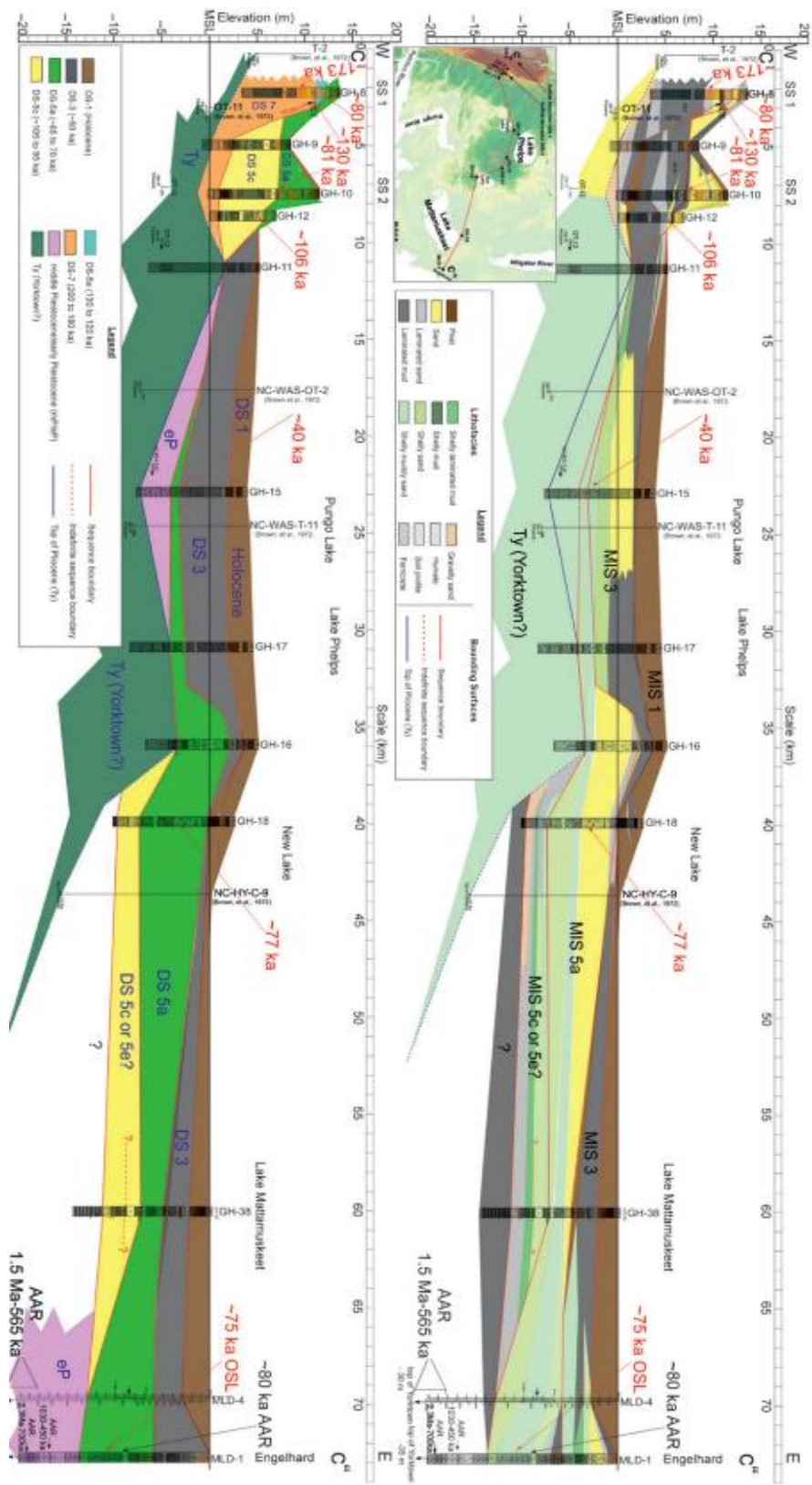


Figure 18. Cross section adapted from Parham (2013). Interpretations presented in this cross section based on 11 sediment cores taken south of the Albemarle Sound between the Suffolk Scarp and Lake Mattamuskeel. Here Parham (2013) has defined 4 late Pleistocene depositional sequences correlative to those in this study.

Along the southern shoreline, a ~2 m thick wedge of flaser bedded muddy fine sands observed in SAS20-GP 1, 2 and 5 ~ -4 to -5 mrsf, overlie the braidplain facies described above and are interpreted to represent the landward encroachment of the tidal flat paleoenvironment as sea level rose during MIS3 (Mallinson et al. 2005; Parham et al. 2013; Daidu et al., 2013) (Figure 14).

Within the first interfluvial east of the Yeopim River (Figure 1 and 12), a medium to fine-grained sand facies recovered in NAS20-GP8 produced an OSL age of 68.8 ± 5.4 ka, observed at similar elevation to MIS 5c aged facies east in NAS20-GP9-10. The age of this sand facies in NAS20-GP8 is consistent with mid – late MIS4. Regression during MIS 4 would have led to incision into MIS 5 marine deposits. Incision at the location of NAS20-GP8 may have exposed sediment from a shallow marine shoal similar to those observed in NAS20-GP9-10. As these facies of sand became exposed at the land surface, aeolian forces would have reworked the body of sand into dunes (Burdette and Mallinson, 2008; Parham et al., 2013).

Still within the interfluvial east of the present day Yeopim River along the northern shoreline, the sand facies just described in NAS20-GP8 is overlain by a 2.8 m thick mixed tidal flat deposit composed of lenticular bedded and burrowed mud (Figure 12). Two interfluvials east of the Perquimans River contain correlative tidal flat deposits. Sediment analysis within the tidal flat facies observed in NAS20-GP9-10 produce medium to fine mean grain sizes of 3.659 phi and 3.502 phi (Appendix B) suggesting an extensive mixed tidal flat system during late MIS3 along the northern shoreline, east of the Perquimans River.

As sea level continued to fluctuate during MIS 3, there is a transition along the modern-day northern shoreline into a 0.5-1 m thick burrowed mud facies 0-3 mrsf, overlying mixed tidal flat facies (Figure 15). These are interpreted to represent mud flat facies, correlative between cores

NAS20-GP6-7 and GP11-12 (Figure 15). These mud deposits make up the upper-most lithofacies of DS-3 along the northern shoreline as sea level receded and the region became less tidally influenced, giving way to a low energy mudflat environment similar to that of the present Albemarle Sound.

Incision during MIS 6 from a diverted Perquimans River, west of the present Yeopim River, was reinitiated during MIS 4, forming a 14 m-deep paleochannel, subsequently filled by DS-3 during MIS 3 (Figure 13). This channel-fill consists of a succession of steeply dipping, laterally accreting clinofolds at the base, to subhorizontal reflections correlating to sand laminated tidal flat muds and burrowed estuarine muds observed in NAS20-VC3 between -3.82 to -4.63 mrs. ^{14}C age results from this mud facies yield a late MIS3 age of 35.6 ± 1.3 ka. MIS 3 deposits within the present Albemarle Sound were incised during MIS2, leaving 0-1 m sections of DS-3 estuarine muds west of the Yeopim River in NAS20-GP6-7 and GP11-12 (Figure 15).

4.1.4 Depositional Sequence 4 (DS-4)

Holocene deposits associated with MIS 1 and DS-4 (Table 3) are ≤ 0.5 m thick along the southeastern flank of the Roanoke River and are composed of sandy peat deposits associated with flooding of the present Roanoke River (Figure 17). On the north side of the Albemarle Sound, lithofacies vary laterally from west to east, from modern shelly shoreface sands at the mouth of the Chowan River (Figure 11), to a 1 m thick peat section associated with the present swamp forest surrounding the northwestern shore of Edenton Bay, and a 1.3 m thick facies of estuarine shoreface sands here as well. East, along the northern shoreline, DS-4 remains < 0.5 m thick transitioning from sandy mud to muddy sand on interfluvial areas east of the Perquimans River (Figure 14). Estuarine shoreface sands comprise DS-4 along the shorelines within the Albemarle Sound (Figure 13, 19, and 21–23). These are products of present transgressive ravinement into

MIS 3 and 5 sand and mud lithofacies preserved in the modern uplands along the estuarine shoreline. DS-4 thickens towards the center of the sound and transitions from shoreface sands along the shoreline to modern estuarine muds towards the center. The base of this Holocene unit is marked by a bay ravinement surface denoted in the seismic data as SH4 (Figure 19, 22, and 23). In NAS20-VC4, this surface is marked by a lithologic transition from peat at the base of the core to medium-fine sand above (Appendix B).

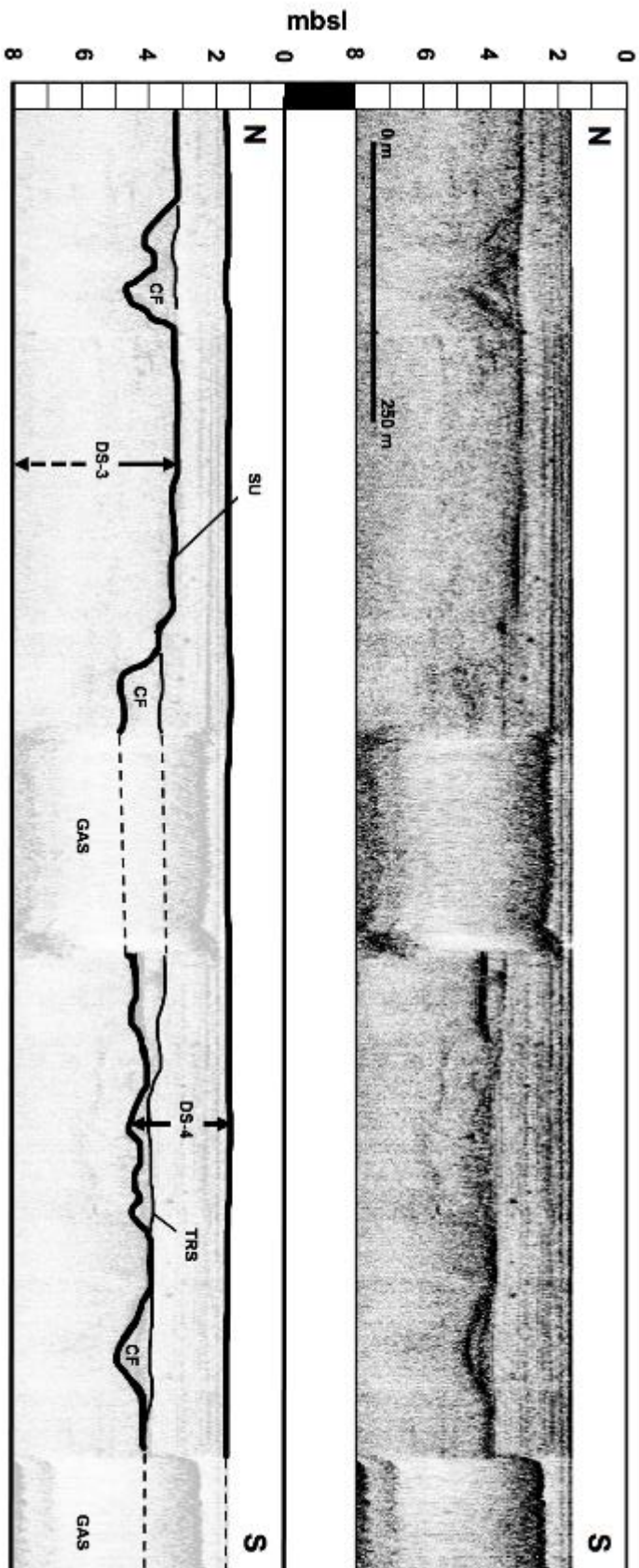
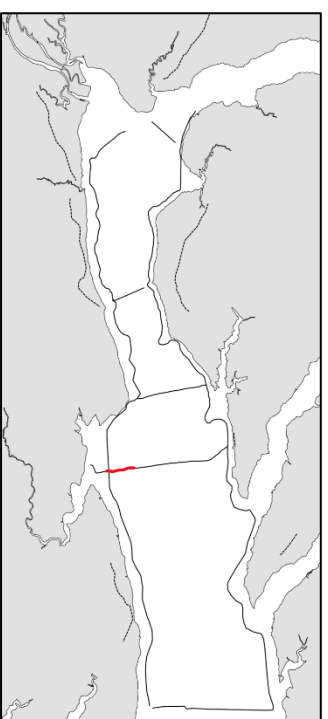


Figure 19. CHIRP seismic N-S crossing line with interpreted depositional sequences based on seismic units defined previously in Figure x. Paleochannel here emitting gas attenuate the seismic data in two locations along this profile. This distinguishable data here is mostly Holocene channel fill (DS-4).



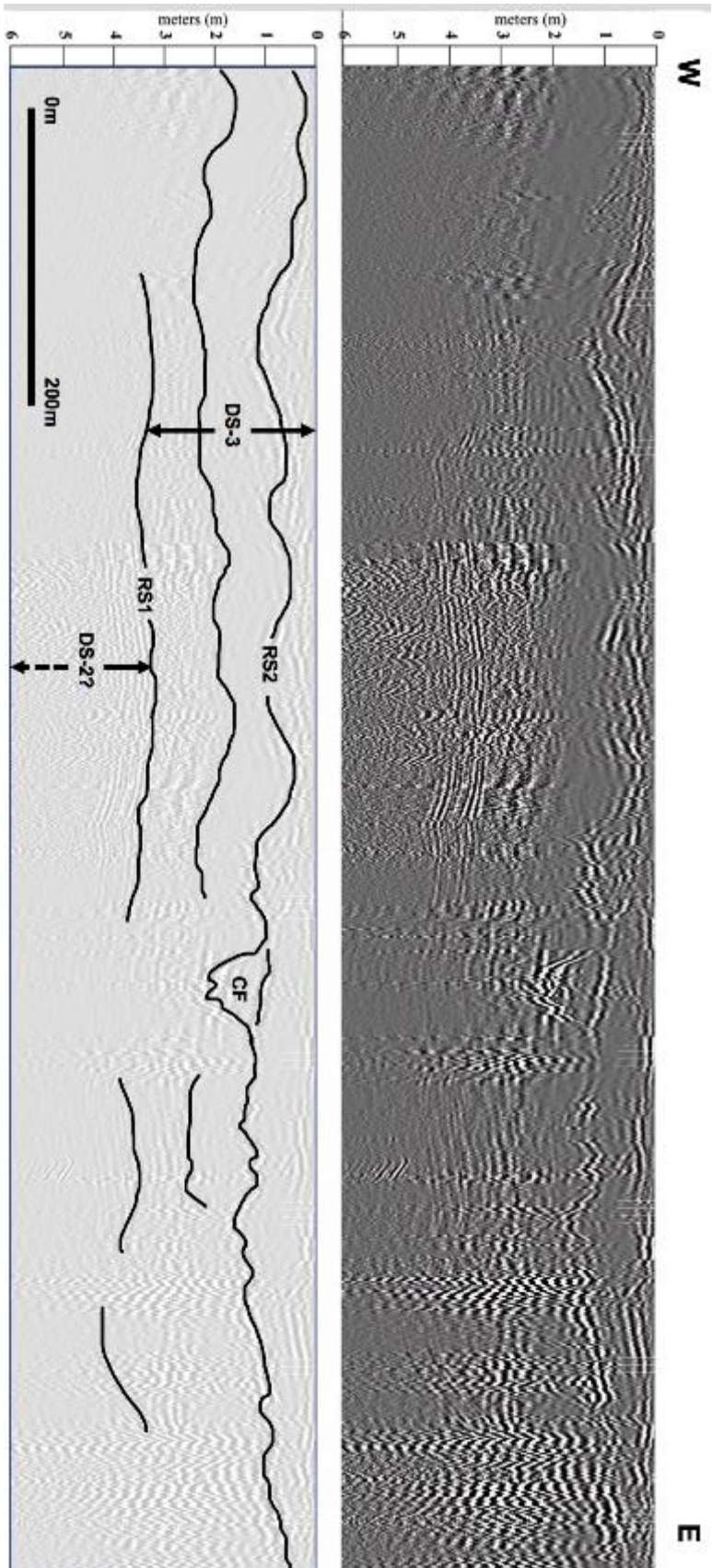


Figure 20. GPR profile collected along the southern shoreline of the Albemarle Sound. Here the depositional sequences (DS) are interpreted from their associated radar facies. DS are bound by subaerial unconformities.

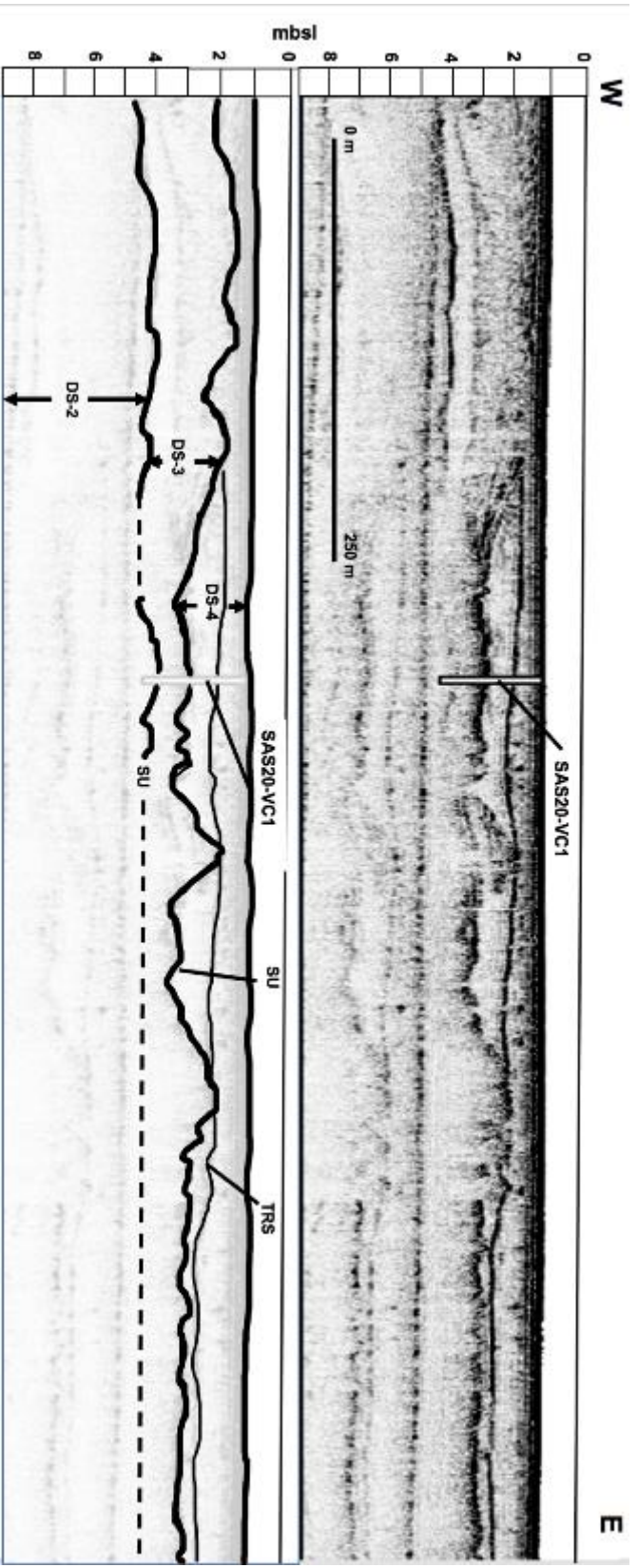
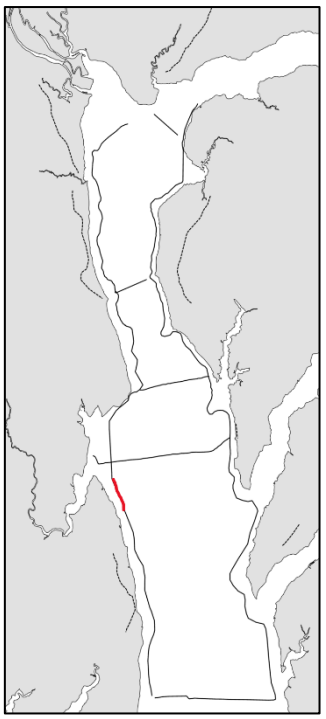


Figure 21. CHIRP seismic W-E profile. Here the depositional sequences (DS) are interpreted from their seismic units. DS are bound by subaerial unconformities including transgressive ravinement surfaces. Vibracore SAS20-VC1 location superimposed on the profile.



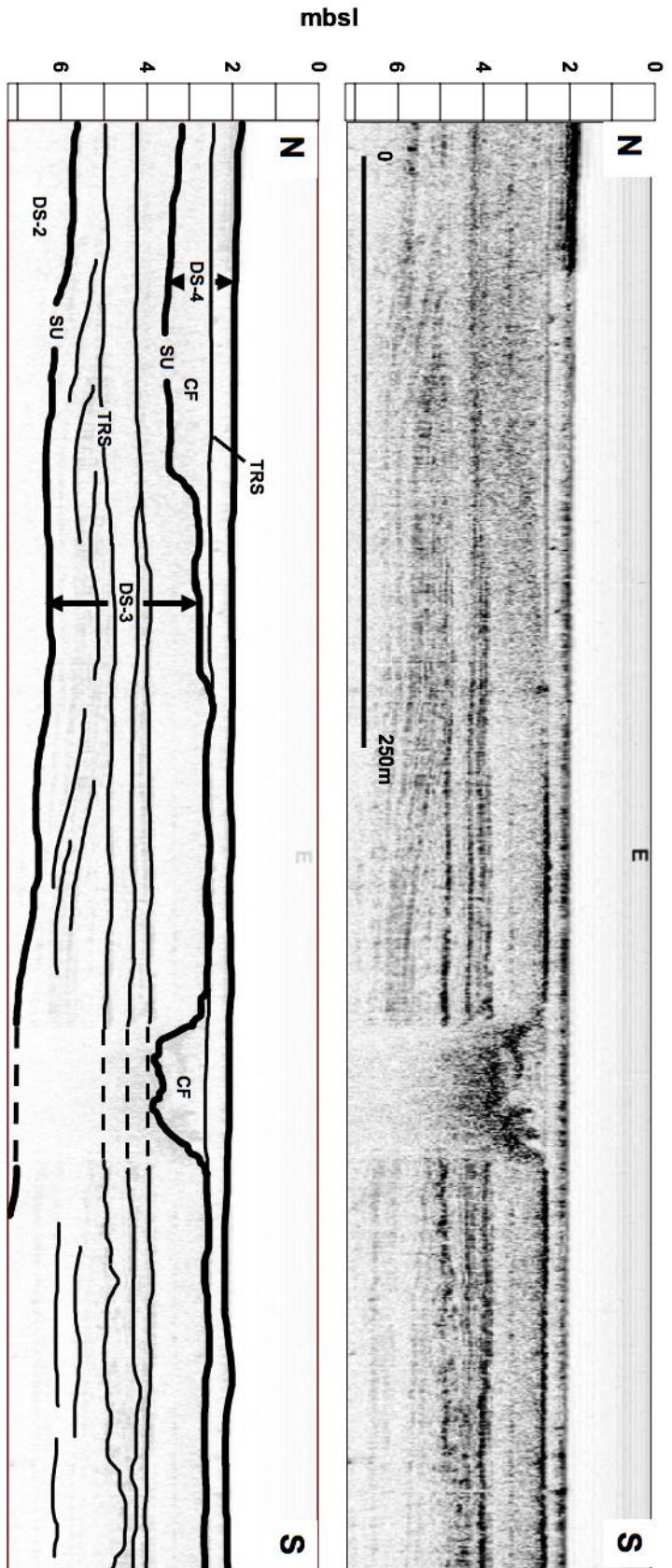
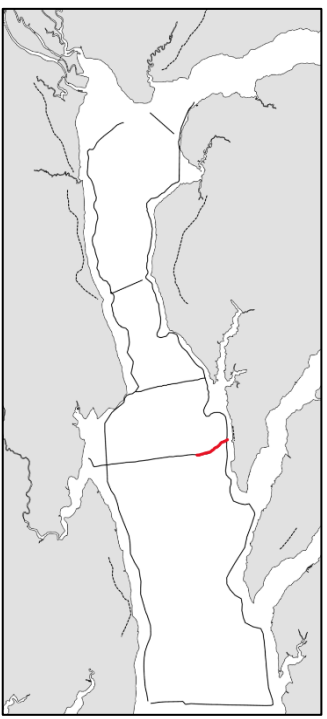


Figure 22. CHIRP seismic N-S crossing line. Here the depositional sequences (DS) are interpreted from their seismic units. DS are bound by subaerial unconformities including transgressive ravinement surfaces.



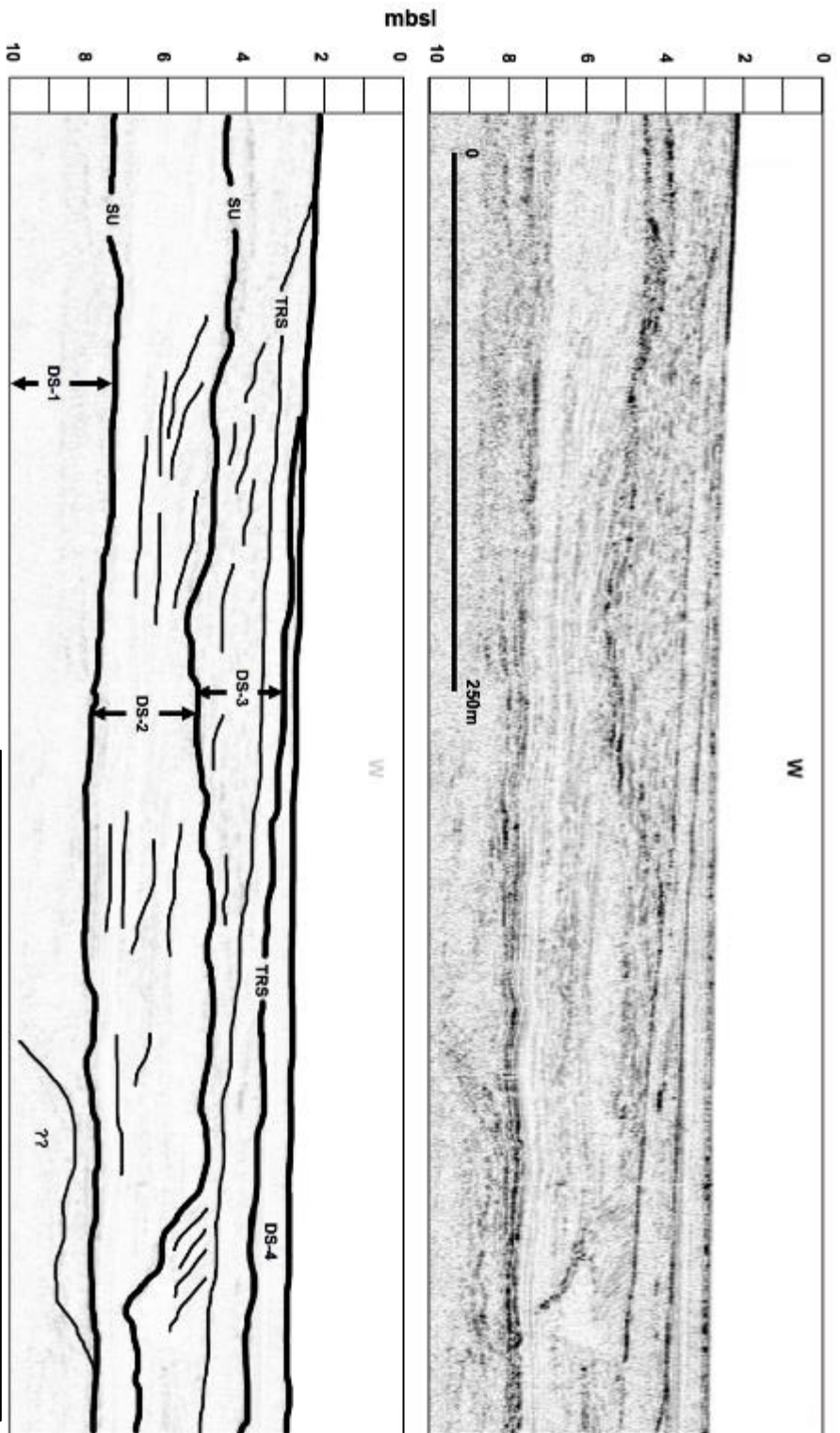
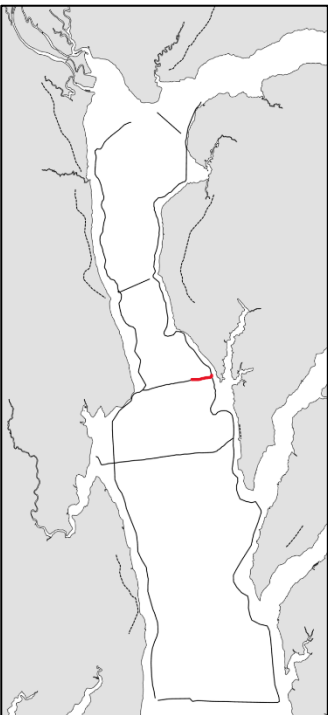


Figure 23. CHIRP seismic N-S crossing line, east of the Yeopim river. Here the depositional sequences (DS) are interpreted from their seismic units. DS are bound by subaerial unconfined units including transgressive ravinement surfaces.



4.2 Evolution of the system and implications for sea-level changes and glacio-isostatic adjustment

Successions of glacial/interglacial cycles characterize the Earth's climate through the Quaternary period. The duration of these cycles has increased from 41,000 yrs to 100,000 yrs following the beginning of the Middle Pleistocene at 780 ka (Pisias and Moore, 1981; Railsback et al., 2015) (Figure 24). Presence of terrestrial glaciers, in North America, specifically the Laurentide ice sheet of the Wisconsin glacial period (ca. 75 ka to 11 ka), has influenced the extent of regional sea-level fluctuations along the western Atlantic coast via glacio-isostatic adjustment (GIA) (Fig 25) (Potter and Lambeck, 2003; Peltier, 2004; Scott et al. 2010; DeJong et al. 2015; and Pico et al. 2017). GIA is the response of the Earth's lithosphere to the loading and unloading of glaciers at the surface as the climate transitions between glacials and interglacials. Presence of the Laurentide Ice Sheet prior to Termination II (the rapid decay of ice sheets at ca. 130 ka) produced a forebulge as mantle material was displaced from the glaciated region to the periphery of the ice sheet (Scott et al., 2010; Stanford et al., 2016). Stanford et al. (2016) studied fluvial, glacial, and estuarine deposits in the Delaware River Basin of New Jersey to model uplift rates following the retreat of glaciers during the middle and late Pleistocene. Models from the Stanford et al. investigations suggest that the crest of the glacioisostatic forebulge is located at the southern shore of Delaware Bay, ~200 km south of the late Wisconsinan glacial limit.

Following the onset of ice sheet retreat and Termination II (MIS 6-5), subsidence of this forebulge produced regional fluctuations in relative sea level that differ from eustatic sea level from MIS 6 to 1, (Walcott 1972; Chappell 2002; Potter and Lambeck, 2003; Mallinson et al. 2008; Scott et al. 2010; Parham et al. 2013; Dejong et al. 2015; Stanford et al. 2016; Pico et al. 2017). A similar phenomenon is observed in the present-day northern North Carolina, including

the study area. Mallinson et al. (2008) show that current GIA in northeastern North Carolina amounts to ca. 26 m above isostatic equilibrium conditions. Here a subsidence rate of approximately 1 mm/yr is experienced in response to ice sheet retreat during Termination I (ca.

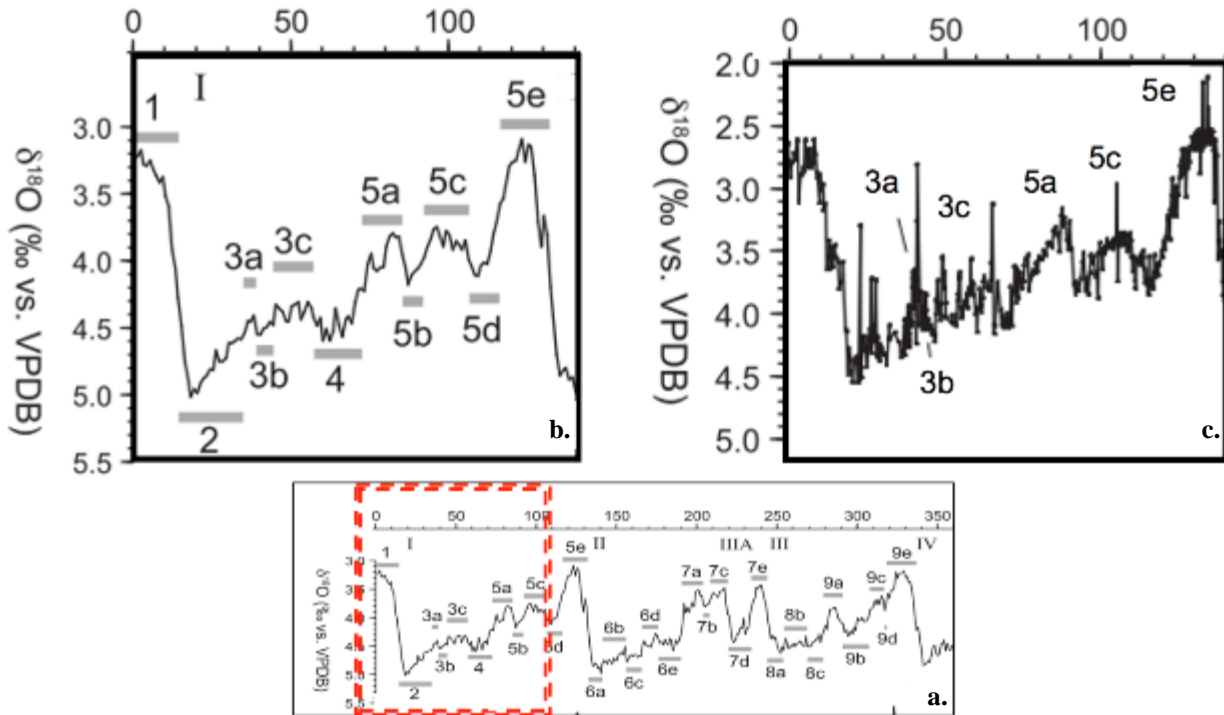


Figure 24. Marine benthic foraminiferal oxygen isotope 18 data adapted from Railsback (2015), including marine isotope stages, from 140kya to the present. **a.** Extended oxygen isotope 18 data showing marine isotope stages 1-9 (From termination IV). **b.** Enhanced view of figure 16a focusing on the marine isotope stages relevant to this study (MIS 1-5). **c.** North Atlantic marine record (MIS 1-5).

20 kya – 10 kya) (Figure 25) (Potter and Lambeck, 2003; Peltier, 2004; Kopp et al., 2015). It should be noted that all elevations described in the following discussion are referenced to mean sea level corresponding to the North American Vertical Datum (NAVD 88).

4.2.1 MIS5

Of the five substages of MIS5, stage 5a (74 ka – 84 ka) deposits are the most abundant in coastal Virginia and North Carolina due to glacio-isostatic influences on the regional topography (Mallinson et al. 2008; Scott et al. 2010; Parham et al. 2013). Based on dated submerged

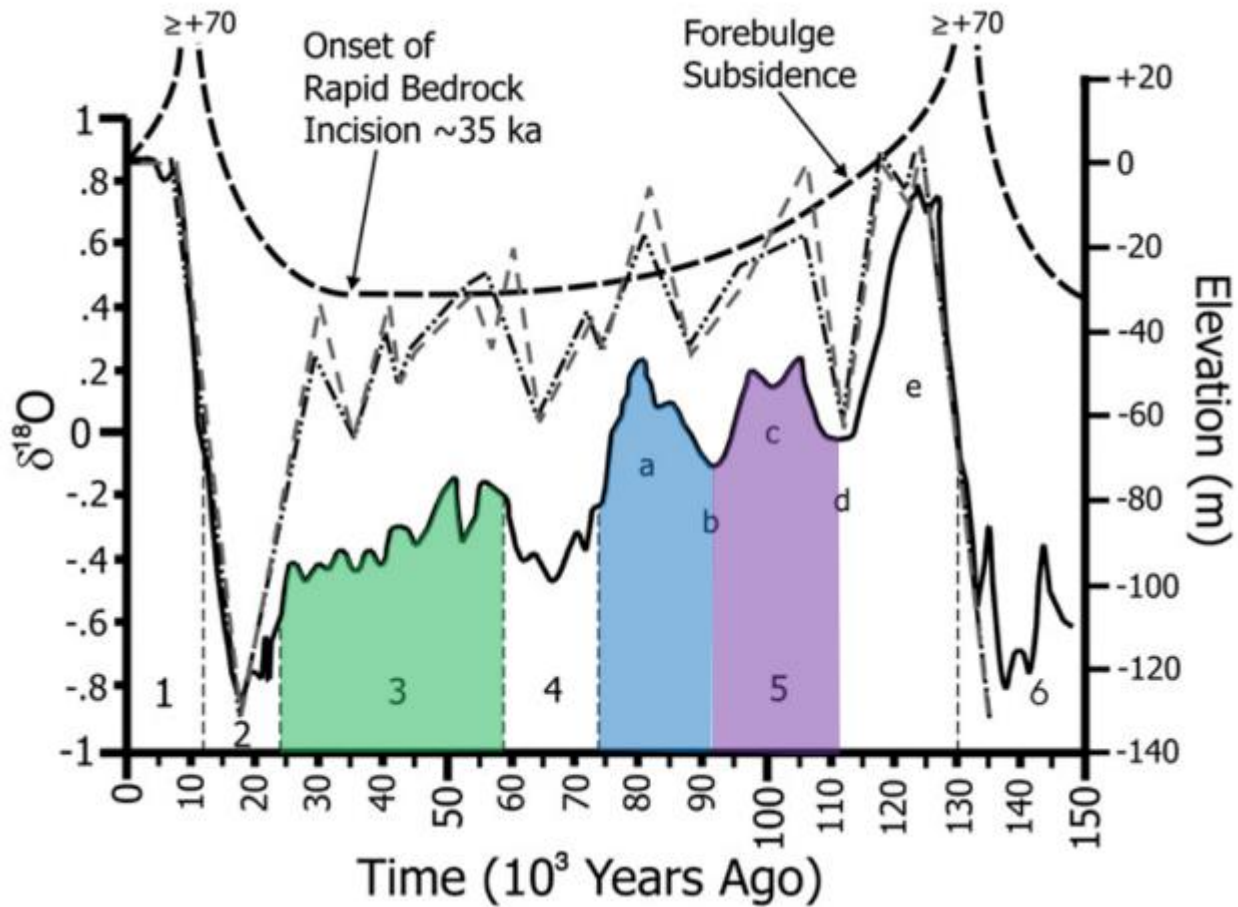


Figure 25. Sea level curve (solid black line) and glacioisostasy curve (dashed black line) compared with oxygen isotope levels for the last glacial/Interglacial cycle (MIS 5-2). Colored polygons point out periods within MIS5 (blue/purple) and MIS3 (green) where relative sea level extended above the Virginia coastal plain (adapted from Scott et al., 2010).

speleothems, Potter and Lambeck (2003) identified a north to south decreasing sea level gradient along the US Atlantic coast, from ca. +7 m in Virginia to -8 m in Florida during MIS 5a. Following Termination II and the onset of the Sangamon interglacial period, subsidence of a peripheral forebulge which accumulated during the Illinoian glacial period led to a rapid elevation decrease in the Virginia and North Carolina region from ca. +20 m at 130 ka to ca. -20 m at 80 ka (Scott et al. 2010).

Deposits in the study area interpreted as MIS5 age, including both MIS 5c and 5a, represent beach/shoreface to shallow shelf marine paleoenvironments consisting of moderately sorted, fine to medium, heavy mineral laminated quartz sands with a mean grain size of ~2 phi

(Cores CR20-VC5–6) (Figure 11). Geologic interpretations from Parham et al. (2013) indicate the presence of MIS 5c deposits east and west of the Suffolk shoreline in coastal North Carolina (Figure 15). Approximately 20 km north of CR20-VC6, Parham et al. (2013) recovered one MIS 5c OSL age (94 ka) from laminated sand deposits 3-6 m above mean sea level (Figure 12). In the cross section shown in Figure 12, Parham et al. (2013) interpreted a laminated sand facies ~ -3 to -4 mrsll as MIS 5c or 5e. Similar laminated sand facies identified in cores CR20-VC5 and CR20-VC6 were collected in the Albemarle Sound at -3.6 to -3.9 mrsll supporting the interpretation that these are likely shoreline deposits associated with MIS 5c. West to east along the Pamlico/Albemarle peninsula, from the Suffolk shoreline to Lake Mattamuskeet (Figure 1), Parham et al. (2013) defines a seaward thickening wedge consisting of MIS5a shelly muddy sand to sand (Figure 18). The succession of MIS 5a and MIS 5c lithofacies shown in Figures 12 and 18 are correlative, both chronostratigraphically and lithostratigraphically, to those identified in terrestrial and marine cores from this study. On the Albemarle interfluvies east of the Yeopim River between the Perquimans and Pasquotank rivers, OSL samples from medium-fine sand deposits ~ -1.5 mrsll, yield late MIS 5c ages of 93.4 ± 5.3 ka (NAS20-GP9) and 91.8 ± 6.3 ka (NAS20-GP10) (Table 3 and Figure 14). Presence of these large shoals suggests that even during late MIS 5c and the onset of a stadial period (MIS 5b), the study area remained an shallow shelf environment, likely with few barrier islands (Figure 26). Shelly muddy sand and muddy sand lithofacies recovered along the northern shoreline -2 to -3 mrsll (NAS20-GP11 and GP12) are similar to those within a thin sequence of MIS 5a observed -2 to -4 mrsll by Parham et al. (2013), south of the study area between Pungo and Alligator Lake (Figure 18). Shells recovered from this facies in NAS20-GP12 and Parham et al. (2013) include *Anadara floridana* and *Spisula*

solidissima raveneli suggesting deposition in a shallow (8–66 m) shelf paleoenvironment (Porter and Houser, 1997; Cargnelli, 1999) (Figure 16).

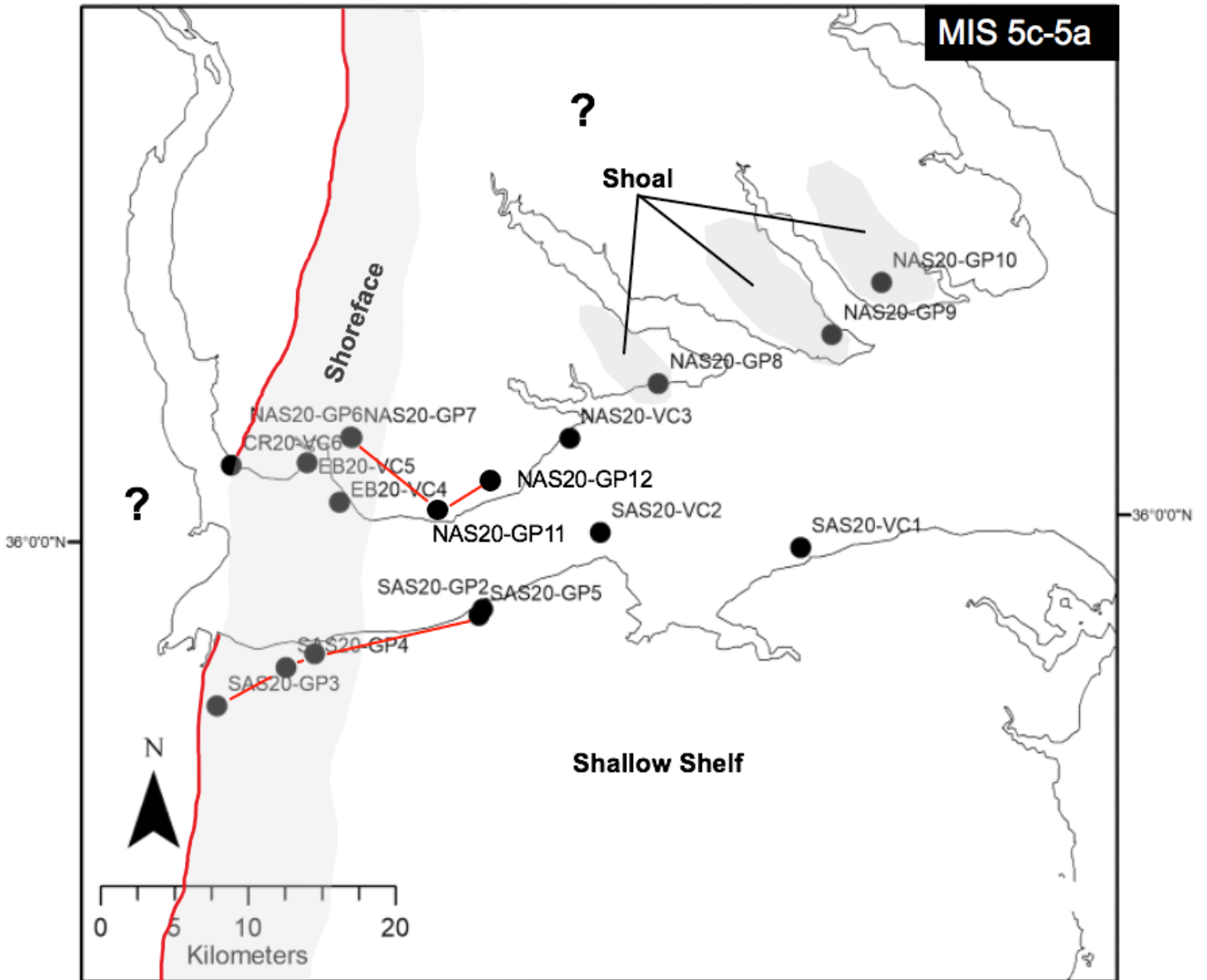


Figure 26. Map showing interpreted extent of paleoenvironments throughout the study area during MIS 5c and 5a. Marine shelf should be open shelf. Red lines connecting core locations on the northern and southern shorelines outline the cross sections defined in figures 15 and 17.

4.2.2 MIS3

Deposition associated with highstand conditions during MIS 3 produced a stratigraphic sequence ranging from -6 m to +4 m in the study area (Figure 13–15 and 20–23). This elevation range aligns well with those recorded by several other regional studies, compiled by Pico et al. (2017) (Figure 27). However, the extensive deposition during this period is contradicted by estimates of global mean sea level (GMSL) estimated to have reached -30 to -60 m between 60 ka and 26 ka (Pico et al. 2017). Similar to MIS 5, this discrepancy is explained by a relative rise in sea level interpreted by several studies to have been produced by regional GIA as peripheral forebulge subsidence persisted from MIS 5 into MIS3 (Potter and Lambeck 2003; Mallinson et al. 2008; Scott et al. 2010; Stanford et al. 2016; and Pico et al. 2016). However, MIS3 is not defined by a single highstand period. Based on dated coral terraces from Papua New Guinea and the Huon peninsula by Chappell (2002), between 33 – 60 ka, five interstadial sea-level peaks were identified and interpreted to have been influenced by Dansgaard-Oeschger oscillations (D-O events). D-O events signify rapid decadal scale atmospheric warming followed by millennial scale cold periods, or Heinrich events, and were abundant during MIS 3 (Voelker 2002). Evidence of these sea-level oscillations are recorded in the present geomorphology of coastal North Carolina within the Hickory Scarp, Powell's Point Ridge, and Land of Promise ridge (Burdette, 2005 Mallinson et al., 2008), and the vertical succession of lithofacies in the study area.

Along the north and south shorelines of Albemarle Sound there is a complex temporal and spatial evolution of paleoenvironments. Based on cross sections along both the north and south of the sound (Figure 19 and 14), DS-3 west of SAS20-GP5 (76° 22'W) began as a

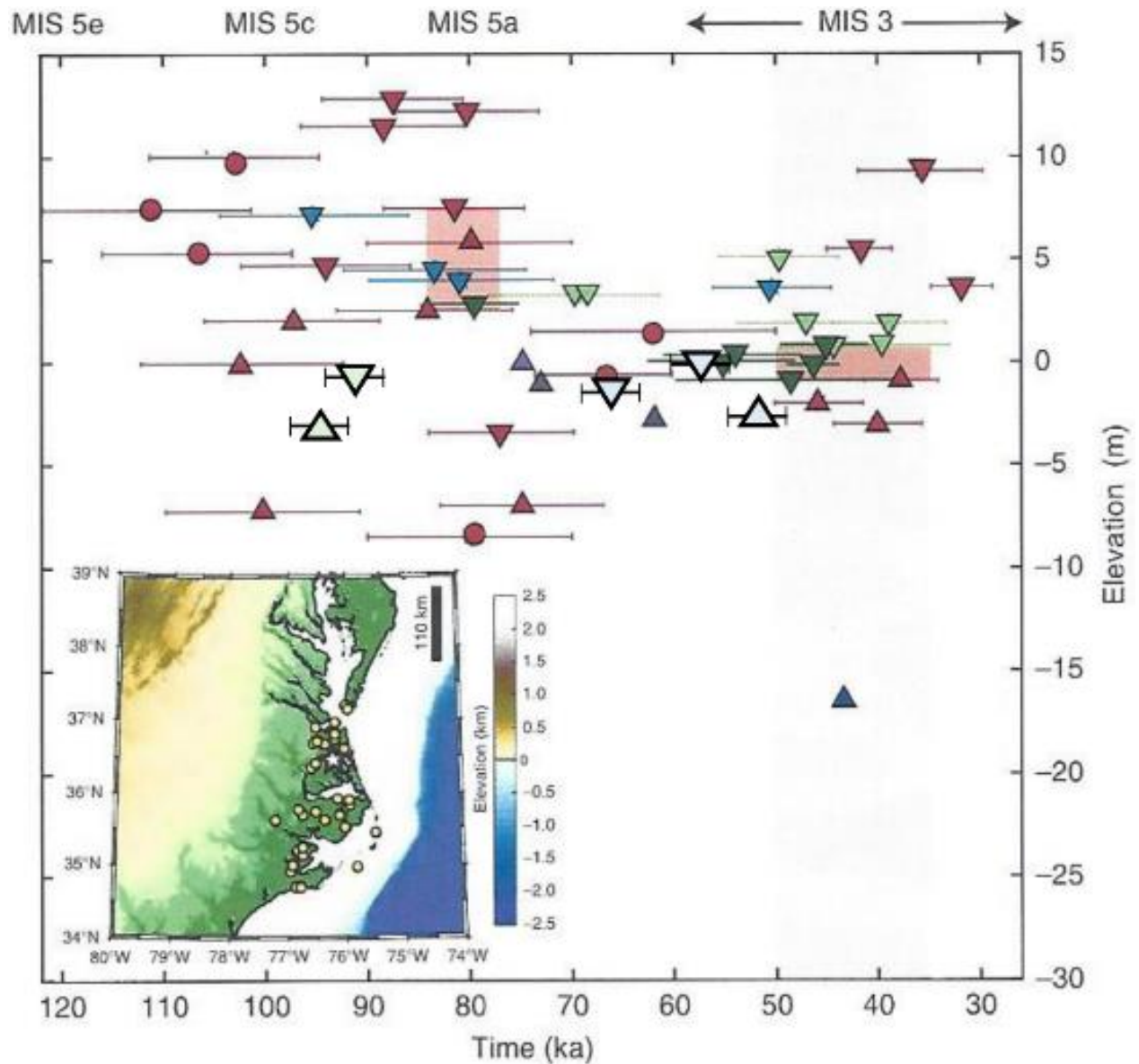


Figure 27. Modified figure from Pico et al, 2017 depicting a compilation of sea level indicators from various studies done in North Carolina and Virginia. Upward pointing triangles represent lower bound marine markers and downward pointing triangles signify upperbound terrestrial markers. Open triangles represent data from this study. The upper bound marker represents the interpreted upper limit of MIS3 age deposits.

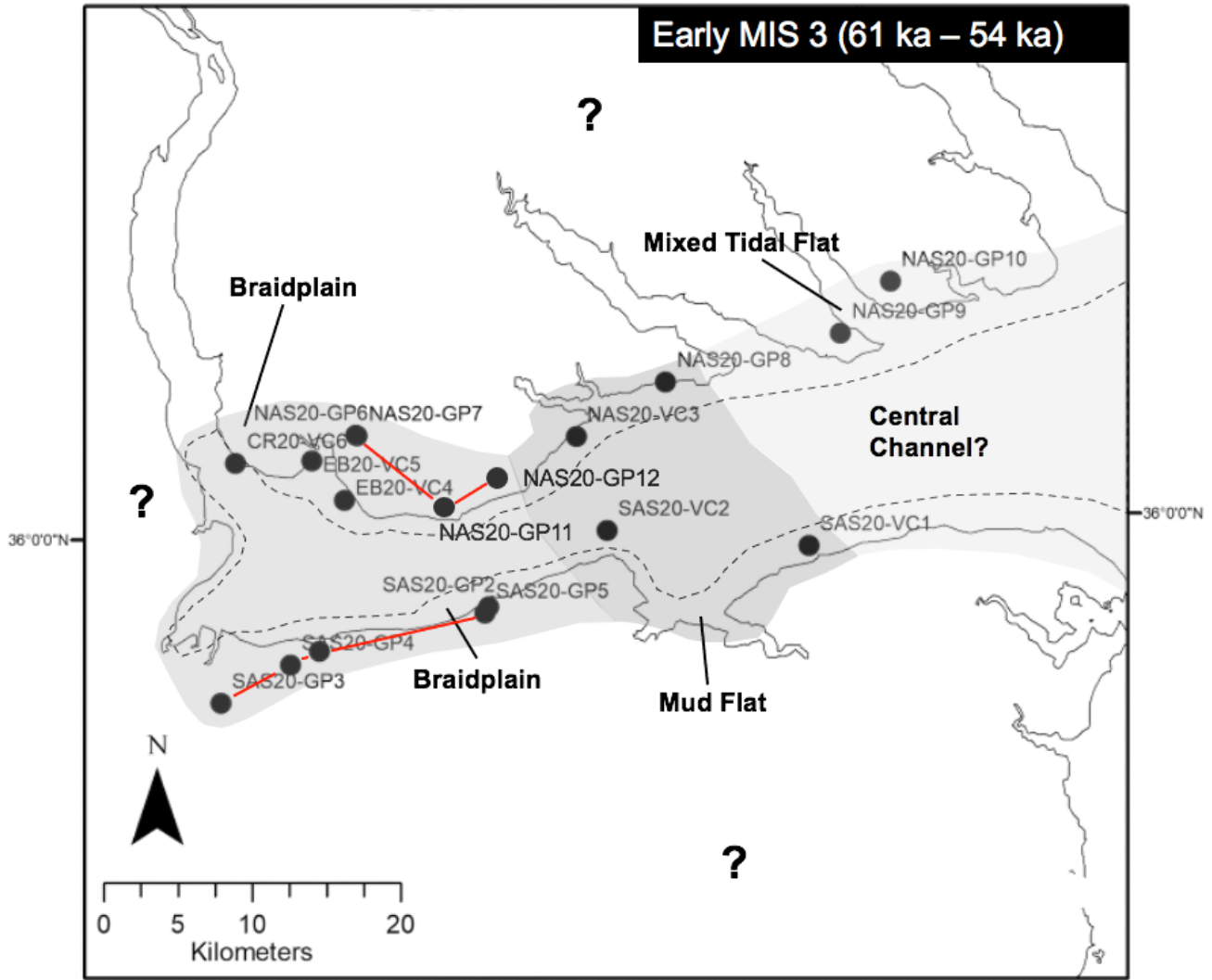


Figure 28. Map showing interpreted extent of paleoenvironments throughout the study area during early MIS 3. Red lines connecting core locations on the northern and southern shorelines outline the cross sections defined in figures 15 and 17.

braidplain system (Figure 28). Gravelly sand – coarse-grained sands are found at the base of DS-3 and recovered in SAS20-GP3 (Figure 29). OSL samples from SAS20-GP1 and GP5 produced dates of 61.6 ± 3.8 and 54.5 ± 3.1 kya B.P., correlative to early MIS 3 and late MIS 4. Up-section, the region changes from braid-plain to mixed tidal flat and mud flat along the southern shoreline (Figure 14). Mud deposits in land cores along the northern shoreline overlay flaser bedded mixed tidal flat

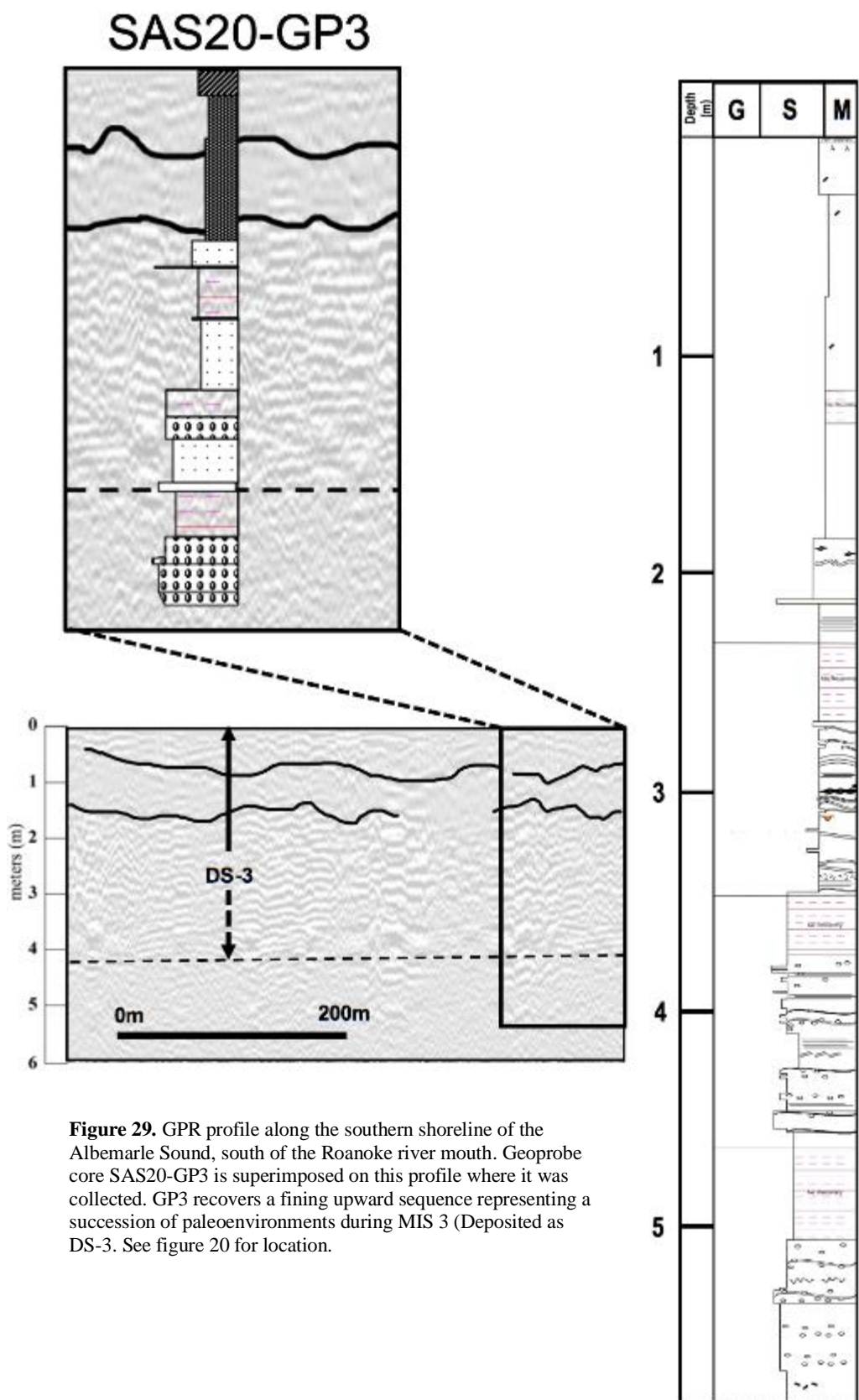


Figure 29. GPR profile along the southern shoreline of the Albemarle Sound, south of the Roanoke river mouth. Geoprobe core SAS20-GP3 is superimposed on this profile where it was collected. GP3 recovers a fining upward sequence representing a succession of paleoenvironments during MIS 3 (Deposited as DS-3. See figure 20 for location.

deposits (Figure 13) at which point a mud flat environment extended eastward. This evolution represents the transgressive systems tract associated with initial sea-level rise during MIS 3, supported by the general fining upward sequence of the lithologies in cores along the northern shoreline (Catuneanu, 2006). Along the southern shoreline a lithologic change from fine flaser bedded sand and sandy muds to coarser sands containing plant fragments represents a change from mixed tidal flat back to braidplain environment following sea level fall. With the resurgence of braidplains here, the underlying mudflat facies are incised by the coarser braidplain sands discovered in the seismic data above.

The majority of DS-3 consists of tidal flat deposits which are correlative to those found in surrounding studies as well. Parham et al. (2013) hypothesized that during MIS 3 the Chowan and Roanoke Rivers would have been more inundated relative to today, producing two major fluvial systems. Based on interpretations from this study, these would have discharged into a major tidal flat system expanding W-E ~50 km between the Suffolk and Hickory scarps. Mallinson (2008) investigated the late Pleistocene coastal lithosomes within three paleoshorelines west of the modern-day Outer Banks. Of these three ridges, the lithology of the Hickory Scarp displayed a vertical succession of tidal flat paleoenvironments. This succession includes tidal sand flat and mixed flat deposits between 1 and -1 m relative to sea level, a similar elevation as those identified in GP-6-10 of this study. The Hickory Scarp deposits produced MIS 3 luminescence ages between 48.9 ± 10.9 ka and 39.6 ± 11.6 ka. No OSL data from these tidal flat deposits are available for this study, however radiocarbon-dated plant debris collected from sandy mud facies within NAS20-VC3 produced an age of 35.6 ± 1.3 ka. Thus, the chronology of this tidal flat system in the Albemarle Sound region can be constrained to 48.9 ± 10.9 ka – 35.6 ± 1.3 ka (Figure 30)

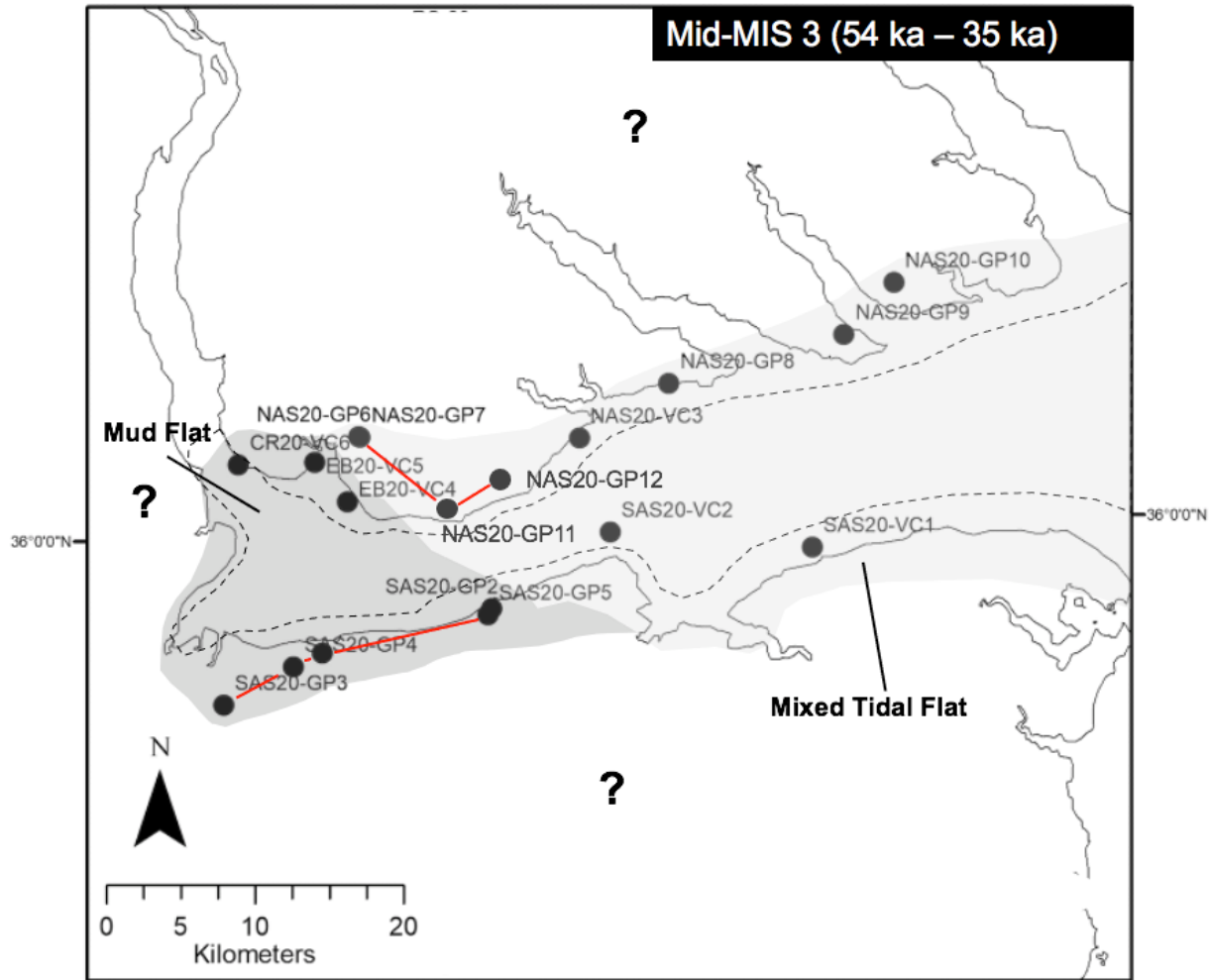
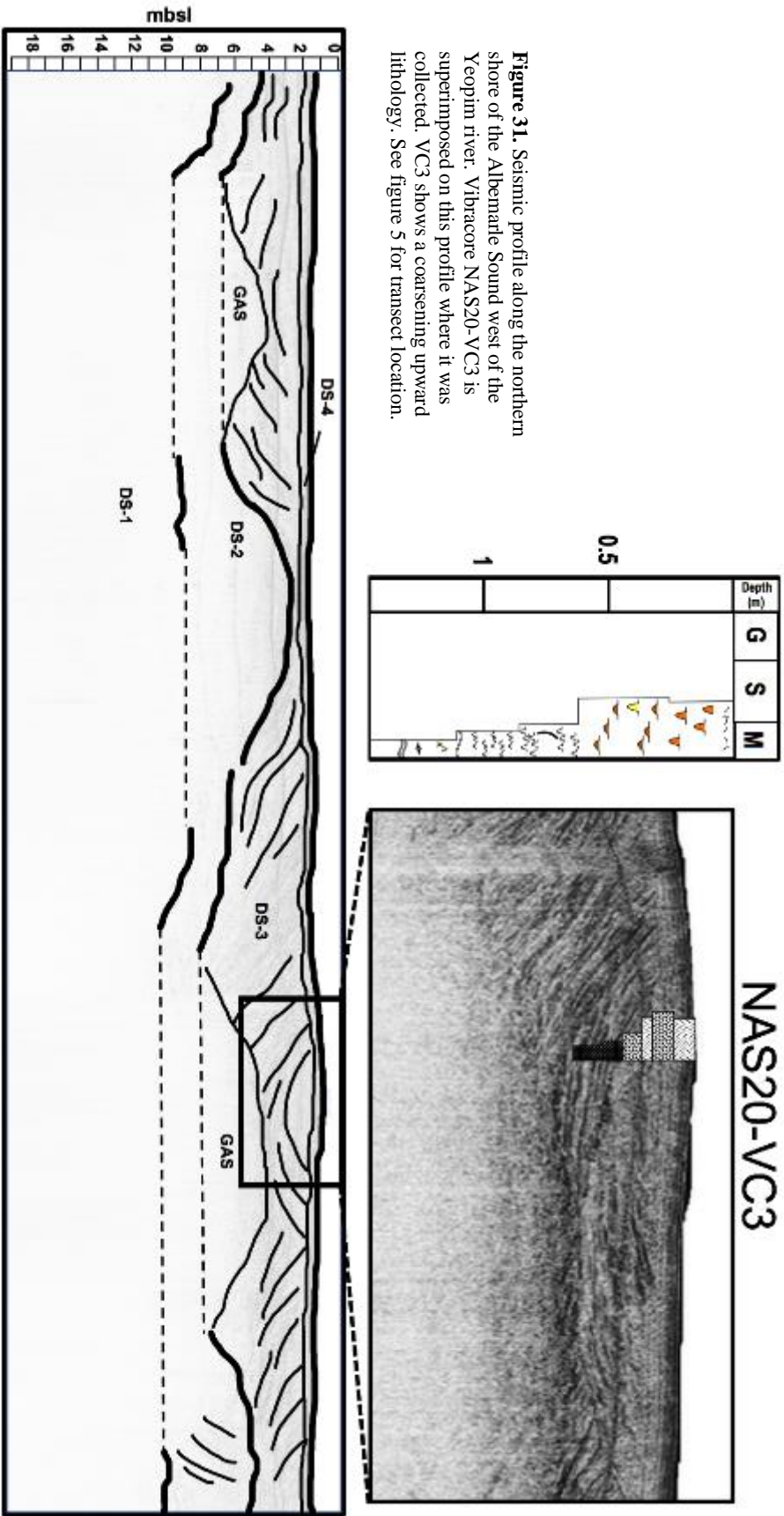


Figure 30. Map showing interpreted extent of paleoenvironments throughout the study area during middle MIS 3. Red lines connecting core locations on the northern and southern shorelines outline the cross sections defined in figures 15 and 17.

These tide-dominated settings typically consist of three major components including tidal sand bars, tidal channels, and tidal flats (Daidu et al., 2013). In this coastal setting, the modern fluvial channels including the Yeopim, Perquimans, Little Rivers as well as the buried channel uncovered in the seismic data west of the modern Yeopim River (Figure 31) may have acted as tributary tidal channels associated with a major tidal channel within the central basin of the modern Albemarle Sound. The presence of a central tidal channel is supported by the seismic profile in figure 22, depicting N-S dipping beds within SSU2 of DS-3 suggesting the infilling of a major channel.

Figure 31. Seismic profile along the northern shore of the Albemarle Sound west of the Yeopim river. Vibracore NAS20-VC3 is superimposed on this profile where it was collected. VC3 shows a coarsening upward lithology. See figure 5 for transect location.



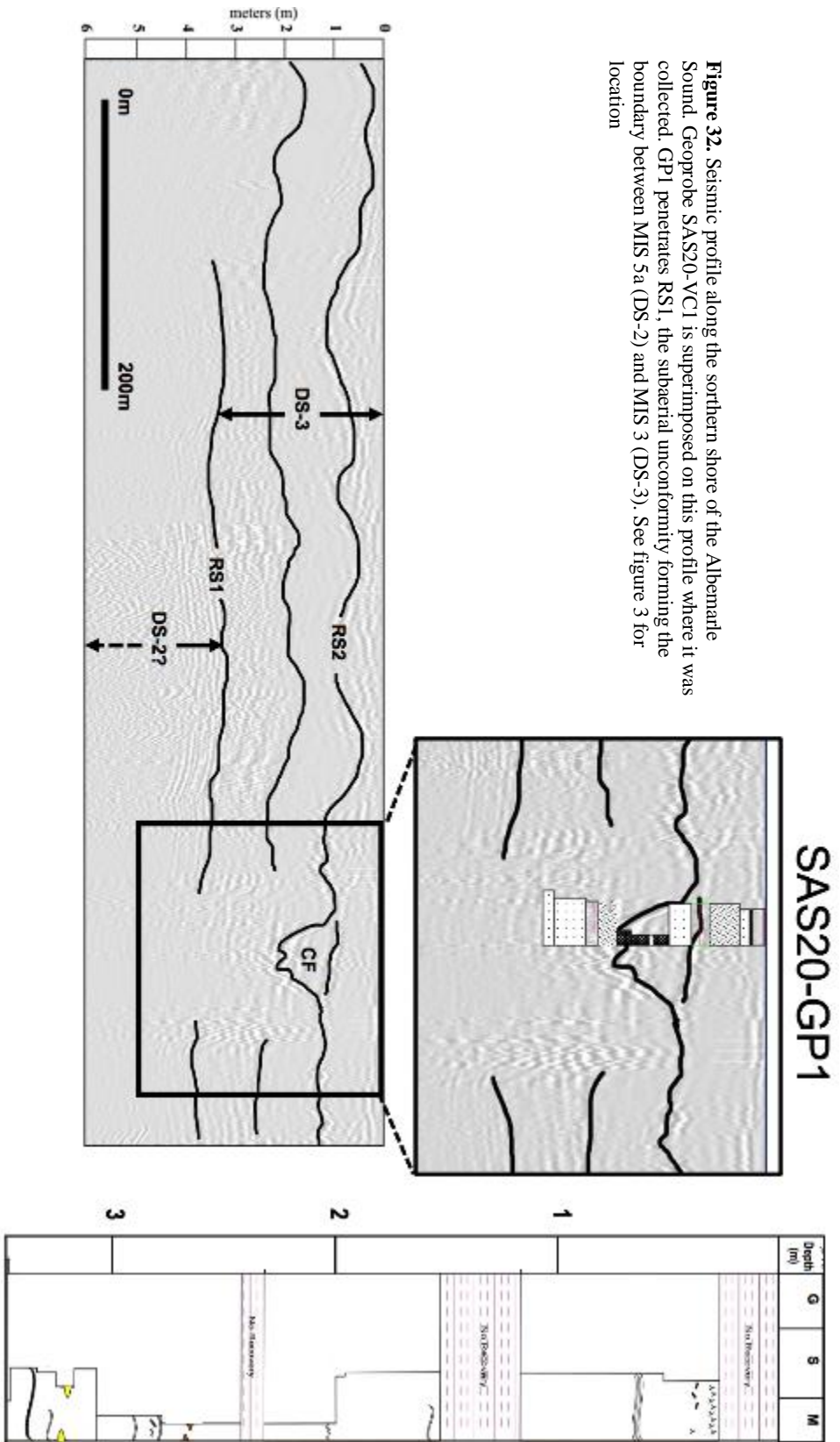


Figure 32. Seismic profile along the southern shore of the Albemarle Sound. Geophone SAS20-VCI is superimposed on this profile where it was collected. GP1 penetrates RS1, the subaerial unconformity forming the boundary between MIS 5a (DS-2) and MIS 3 (DS-3). See figure 3 for location

4.3 Expectations for the future

Coastal North Carolina's response to sea level rise is expected to be analogous with that during MIS 3 which produced a peak sea level similar to that of the present (Mallinson et al.,

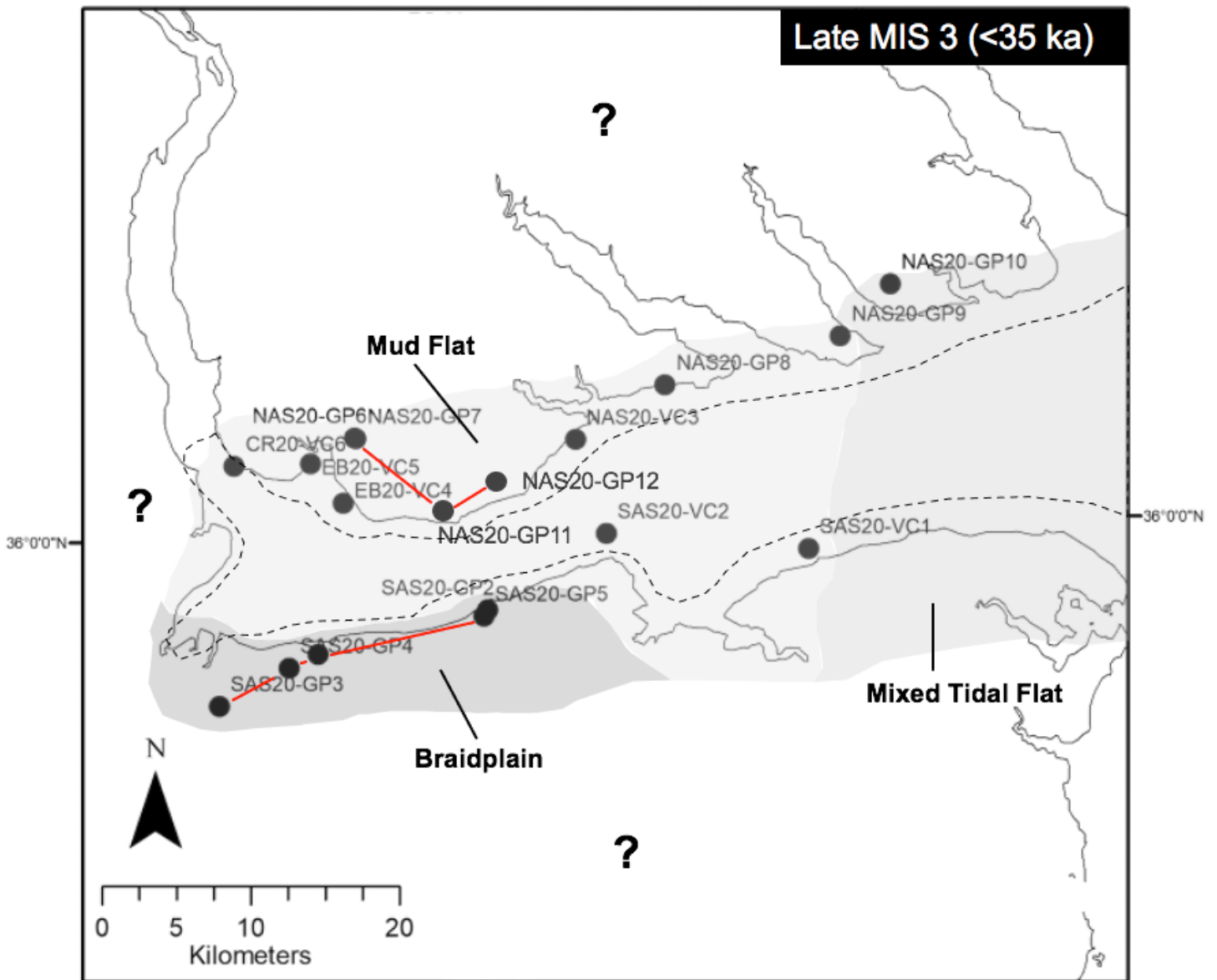


Figure 33. Map showing interpreted extent of paleoenvironments throughout the study area during late MIS 3. Red lines connecting core locations on the northern and southern shorelines outline the cross sections defined in figures 15 and 17.

2008; Parham et al. 2013). The IPCC assessment report (AR6) of 2021 provides short term (relative to geologic timescales) predictions of sea-level rise along the east coast of North America (Table. 4). This report states that by the end of the 21st century sea level along the east coast will have risen ~1 m above the present. Considering the ongoing peripheral forebulge subsidence in the region, coastal North Carolina should experience sea-level rise at an accelerated rate relative to the North American east coast north of New Jersey (~ Lat. 40° 30') (Stanford et al., 2016). Considering the sea-level trend produced by the IPCC AR6 it can be estimated that by the end of the 23rd century regional sea level will have risen ≥ 3 m above the present, producing coastal conditions similar to those experienced during MIS 3 (Parham et al., 2013).

In the study area, peak sea level during MIS 3 would have produced an extensive tidal flat system (Figure 30). This coastal environment and its relationship to the Chowan and Roanoke paleoestuaries is comparable to that of the Wadden Sea tidal flat system along the northern coast of Germany and the Netherlands (Scheel, 2012 and Fitzgerald et al., 2018). Separated from the North Sea by the Frisian barrier island system, the Weser and Elbe estuaries both feed into intertidal areas of exposed tidal flats, also known as the Wadden Sea (Fitzgerald et al., 2018). Daidu et al. (2013) classifies the Wadden Sea as a barrier flat system, where tidal flats occupy the landward side of barrier islands. Tidal strength here is upper mesotidal with a tidal range of 2 – 3.5 m (Flemming, 2012). This tidal flat system exists as the largest of its kind in the world, extending ~30 km off the coast (Wang et al., 2013). The lithologic characteristics of this environment are consistent with those identified in this study as well. Karle et al. (2021) describes the lithology of sand-mixed flats in the Wadden Sea as fine sand with flaser and lenticular bedding, and mud flats with occasional fine sand laminations. These lithologies are

consistent with those interpreted as mixed and sand tidal flats in this study from cores NAS20-GP6-10 between 1 and -1 mrs1 as well as those present in the Hickory Scarp stratigraphy (Mallinson, 2008) (Figure 19 and 30).

Elevation of Wadden Sea tidal flats ranges from 0 to -4 mrs1 and the flats are divided by tidal channels reaching depths of -15 mrs1 (Figure 34) (Scheel, 2012, Fitzgerald, 2018). Data discussed in the previous section of this study suggest tidal channels were abundant in the tidal flat system present during MIS 3 much like the tidal channel network of the modern day Wadden Sea (Figure 34). Another morphologic similarity with the Wadden Sea region would be the separation between the open ocean and tidal flat environment by a highly segmented barrier island system. North of the Wadden Sea the Frisian barrier island chain is divided by >5 inlets (Figure 34). The existence of a tidal flat system here is dependent on marine sediment supply via

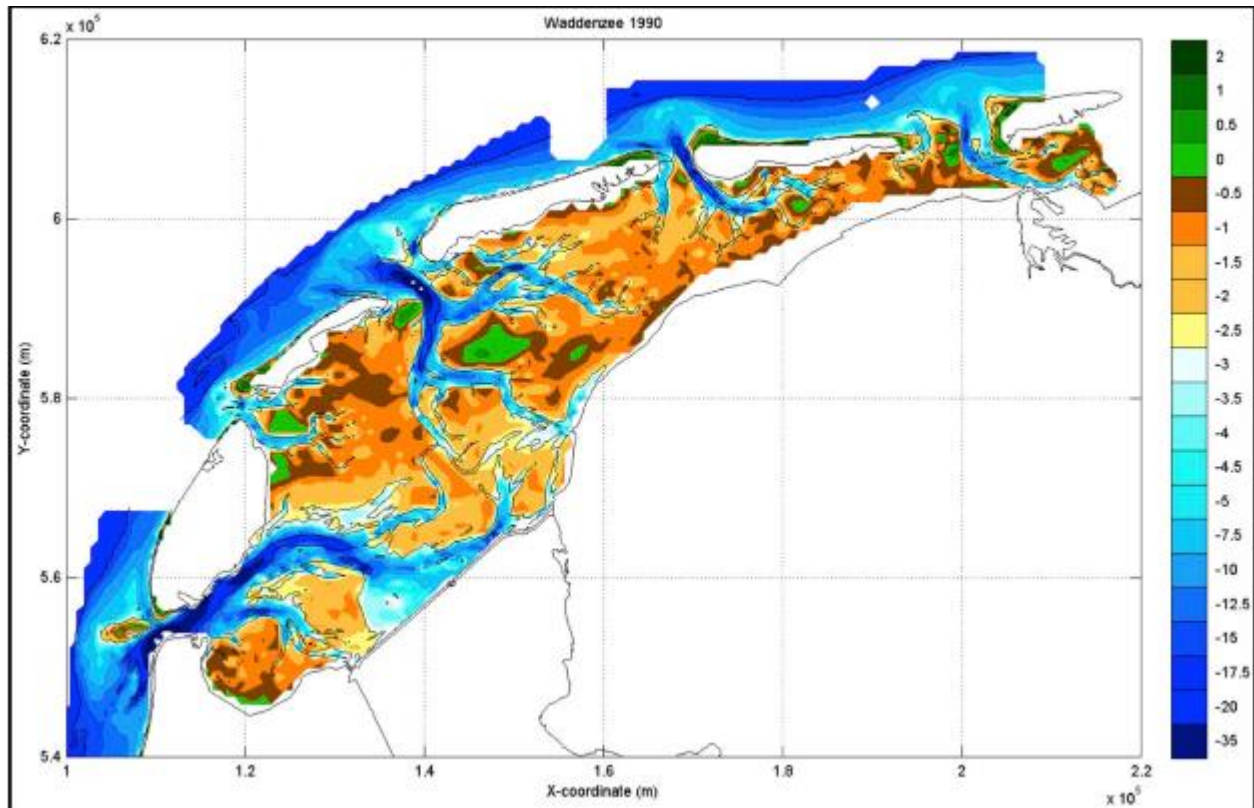


Figure 34. Bathymetry map (m) of the Wadden Sea along the northern shoreline of the Netherlands. Map is adapted from Scheel, 2012)

barrier inlets. Much like coastlines in northern Europe bordering the North Sea, the North American Atlantic coast relies on marine sediment as fluvial influx is limited (Daidu et al., 2013). Considering the lateral extent of MIS 3 tidal flat deposits, and the region's dependence on marine sediment supply, it can be inferred that the Hickory, Powell's Point, and Land of Promise paleoridges represent a backstepping barrier island system with multiple inlets. A highly segmented barrier system would have had a similar influence of sediment transport to that of the present-day Frisian Islands.

5. Conclusion

The shallow stratigraphy of the Albemarle Sound region east of the Suffolk scarp and west of the Alligator and Pasquotank rivers reveal a geomorphic evolution of late Pleistocene paleoenvironments. Stratigraphic sequences best defined by their lithology and chronology reveal how the study area responded to sea level highstand periods during MIS 5 (a/c) and MIS 3. Considering the lack of foraminifera in samples, geomorphologic interpretations for this study depended on lithologic correlations with surrounding studies, geophysical interpretations, and OSL ages to constrain environments and chronology.

Based on shoreface deposits uncovered in Edenton Bay, shoreline transgression between 110 ka – 92 ka extended ~90 km west, periodically occupying the modern-day Suffolk scarp. Tidal shoal facies with OSL ages of 93.4 ± 5.3 ka and 91.8 ± 6.3 ka present within interfluves adjacent to the Little River, suggests minimal shoreline regression during MIS 5b stadial event. Transitioning into MIS 5a interstadial, the study area experienced a return to highstand conditions. Facies comprised of shelly material found at similar elevations as MIS 5a-aged facies ~30 km north in a comparable study support this interpretation. Between 3.8 ka and 54.5 ± 3.1 ka, extensive braid-plain deposits preserved in the shorelines of the Albemarle Sound west of the Perquimans River represent the end of MIS 4 regression, marking the end of fluvial environment (Catuneanu, 2006). During maximum highstand conditions throughout mid MIS 3 (54.5 ± 3.1 ka – 35.6 ± 1.3 ka), tidal flat environments dominated the study area. OSL ages from paleoridges including the Hickory and Powell's Point Ridge (Mallinson et al., 2008) indicate that a barrier island system was present during mid MIS 3. However, this barrier system was highly segmented and allowed for the transport of marine sediment into the back-barrier system via tidal influx.

Literature Cited

- Artyushkov, Y.V., 1967. Establishment of Isostatic Equilibrium in Earth's Crust. *International Geology Review*, vol. 9, no. 11, pp. 1483–1489.
- Blott, S.J., and Pye, K., 2001. Gradstat: A Grain Size Distribution and Statistics Package for the Analysis of Unconsolidated Sediments.” *Earth Surface Processes and Landforms*, vol. 26, no. 11, pp. 1237–48, doi:10.1002/esp.261.
- Boss, S.K., Hoffman, C.W., Cooper, B., 2002. Influence of fluvial processes on the Quaternary geologic framework of the continental shelf, North Carolina, USA. *Mar. Geol.* 183, 45–65.
- Bradley, R.S., 1999. *Paleoclimatology: Reconstructing Climates of the Quaternary*. International Geophysics Series 64, Harcourt, San Diego, CA, 613 p.
- Catuneanu, O., 2006. *Principles of Sequence Stratigraphy*. Elsevier.
- Chappell, J., 2002. Sea level changes forced ice breakouts in the Last Glacial cycle: new results from coral terraces, *Quaternary Science Reviews*, Volume 21, Issue 10, Pages 1229-1240.
- Cargnelli, L. M. 1999. Essential fish habitat source document. Atlantic surfclam, *Spisula solidissima*, life history and habitat characteristics.
- Corbett, D.R., Vance, D., Letrick, E., Mallinson, D., Culver, S., 2007. Decadal-Scale Sediment Dynamics and Environmental Change in the Albemarle Estuarine System, North Carolina. *Estuarine, Coastal and Shelf Science*, vol. 71, no. 3–4, pp. 717–29.
- Culver, S.J., Farrell, K.M., Mallinson, D.J., Willard, D.A., Horton, B.P., Riggs, S.R., Thieler, E.R., Wehmiller, J.F., Parham, P.R., Moore, J.P., Snyder, S.W., Hillier, C., 2011, Micropaleontologic Record of Quaternary Paleoenvironments in the Central Albemarle Embayment, North Carolina, U.S.A. *Palaeogeography, Palaeoclimatology, Palaeoecology*, vol. 305, no. 1–4, pp. 227–49.
- Culver, S.J., Farrell, K.M., Mallinson, D.J., Willard, D.A., Horton, B.P., Riggs, S.R., Thieler, E.R., Wehmiller, J.F., Parham, P.R., Moore, J.P., Snyder, S.W., Hillier, C., 2016. Micropaleontologic Record of Pliocene and Quaternary Paleoenvironments in the Southern Albemarle Embayment, North Carolina, U.S.A. *Palaeogeography, Palaeoclimatology, Palaeoecology*, vol. 457, pp. 360–79.
- Culver S.J., Grand Pre C.A., Mallinson D.J., Riggs S.R., Corbett D.R., Foley J., Hale M., Metger L., Ricardo J., Rosenberger J., Smith C.G., Smith C.W., Snyder S.W., Twamley D. 2007, Late Holocene barrier island collapse: Outer Banks, North Carolina, USA. *Sediment Record*, vol. 5, no. 4, pp. 4-8.

- Chua, V. P., and Ming X. 2014, Impacts of Sea-Level Rise on Estuarine Circulation: An Idealized Estuary and San Francisco Bay. *Journal of Marine Systems*, vol. 139, Elsevier B.V. pp. 58–67.
- Daidu, F., Yuan, W., Min, L., 2013. Classifications, Sedimentary Features and Facies Associations of Tidal Flats. *Journal of Palaeogeography*, vol. 2, no. 1, pp. 66–80.
- Dejong, B.D., Newell, W.L., Rittenour, T.M., Mahan, S.A., Balco, G., Rood., D.H., 2015. Pleistocene Relative Sea Levels in the Chesapeake Bay Region and Their Implications for the next Century.” *GSA Today*, vol. 25, no. 8, pp. 4–10.
- Farrell, K.M., Harris, W.B., Mallinson, D.J., Culver, S.J., Riggs, S.R., 2013. Graphic logging For interpreting process-generated stratigraphic sequences and aquifer/reservoir potential: with analog shelf to shoreface examples from the Atlantic coastal plain province, U.S.A. *Journal of Sedimentary Research*, 83, 723-745.
- Fitzgerald, D.M., Hein, C.J., Hughes, Z., Kulp, M., Georgiou, I., and Miner, M., 2018. Runaway Barrier Island Transgression Concept: Global Case Studies. *Barrier Dynamics and Response to Changing Climate*, no. 2013.
- Flemming, B.W., 2012. Siliciclastic Back-Barrier Tidal Flats. *Principles of Tidal Sedimentology*, ch. 10, pp. 231-267.
- IPCC, 2021: Climate Change 2021: The Physical Science Basis. Contribution of Working Group I to the Sixth Assessment Report of the Intergovernmental Panel on Climate Change [Masson-Delmotte, V., P. Zhai, A. Pirani, S.L. Connors, C. Péan, S. Berger, N. Caud, Y. Chen, L. Goldfarb, M.I. Gomis, M. Huang, K. Leitzell, E. Lonnoy, J.B.R. Matthews, T.K. Maycock, T. Waterfield, O. Yelekçi, R. Yu, and B. Zhou (eds.)]. Cambridge University Press. In Press.
- Karle, M., Bungenstock, F. and Wehrmann, A., 2021. Holocene coastal landscape development in response to rising sea level in the Central Wadden Sea coastal region. *Netherlands Journal of Geosciences*, pp. 100.
- Kemp, A.C., Horton, B.P., Culver, S.J., Corbett, D.R., Plassche, O., Gehrels, W.R., Douglas, B.C., and Parnell, A.C. 2009, Timing and Magnitude of Recent Accelerated Sea-Level Rise, North Carolina, United States. *Geology*, vol. 37, no. 11, pp. 1035–38.
- Kopp, R.E., Horton, B.P., Kemp, A.C., Tebaldi, C., 2015. Past and Future Sea-Level Rise along the Coast of North Carolina, USA. *Climatic Change*, vol. 132, no. 4, Kluwer Academic Publishers, pp. 693–707.
- Lazar, K.B., Mallinson, D.J., Culver, S.J., 2016. Late Quaternary Development of the Croatan Beach Ridge Complex, Bogue Sound, Bogue Banks, NC, USA and Implications for Coastal Evolution.” *Estuarine, Coastal and Shelf Science*, vol. 174, Academic Press, pp. 49–64.

- Lisiecki, L.E., Raymo, M.E., 2005. Pliocene-Pleistocene stack of 57 globally distributed benthic $\delta^{18}\text{O}$ records. *Paleoceanography* 20, PA 1003.
- Mallinson, D., Riggs, S., Thieler, E.R., Culver, S., Farrell, K., Foster, D.S., D. Corbetta, D.R., Benjamin Horton, B., Wehmiller J.F., 2005. Late Neogene and Quaternary Evolution of the Northern Albemarle Embayment (Mid-Atlantic Continental Margin, USA). *Marine Geology*, vol. 217, no. 1–2, pp. 97–117.
- Mallinson, D.J., Burdette, K., Mahan, S., Brook., 2008. Optically Stimulated Luminescence Age Controls on Late Pleistocene and Holocene Coastal Lithosomes, North Carolina, USA. *Quaternary Research*, vol. 69, no. 1, pp. 97–109.
- Mallinson, D.J., Culver, S.J., Riggs, S.R., Thieler, E.R., Foster, D., Wehmiller, J., Kathleen M. Farrell, K.M., Pierson, J., 2010. Regional Seismic Stratigraphy and Controls on the Quaternary Evolution of the Cape Hatteras Region of the Atlantic Passive Margin, USA. *Marine Geology*, vol. 268, no. 1–4, Elsevier B.V., pp. 16–33.
- Mallinson, D., Culver, S., Leorri, E., Mitra S., Mulligan, R., Riggs, S., 2018. Barrier Island and Estuary Co-Evolution in Response to Holocene Climate and Sea-Level Change: Pamlico Sound and the Outer Banks Barrier Islands, North Carolina, USA. *Barrier Dynamics and Response to Changing Climate*, Springer International Publishing, pp. 91–120.
- Miall, A. D., 1995, Whither Stratigraphy. *Sedimentary Geology*, vol. 100, no. 1–4, pp. 5–20.
- Munsterman, D., and Kerstholt, S., 1996. Sodium Polytungstate, a New Non-Toxic Alternative to Bromoform in Heavy Liquid Separation. *Review of Palaeobotany and Palynology*, vol. 91.
- Murray, A.S., Wintle, A.G., 2000. Luminescence of dating of quartz using an improved single-aliquot regenerative-dose protocol. *Radiation Measurements* 32, 57–73.
- Parham, P.R., Riggs, S.R., Culver, S.J., Mallinson, D.J., Wehmiller, J.F., 2007. Quaternary Depositional Patterns and Sea-Level Fluctuations, Northeastern North Carolina. *Quaternary Research*.
- Parham, P. R., 2009. The late quaternary stratigraphy and geologic history of northeastern North Carolina and southeastern Virginia, Greenville, North Carolina, East Carolina University, p. 315.
- Parham, P. R., Riggs, S.R., Culver, S.J., Mallinson, D.J., Rink, J.W., Burdette, K., 2013. Quaternary Coastal Lithofacies, Sequence Development and Stratigraphy in a Passive Margin Setting, North Carolina and Virginia, USA. *Sedimentology*, vol. 60, no. 2, Blackwell Publishing Ltd, pp. 503–47.

- Peebles, P. C., 1984. Late Cenozoic landforms, stratigraphy and history of sea level oscillations of southeastern Virginia and northeastern North Carolina. Dissertations, Theses, and Masters Projects. Paper 1539616804.
- Peltier, W. R., 2004. Global Glacial Isostasy and the Surface of the Ice-Age Earth: The ICE-5G (VM2) Model and GRACE.” *Annual Review of Earth and Planetary Sciences*, vol. 32, pp. 111–49.
- Pico, T., Creveling, J. & Mitrovica, J., 2017. Sea-level records from the U.S. mid-Atlantic constrain Laurentide Ice Sheet extent during Marine Isotope Stage 3. *Nat Commun* 8, 15612.
- Pisias, N.G., and Moore, T.C.Jr., 1981. The evolution of the Pleistocene climate: A time series approach. *Earth and Planetary Science Letters* 52, 450–458.
- Porter, H. J., Houser, L., 1997. *Seashells of North Carolina*. North Carolina Sea Grant Program.
- Potter, E.K., and Lambeck, K., 2003. Reconciliation of Sea-Level Observations in the Western North Atlantic during the Last Glacial Cycle. *Earth and Planetary Science Letters*, vol. 217, no. 1–2, Elsevier B.V., pp. 171–81.
- Railsback, L. B., Gibbard, P.L., Head, M.J., Voarintsoa, N. G., Toucanne, S., 2015. An Optimized Scheme of Lettered Marine Isotope Substages for the Last 1.0 Million Years, and the Climatostratigraphic Nature of Isotope Stages and Substages. *Quaternary Science Reviews*, vol. 111, Elsevier Ltd, pp. 94–106.
- Rhodes, E.J., 2011. Optically Stimulated Luminescence Dating of Sediments over the Past 200,000 Years. *Annual Review of Earth and Planetary Sciences*, 39, 461–488.
- Riggs, S., York, L., Wehmiller, J., Snyder, S., 1992. Depositional patterns resulting from high-frequency Quaternary sea-level fluctuations in North- eastern North Carolina. *Quaternary Coasts of the United States: Marine and Lacustrine Systems. SEPM Special Publication*, vol. 48, pp. 141–153.
- Riggs, S.R., Cleary, W.J., Snyder, W.S., 1996. Morphology and Dynamics of Barrier and Headland Shorefaces in Onslow Bay, North Carolina. *Carolina Geological Society Fieldtrip Guidebook*, 29-40.
- Scavia, D., Field, J. C., Boesch, D. F., Buddemeier, R. W., Burkett, V., Cayan, D. R., et al., 2002. Climate change impacts on U.S. coastal and marine ecosystems. *Estuaries*, 25(2), 149–164.
- Scheel, F., 2012. *Simulating and Classifying Large-Scale Spatial Sand-Mud Segregation Using a Process-Based Model for a Tidal Inlet System*. p. 116.

- Scott, T.W., Swift, D.J.P., Whittecar, G.R., Brook, G.A., 2010. Glacioisostatic influences on Virginia's Late Pleistocene Coastal Plain Deposits. *Geomorphology*.
- Shackleton, N.J., and Turner, C., 1967. Correlation between Marine and Terrestrial Pleistocene Successions. *Nature*, vol. 216, no. 5120, pp. 1079–82.
- Shackleton, N.J., Sa´nchez-Gon˜i, M.F., Paillerc, D., Lancelot, Y., 2003 Marine Isotope Substage 5e and the Eemian Interglacial.” *Global and Planetary Change*, vol. 36, no. 3, Elsevier B.V., pp. 151–55.
- Stanford, S.D., Witte, R.W., Braun, D.D., Ridge, J.C., 2016. Quaternary Fluvial History of the Delaware River, New Jersey and Pennsylvania, USA: The Effects of Glaciation, Glacioisostasy, and Eustasy on a Proglacial River System. *Geomorphology*, vol. 264, Elsevier B.V., pp. 12–28.
- Siddall, M., Rohling, E.J., Thompson, W.G., Waelbroech, C., 2008. Marine isotope stage 3 sea level fluctuations: Data synthesis and new outlook: *Reviews of Geophysics*, v. 46.
- Voelker, A.H.L., 2002. Global Distribution of Centennial-Scale Records for Marine Isotope Stage (MIS) 3: A Database. *Quaternary Science Reviews*, vol. 21.
- Walcott, R.I., 1972. Late Quaternary Vertical Movements in Eastern North America: Quantitative Evidence of Glacio-isostatic Rebound. *Reviews of Geophysics*, vol. 10, no. 4, 1972, pp. 849–84.
- Wang, Z.B., Vroom, J., VanProoijen, B.C., Labeur, R.J., Stive, M.J., 2013. Movement of Tidal Watersheds in the Wadden Sea and Its Consequences on the Morphological Development. *International Journal of Sediment Research*, vol. 28, no. 2, International Research and Training Centre on Erosion and Sedimentation and the World Association for Sedimentation and Erosion Research, 2013, pp. 162–71,
- Wehmiller, J.F., Thieler, E.R., Miller, D., Pellerito, V., Bakeman Keeney, V., Riggs, S.R., Culver, S., Mallinson, D., Farrell, K.M., York, L.L., Pierson, J., Parham, P.R., 2010. Aminostratigraphy of Surface and Subsurface Quaternary Sediments, North Carolina Coastal Plain, USA. *Quaternary Geochronology*, vol. 5, no. 4, Elsevier Ltd, pp. 459–92.
- Wells, J.T., Adams Jr, C.E., Park, Y., Frankenburg, E.W., 1990. Morphology, Sedimentology and Tidal Channel Processes on a High-Tide-Range Mudflat, West Coast of South Korea.” *Marine Geology*, vol. 95, no. 2, pp. 111-130.
- Zaremba, N., Mallinson, D.J., Leorri, E., Culver, S., Riggs, S., Mulligan, R., Horsman, E., Mitra, M., 2016. Controls on the Stratigraphic Framework and Paleoenvironmental Change within a Holocene Estuarine System: Pamlico Sound, North Carolina, USA. *Marine Geology*, vol. 379, Elsevier B.V., pp. 109–23,

APPENDIX A: GEOPROBE CORE LOCATIONS

Core locations along with penetration depths. Geoprobe elevations measure the ground level height above msl where the core was collected. Vibracore elevations measure the water depth at the coring location.

	Core ID	Latitude	Longitude	Penetration (m)	Elevation (m)
GeoProbe	SAS20-GP1	35.928889 N	76. 618889 W	4.8	3.7
	SAS20-GP2	35.953303 N	76.4913 W	4.8	4.0
	SAS20-GP3	35.898694 N	76.693019 W	6.0	4.9
	SAS20-GP4	35.921081 N	76.640308 W	4.8	3.0
	SAS20-GP5	35.949506 N	76.493908 W	6.0	2.7
	NAS20-GP6	36.05995 N	76.587467 W	5.2	2.7
	NAS20-GP7	36.059444 N	76.586389 W	6.0	3.0
	NAS20-GP8	36.087703 N	76.354397 W	4.8	2.4
	NAS20-GP9	36.114408 N	76.222236 W	3.7	2.1
	NAS20-GP10	36.145403 N	76.183467 W	4.8	1.2
Vibracore	SAS20-VC1	35.98565 N	76.250133 W	3.2	3.0
	SAS20-VC2	35.9983 N	76.401133 W	1.7	3.0
	NAS20-VC3	36.055883 N	76.42235 W	1.5	3.2
	EB20-VC4	36.020633 N	76.596983 W	1.3	2.2
	EB20-VC5	36.0449 N	76.620783 W	2.9	2.5
	CR20-VC6	36.044733 N	76.678033 W	2.6	3.0
	SAS =	Southern Albemarle Sound			
	NAS =	Northern Albemarle Sound			
	EB =	Edenton Bay			
	CR =	Chowan River			

APPENDIX B: GRAIN SIZE ANALYSIS DATA

Grain size analysis results for 24 samples collected from 14 cores (Geoprobe and vibracore). Elevation of sampled sections are measured in meters relative to sea level.

Sample Name	cm below core top	Sorting Φ	Skewness Φ	Mean Φ	Mode Φ	D ₅₀ (μm)	Sediment Type	
SAS20-GP1	2.15-2.19	215					Unimodal, Moderately Sorted	
			0.769	-0.806	2.778	3.237	137.123	
SAS20-GP4	2.01-2.05	201					Bimodal, Poorly Sorted	
			0.816	-0.222	2.596	2.237	168.325	
SAS20-GP5	3.18-3.22	318					Bimodal, Moderately Sorted	
			0.760	0.188	2.504	2.237	192.756	
SAS20-GP5	4.27-4.31	427					Unimodal, Well Sorted	
			0.381	-0.067	2.224	2.237	214.648	
NAS20-GP6	.92-.96	92					Unimodal, Moderately Sorted	
			0.856	-0.937	2.710	2.737	139.450	
SAS20-GP6	1.80-1.84	180					Unimodal, Moderately Sorted	
			0.747	-0.832	2.672	2.737	149.270	
NAS20-GP7	5.39-5.43	539					Bimodal, Poorly Sorted	
			1.306	-0.163	1.443	0.747	390.270	
NAS20-GP7	3.05-3.09	305					Bimodal, Moderately Sorted	
			0.670	0.558	2.447	2.237	206.868	
NAS20-GP8	.58-.62	58					Bimodal, Poorly Sorted	
			0.773	-1.268	3.256	3.731	81.729	
NAS20-GP8	2.76-2.80	276					Bimodal, Moderately Sorted	
			0.773	0.404	2.386	3.731	211.821	
NAS20-GP9	1.80-1.84	180					Unimodal, Poorly Sorted	
			0.295	-5.834	3.659	3.731	76.566	
NAS20-GP10	.70-.74	70					Unimodal, Poorly Sorted	
			0.517	-2.738	3.502	3.731	79.237	

NAS20-GP10	2.06-2.10	206							Unimodal, Poorly Sorted
			0.185	-6.310	3.691	3.731	76.144		
SAS20-VC1	.35-.37	35							Unimodal, Well Sorted
			0.421	-0.186	2.426	2.237	188.460		
SAS20-VC1	1.25-1.27	125							Unimodal, Well Sorted
			0.444	0.326	2.487	2.237	185.554		
SAS20-VC1	2.28-2.30	228							Unimodal, Moderately Well Sorted
			0.637	-0.154	2.414	2.237	190.025		
SAS20-VC1	3.24-3.26	324							Bimodal, Moderately Well Sorted
			0.627	0.040	2.338	1.747	198.166		
SAS20-VC2	1.00-1.02	100							Unimodal, Moderately Sorted
			0.471	-0.284	2.064	2.237	234.013		
SAS20-VC2	1.67-1.69	167							Bimodal, Poorly Sorted
			0.901	-1.302	3.052	3.731	93.773		
NAS20-VC3	1.26-1.28	126							Bimodal, Moderately Sorted
			0.576	-0.678	3.181	3.731	102.346		
EB20-VC4	.72-.74	72							Unimodal, Well Sorted
			0.470	-0.051	2.172	2.237	220.590		
EB20-VC5	1.14-1.16	114							Unimodal, Moderately Sorted
			0.742	-0.618	2.540	2.737	162.923		
EB20-VC5	.90-.92	90							Unimodal, Moderately Sorted
			0.471	-0.233	2.780	2.737	147.700		
CR20-VC6	1.43-1.45	143							Bimodal, Poorly Sorted
			0.560	0.267	2.013	1.747	253.591		

APPENDIX C: RADIOCARBON ANALYSIS

Sampled Core	Sample Depth (mbsl)	Sample Type	Fm Error	Age (ka)	Age Error (ka)	d13C	d14C
NAS20-VC3	4.3	Sediment Organic Carbon	0.0120	35	1.3	-23.86	-988.1
SAS20-VC1	4.4	Plant/Wood	0.6205	3.83	0.02	-14	-384.8








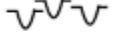





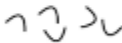







APPENDIX D: OPTICALLY STIMULATED LUMINECENSE RESULTS

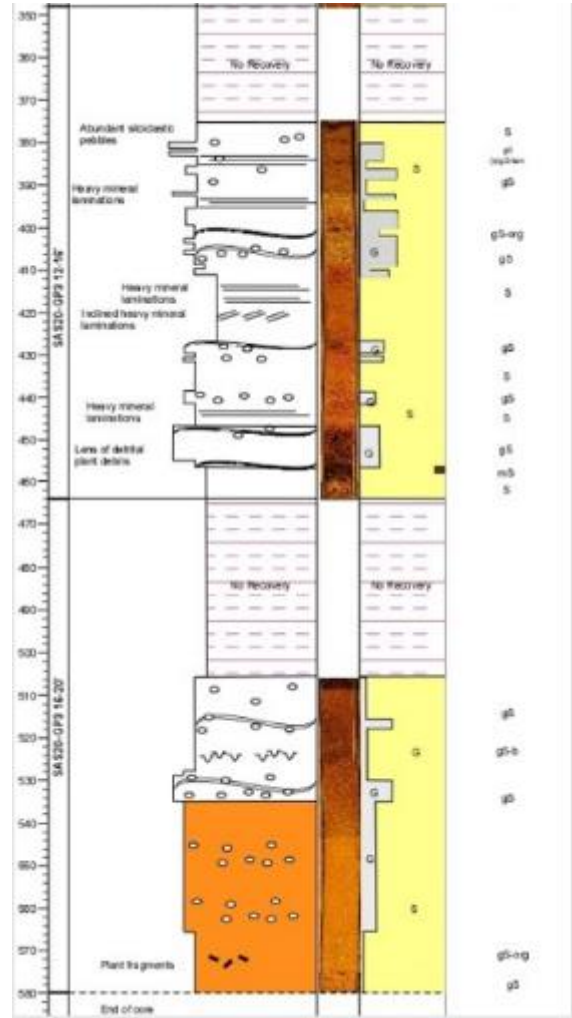
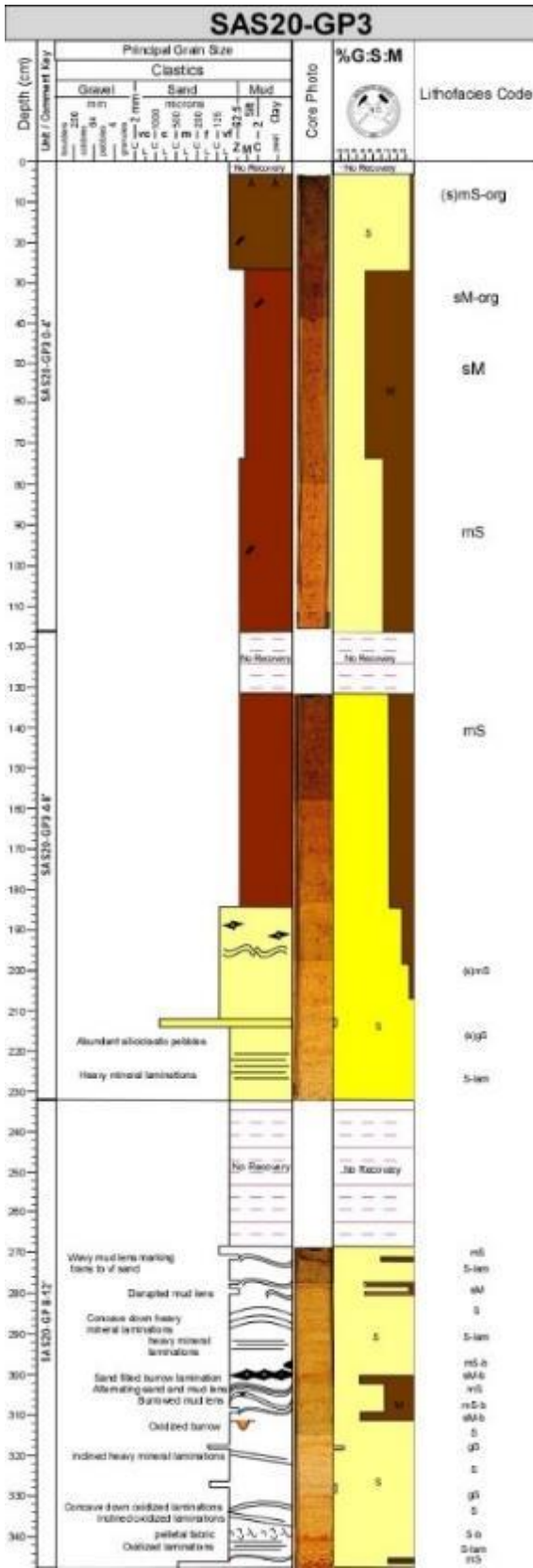
OSL data for 5 samples analyzed in this study. Elevation of each samples is measured in cm relative to sea level. OSL ages (ka) are calculated by dividing the paleo dose (equivalent dose) by the dose rate. Format tables per the instructions in the journal that this paper will be submitted to. Your tables have different formats.

Sample ID	Core	Elev. (cm)	Longitude	Latitude	Th(ppm)	Pb214 (U ppm)	K (%)	Dose rate(Gy/ka)	Paleo dose (Gy)	Age (ka)
OSL1	SAS20-GP1	-29	35.928889 N	76.618889 W	2.06 ± 0.17	0.70 ± 0.04	1.01 ± 0.06	1.238 ± 0.046	76.3 ± 3.8	61.6 ± 3.8
OSL2	SAS20-GP5	-244	35.949506 N	76.493908 W	2.77 ± 0.23	1.04 ± 0.06	1.05 ± 0.06	1.345 ± 0.047	73.3 ± 3.3	54.5 ± 3.1
OSL3a	NAS20-GP8	-163	36.087703 N	76.354397 W	0.43 ± 0.03	0.81 ± 0.06	0.80 ± 0.05	1.354 ± 0.053	93.1 ± 6.4	68.8 ± 5.4
OSL3b					2.77 ± 0.21	0.82 ± 0.05	1.05 ± 0.06			
OSL3c					3.52 ± 0.27	0.95 ± 0.06	1.01 ± 0.06			
OSL4	NAS20-GP9	-72	36.114408 N	76.222236 W	1.20 ± 0.11	0.37 ± 0.03	0.59 ± 0.03	0.806 ± 0.029	75.3 ± 3.3	93.4 ± 5.3
OSL5a	NAS20-GP10	-162	36.145403 N	76.183467 W	4.76 ± 0.35	1.20 ± 0.07	1.80 ± 0.10	1.023 ± 0.052	93.9 ± 4.3	91.8 ± 6.3
OSL5b					1.95 ± 0.16	0.64 ± 0.04	1.07 ± 0.06			

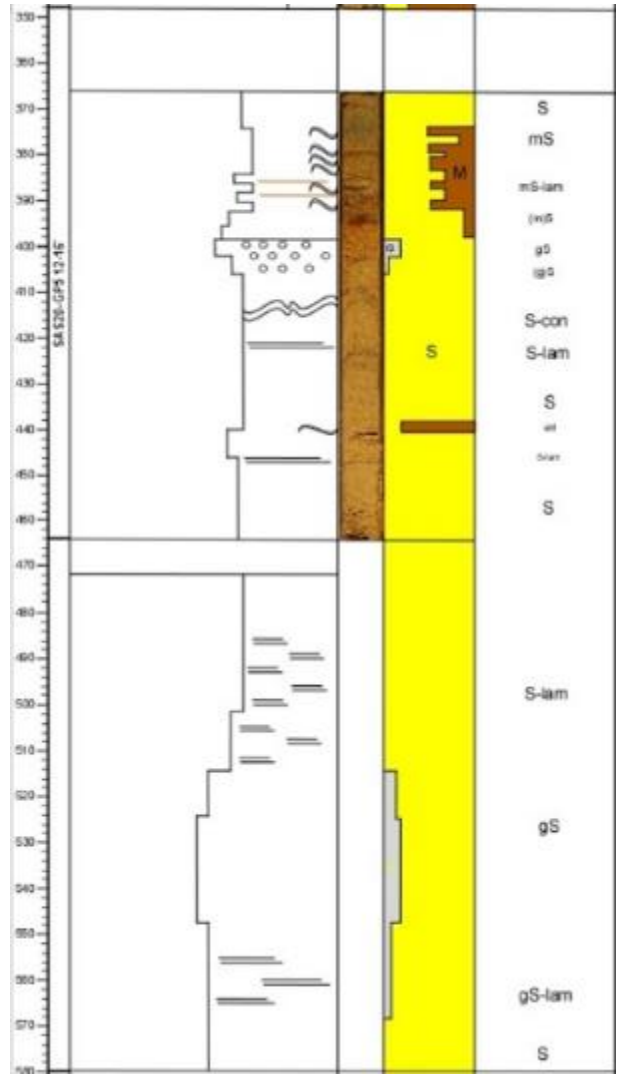
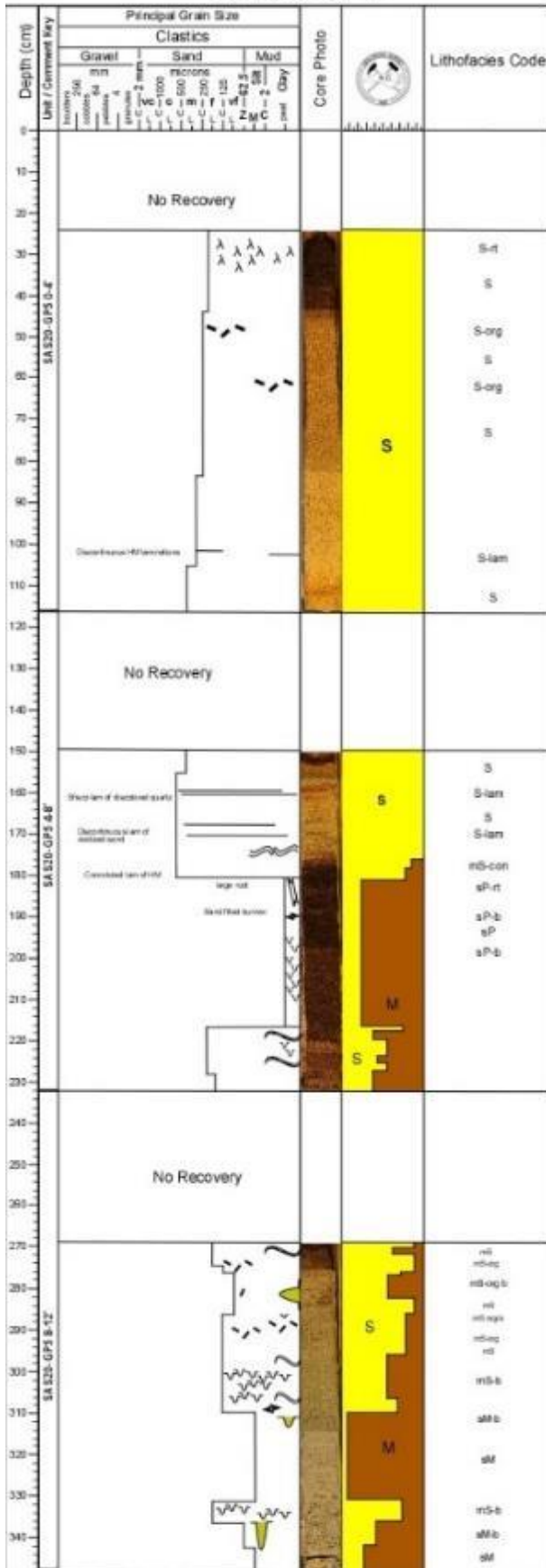
APPENDIX E: GEOPROBE AND VIBRACORES

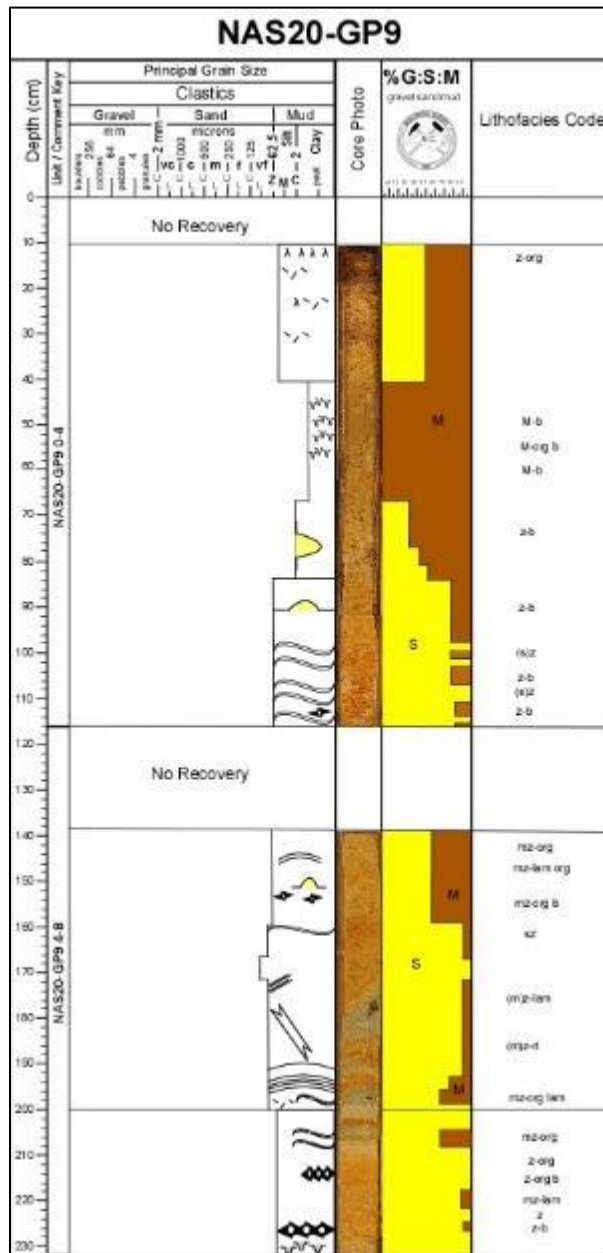
Core Symbol Key

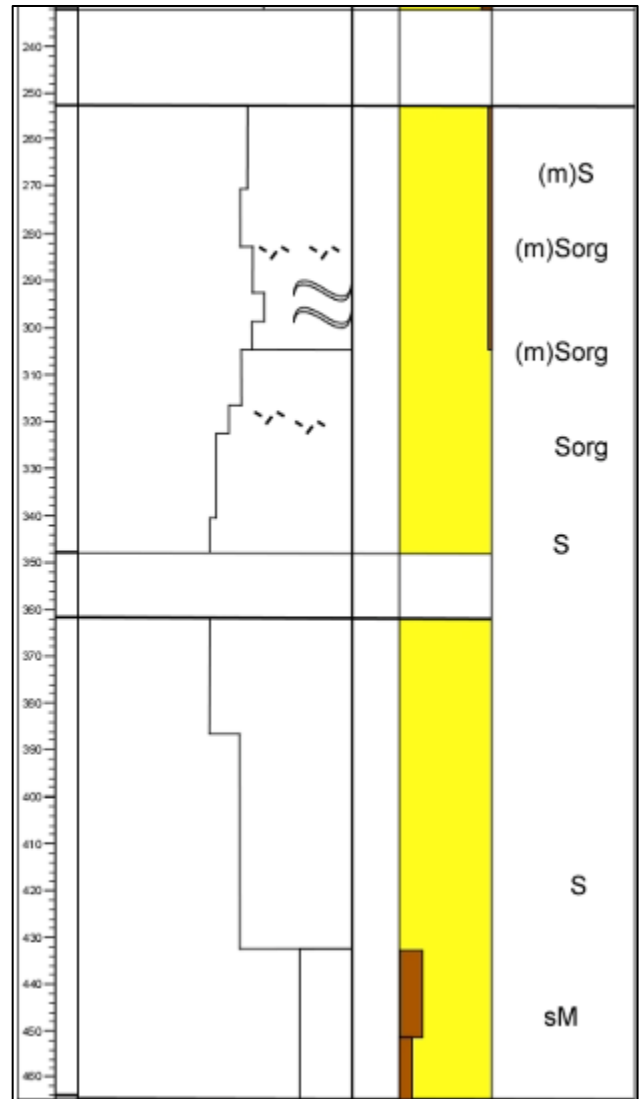
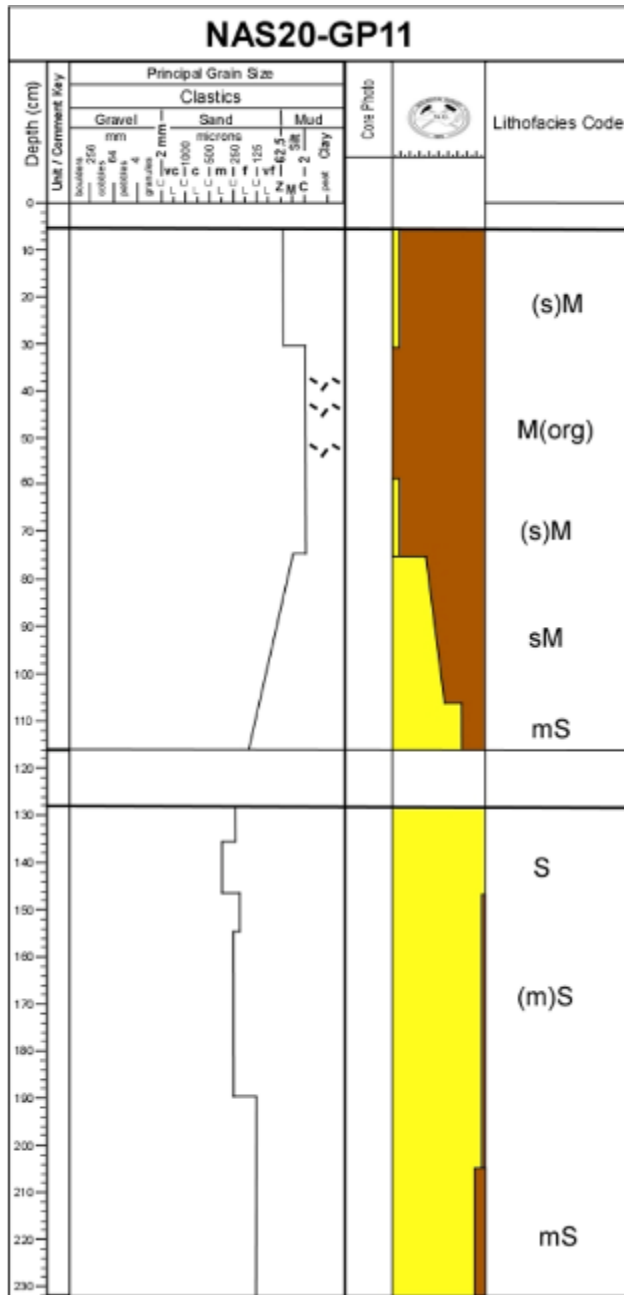
	Small root traces		Flaser bedding (mud)		Shell fragment
	Swirling lamination		Inclined lamination		Disrupted lamination
	Convolute lamination		Undifferentiated burrows		
	Wavy lamination		Burrow lamination		
	Concave down lamination		Bored		
	Horizontal laminations		Pelletal fabric		
	Siliclastic pebbles		Large root trace		
	Plant fragments		<i>Thalassinoides</i> -like burrows		
	Flat lamination of plant debris				
	Lens of detrital plant debris				
	Lenticular bedding (sand)				

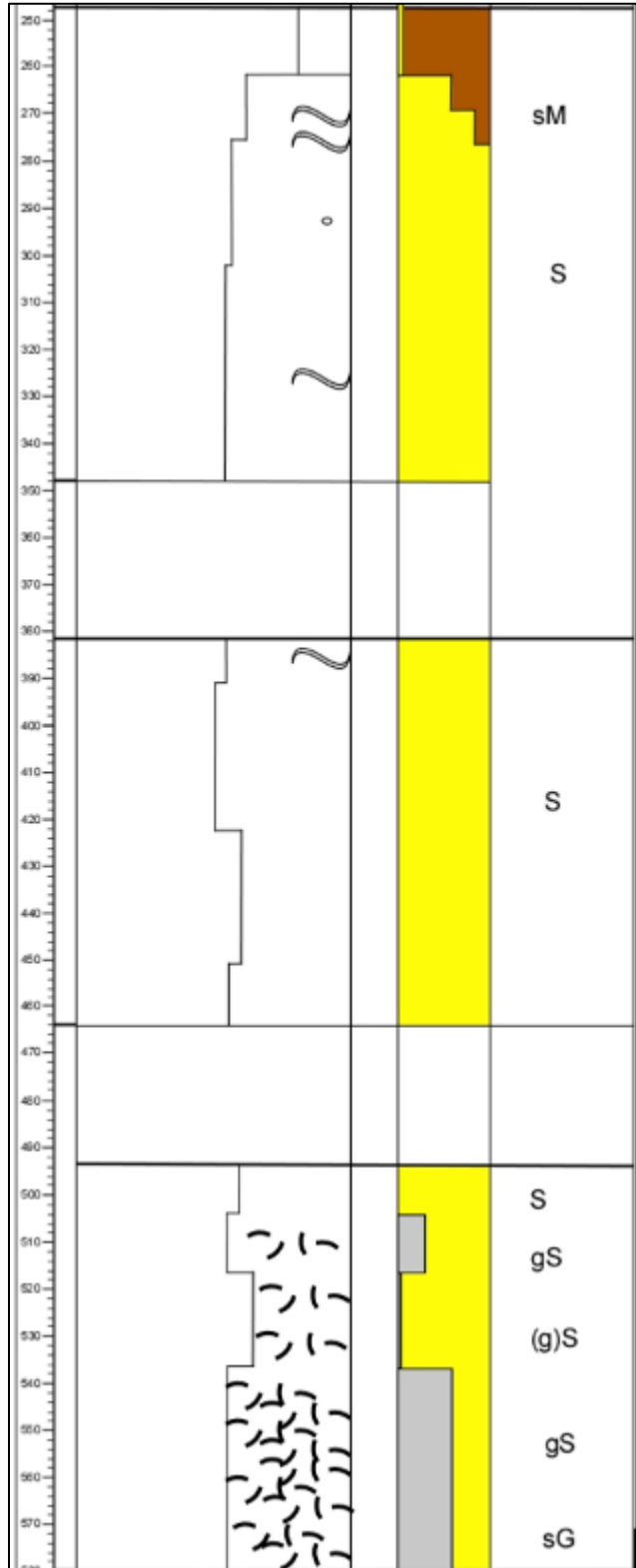
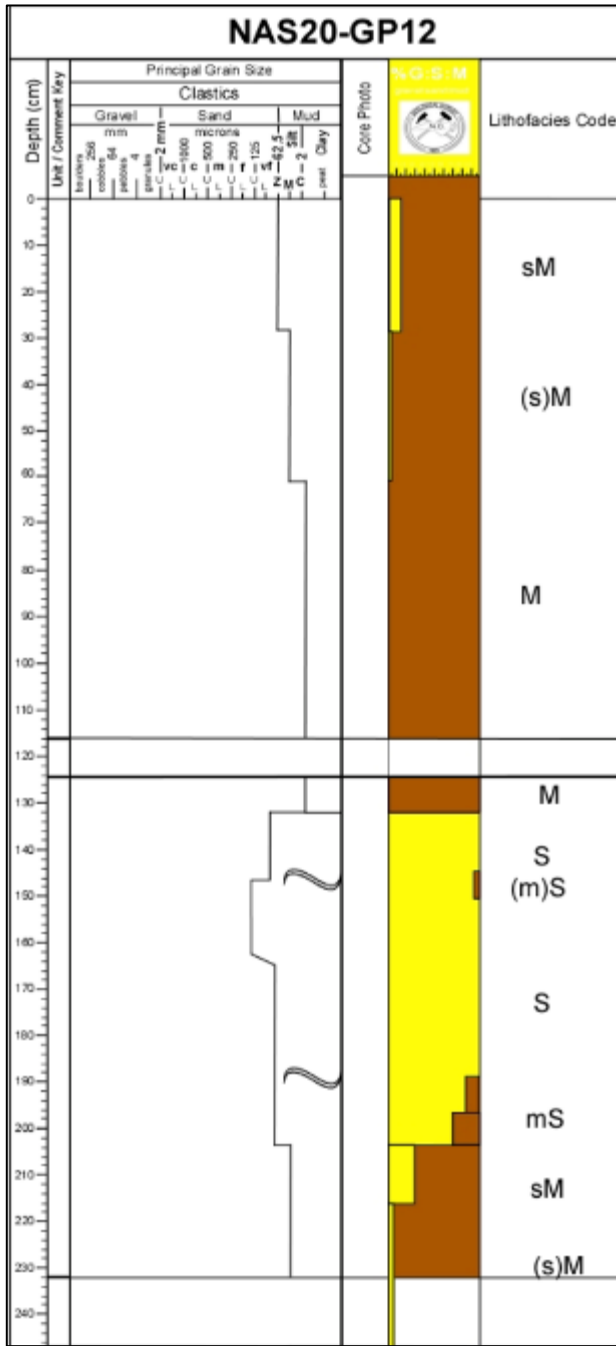


SAS20-GP5

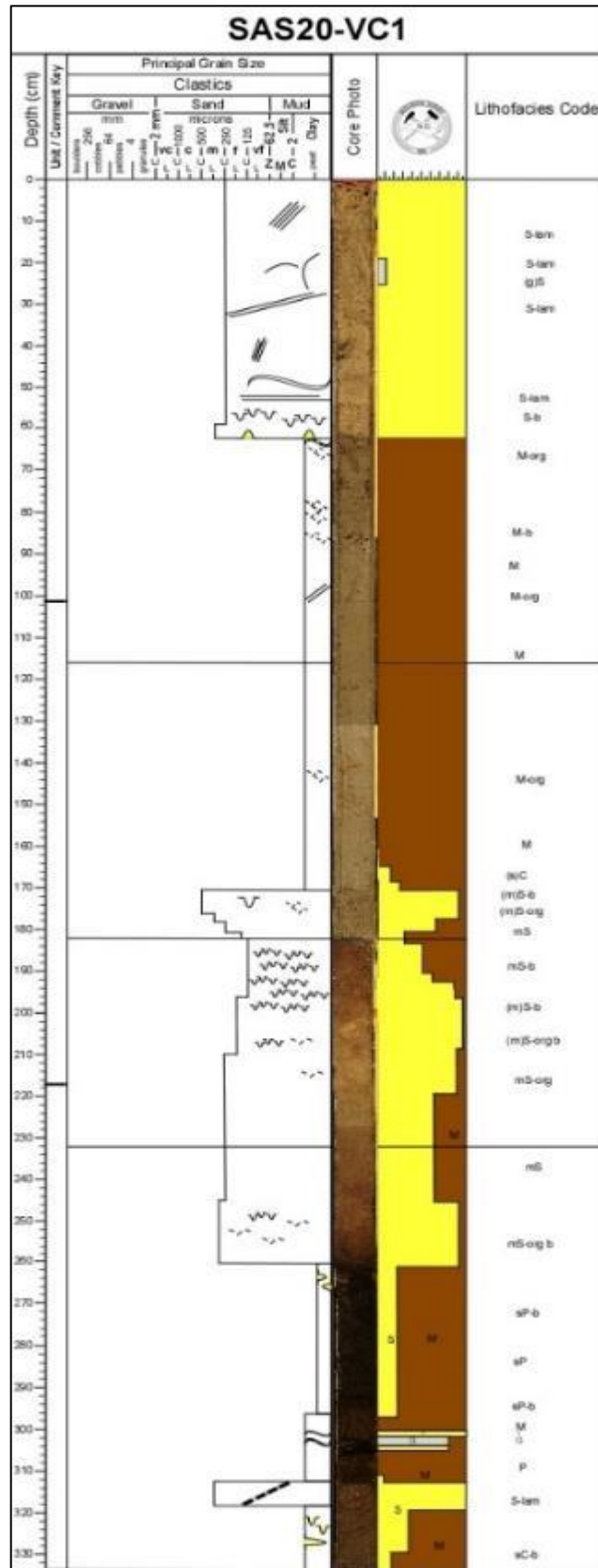


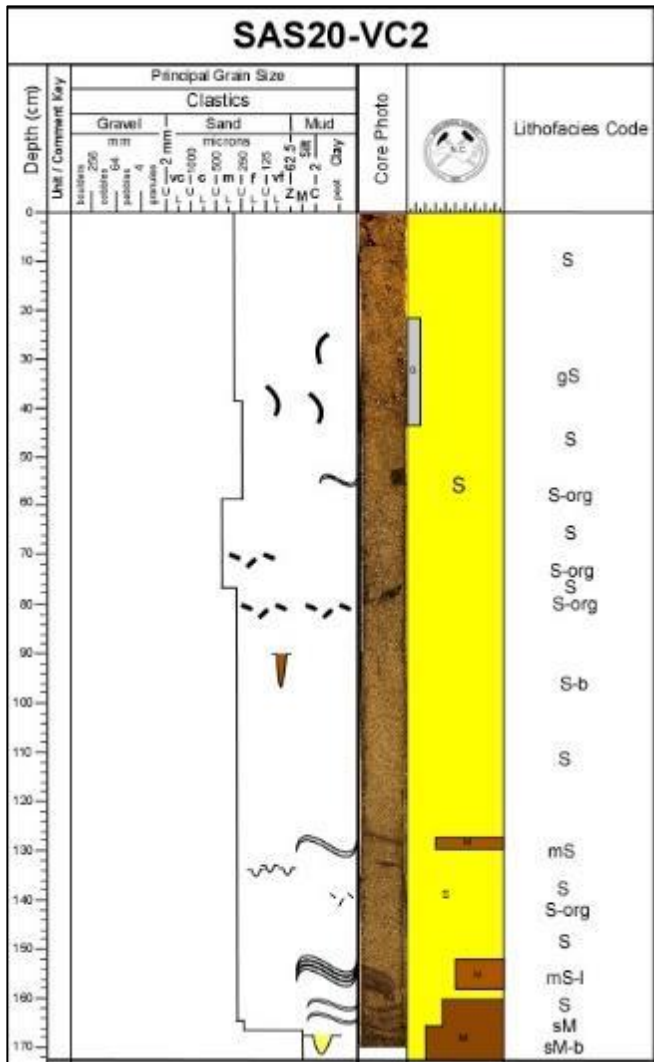


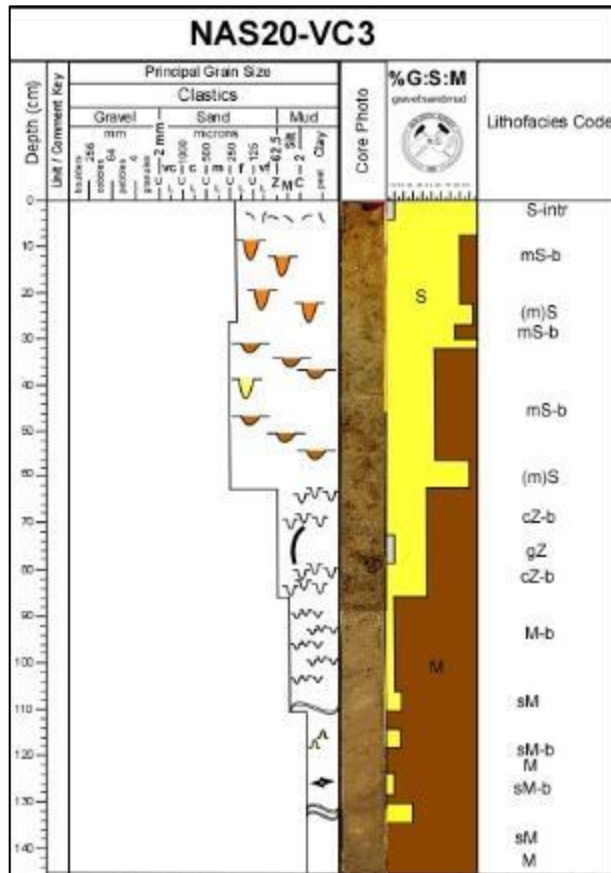


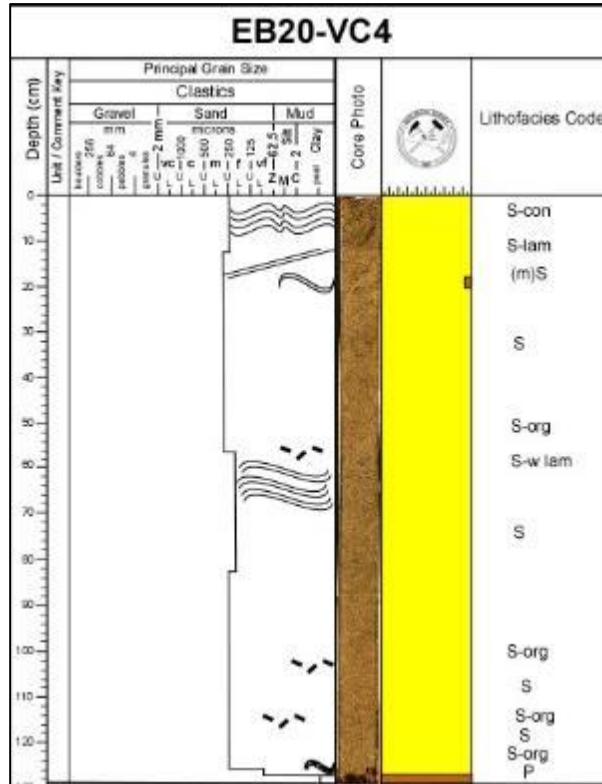


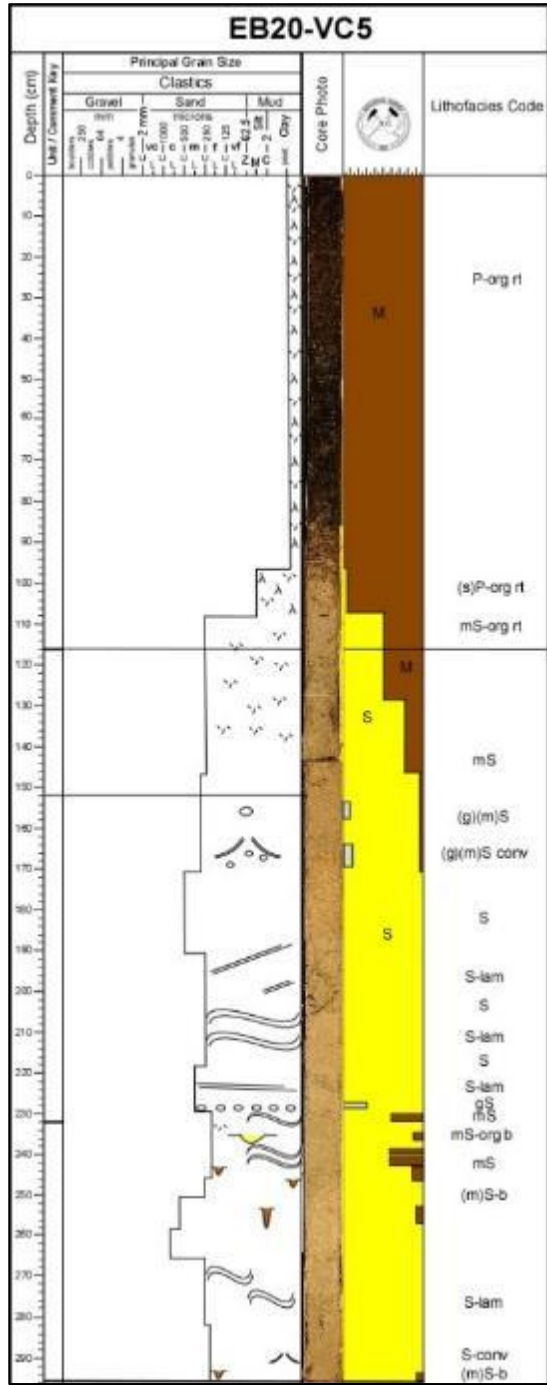
APPENDIX C: VIBRACORES











CR20-VC6

